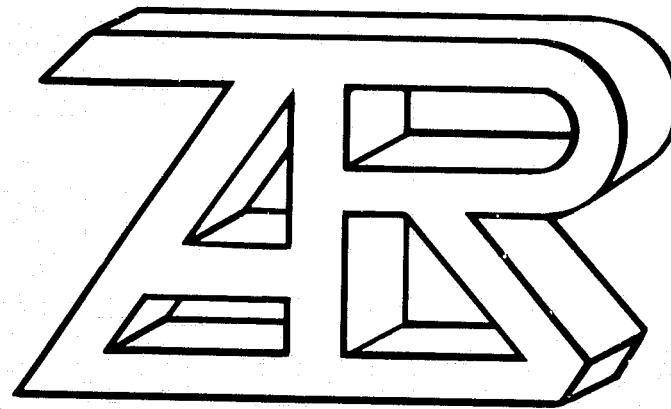


General Disclaimer

One or more of the Following Statements may affect this Document

- This document has been reproduced from the best copy furnished by the organizational source. It is being released in the interest of making available as much information as possible.
- This document may contain data, which exceeds the sheet parameters. It was furnished in this condition by the organizational source and is the best copy available.
- This document may contain tone-on-tone or color graphs, charts and/or pictures, which have been reproduced in black and white.
- This document is paginated as submitted by the original source.
- Portions of this document are not fully legible due to the historical nature of some of the material. However, it is the best reproduction available from the original submission.

NASA CR-175217



**ADVANCED TECHNOLOGY
&
RESEARCH, INCORPORATED**

(NASA-CR-175271) INERTIAL ENERGY STORAGE
HARDWARE DEFINITION STUDY (RING ROTOR)
(Advanced Technology and Research, Inc.)
123 P HC A06/MF A01

CSCL 10C

N84-20015

Unclassified

G3/44 12502

**INERTIAL ENERGY STORAGE HARDWARE
DEFINITION STUDY
(RING ROTOR)**

J. A. Kirk

H. E. Evans

**Advanced Technology and Research, Inc.
3933 Sandy Spring Road
Burtonsville, MD 20866**

Prepared for

**Goddard Space Flight Center
Greenbelt, MD 20771**

January 1984

Report No. 18401

TABLE OF CONTENTS

PREFACE

I. Design Background

II. Rotor Analysis

1. Introduction

2. Rotor Analysis Methods

2.1. FLYANS

- a. Background
- b. Interference Stresses
- c. Constraints
- d. Summary

2.2. FLYSIZE

3. Results

4. Discussion

5. References

III. Fabrication/Assembly

A. Materials

B. Techniques

C. Drawings

D. Companies

E. Testing

IV. Specification

V. Summary

VI. Recommendations

VII. Appendices

- 1. Reference paper for FLYANS code
- 2. Failure Analysis
- 3. FLYSIZE listing
- 4. FLYSIZE formulas
- 5. Ring tolerances
- 6. Stress plots
- 7. Drawings

ORIGINAL PAGE IS
OF POOR QUALITY

ORIGINAL PAGE IS
OF POOR QUALITY

PREFACE

This report contains the results and details of a design study and analysis performed by Advanced Technology and Research, Inc. (ATR) for the NASA Goddard Space Flight Center (GSFC) as part of the overall Inertial Energy Storage Hardware Definition Study. The study was confined to include only the composite ring rotor element. The GSFC technical officer for this task was Mr. G. Ernest Rodriguez.

The objectives of this study were:

1. Detailed design definition of a composite ring rotor meeting the stated performance requirements.
2. Definitive specifications for ring rotor fabrication and assembly.
3. Identification of potential sources for fabrication and assembly.

This design effort centered around the use of graphite-epoxy composite materials. The study is significant because it resulted in the following:

1. High energy density "thick ring" composite rotor design compatible with the "Mechanical Capacitor" concept.
2. Unique multiring prestressed design configuration.
3. Successful application of a modified Tsai-Hill Quadratic Interaction Analysis technique.
4. Demonstrated usefulness and versatility of previously developed computer codes (FLYANS and FLYSIZE), which include the presence of an iron inner ring.

I. DESIGN BACKGROUND

This report covers the design definition of the composite fiber ring-rotor portion of an Inertial Energy Storage Hardware Definition Study managed by the NASA Goddard Space Flight Center (GSFC). Genesis for this effort stems from early work done at GSFC on the "Mechanical Capacitor" program. This early work showed the potential merits of a magnetically suspended ring rotor with integral ironless armature motor/generator construction. The three major elements of this design concept are:

1. Composite material ring-rotor flywheel
2. Magnetic suspension
3. Permanent magnet ironless armature motor/generator

The GSFC selected item 1. as the logical starting point for a complete design definition of the inertial energy storage system.

Stated requirements for this effort were to provide design definition and a specification for a Inertial Energy Storage wheel comprised of composite materials to yield high energy density and be capable of interfacing with an appropriate magnetic suspension system and motor/generator.

Performance requirements:

Energy Storage (at max. speed)	1.6 KWh
Weight (total system)	60 kg(132 lbm)
Volume	Less than 0.05 m ³ (1.77 ft ³)
Environment	
Temperature (operating)	-10°C to +50°C (14°F to 122°F)
Pressure (operating)	< 10 ⁻⁴ torr

The basic requirement that establishes the size of the storage element is the 1.6 KWh capacity. Before determining specific parameters it was necessary to select a best estimate composite material. Previous work supported by the Department of Energy, Mechanical Energy Storage Technology (MEST) program showed that graphite fiber epoxy matrix material demonstrated best overall technical performance and ease of manufacturing when compared to other materials and fabrication technique.. Thus, a graphite/epoxy fiber (Celion 6000) and an epoxy matrix (EPON 826) were selected for this study.

Two form factors (ID/OD ratio) of 0.5 and 0.4 were selected and the design sizing and analysis were conducted using these stated parameters.

ORIGINAL PAGE IS
OF POOR QUALITY

II. ROTOR ANALYSIS

1. Introduction

In designing a magnetically suspended flywheel rotor it is necessary to consider a reasonable geometry upon which the design/analysis will be based. Early work in this area by Kirk, Studer and Evans of GSFC [1, 2, 3]* has shown that a pierced disk of uniform thickness provides a desirable rotor geometry from both a performance and manufacturing point of view.

Shown in Figure II.1 is a cross sectional view of the original GSFC magnetically suspended flywheel design. The original design consists of 2 rings with the outermost ring being made of a filamentary wound composite material and the inner ring being made of continuous iron bonded to the filamentary wound ring. The stator of this design fits in the "hole" of the 2 ring rotor and it carries the magnetic suspension and motor/generator electronics.

RCA [4] and Kirk [5], under contract to GSFC, have done additional work on the original GSFC design. Kirk concluded that a multiring, interference assembled rotor, such as shown in Figure II.2, would provide for substantial improvements in the original GSFC design. The modified GSFC design, shown in Figure II.2, differs from the original GSFC design in the following areas:

1. The rotor is composed of a number of individual filamentary wound rings, rather than being one continuous ring.
2. The inside diameter (ID) to outside diameter (OD) rotor ratio (ID/OD) is smaller than the original GSFC design.

*Brackets denote references at the back of this section.

ORIGINAL PAGE IS
OF POOR QUALITY

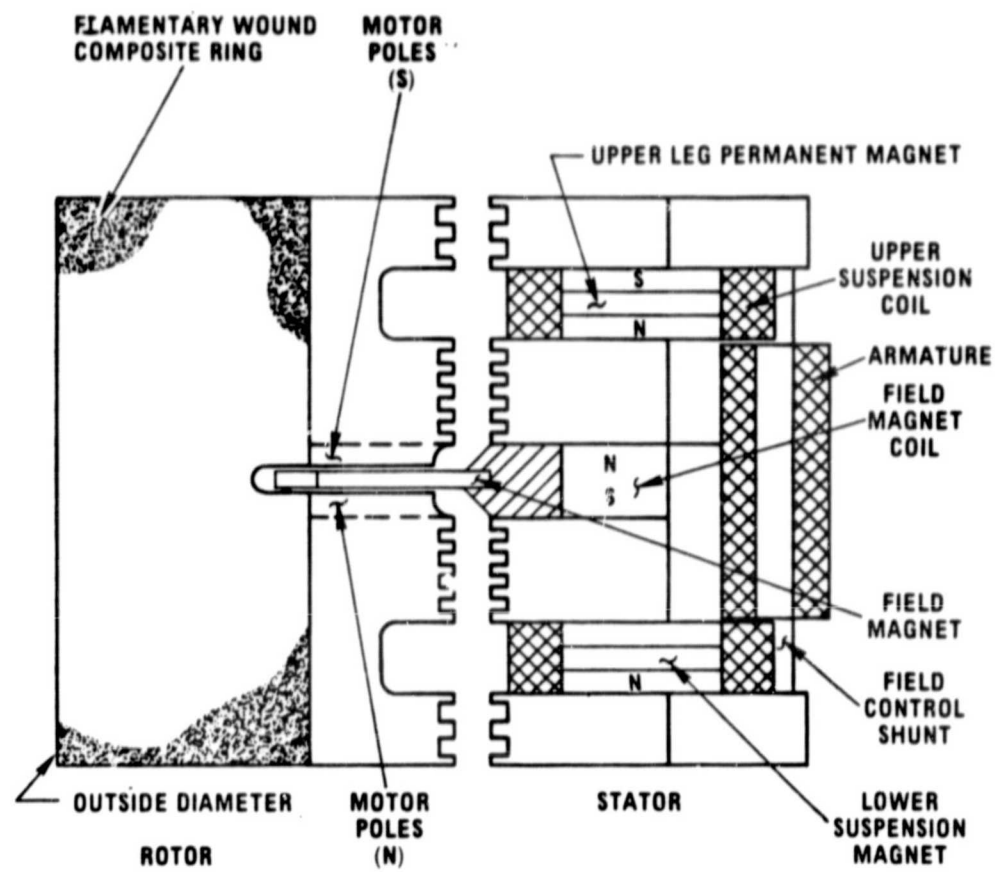
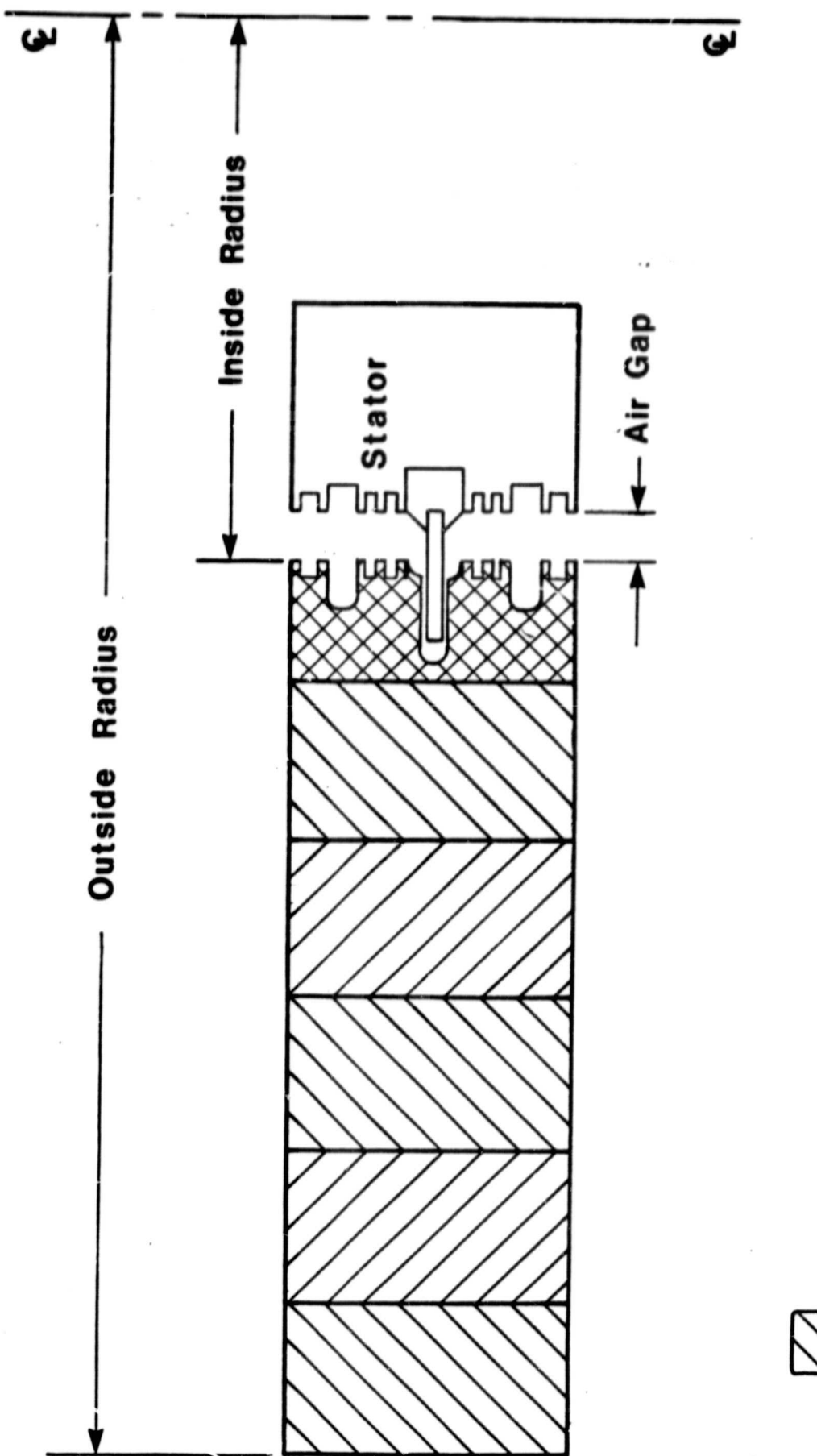


Figure II.1

Cross Sectional View of Rotor/Stator in Original GSFC
Magnetically Suspended Flywheel Design (from reference 1)



ORIGINAL PAGE IS
OF POOR QUALITY

= Composite Material Rings



= Iron Ring



Figure II.2

Cross sectional view of the modified GSFC design.
The design has a smaller ID/OD ratio and the iron
ring is segmented.

3. The innermost ring is made of iron and is segmented into discrete pie shaped "chunks".

Each of the above changes was made in the original GSFC design in order to improve the overall performance of the energy storage system. The reasoning behind the changes has been documented by Kirk and Huntington [6, 7, 8, 9] and a brief explanation follows:

1. The rotor is made of a number of composite material rings which are interference assembled. The reason behind this change is to favorably prestress the rotor so higher rotational speeds and energy densities can be obtained before a limiting performance constraint is encountered.
2. The ID/OD ratio has been lowered. The reason behind this change is that the original GSFC design was of a "thin hoop" type and suffered excessive "gap" growth between the rotor and the stator as it spun. Since gap growth will degrade electrical performance it must be controlled and the best way to achieve this control is by decreasing the ID/OD ratio.
3. The innermost ring must be made of iron and is now segmented instead of being continuous. This change has been made because the iron ring would always reach the limiting strength long before the filamentary wound composite ring(s) reached their strength limit. To overcome this limitation a "segmented" inner ring is now proposed for use on the magnetically suspended flywheel system. The important point to note is that the inner iron ring will have all the necessary magnetic properties but will consist of a number of pie shaped segments which are bonded to the inside diameter of the first filamentary wound ring.

The iron ring thus has no stiffness in a "hoop" or tangential direction and presents an "inner loading" on the filamentary wound composite ring to which it is attached.

The result of making the above changes in the original GSFC design are all intended to bring the original design's excellent theoretical performance to fruition in a physical system.

2. Rotor Analysis Methods

It is clear that the design dimensions for the GSFC rotor must evolve in parallel with the magnetic suspension and motor generator designs (as they impact on the dimensions and weight of iron inner ring). Obviously then, the most useful rotor design and analysis tools are those which most closely model the real physical system and are convenient to apply as the iron inner ring design evolves. One such tool has already been reported by Kirk and Huntington [6, 7, 8, 9] and was used for this project. This tool, an interactive computer code called FLYANS (FLYwheel ANalySis), represents the most complete stress and failure analysis ever performed on a pierced disk multiring rotor. A second tool has been developed for this project and is a computer code called FLYSIZE (FLYwheel SIZE), to size all dimensions for a given rotor design. Each of these codes will be discussed in more detail in the following sections.

2.1. FLYANS - Flywheel Analysis Computer Code

A. Background

Shown in Appendix 1 is the background theory which was used in developing FLYANS. The computer code was originally written by R.A. Huntington [9], as part of his Master's thesis, while working with his thesis advisor, Dr. J.A. Kirk. The code has since been modified by Dr. Kirk, and the modified version was used for this project.

Shown in Figure II.3 is a schematic diagram of the multiring rotor which is modeled in the FLYANS code. Each of the rings are the same axial thickness and the stresses in each ring consist of a hoop or tangential stress (σ_θ) and a radial stress (σ_r). If power is being put in or taken out of the system there is an additional shear stress ($\tau_{r\theta}$) in each ring. This stress is assumed to be zero for this design (i.e., power transfer occurs "slowly") although the FLYANS code is set up to allow any stress input the user wishes. It is also assumed that the flywheel rings are in a state of plane stress, meaning that there is no variation of the σ_θ and σ_r stresses in the axial direction.

The materials which comprise the multiring rotor are modeled as homogeneous linearly elastic, specially orthotropic [10] materials, with material properties specified in the radial and tangential direction. For this project ring #1 is always segmented iron and ring #2 through ring #n are CELION 6000/EPOXY. The properties for these 2 materials are shown in Table II.1. For comparison purposes a number of other materials and their properties are also shown. The source of information for properties on Celion 6000/EPOXY was a Celanese data sheet provided to us by Mr. Alan Hannibal (Section Manager Materials & Process, R & D Department), of Lord Corporation. The other materials listed in the table were from an earlier report to GSFC by Dr. J. A. Kirk [5]. These other materials are shown here because they constitute the working database used by the FLYANS code. It should also be pointed out that any new or hypothetical materials can easily be added to the database with minimal effort.

The total stress distribution in one ring of the multiring flywheel is the superposition of the five stress distributions due to the following:

ORIGINAL PAGE IS
OF POOR QUALITY

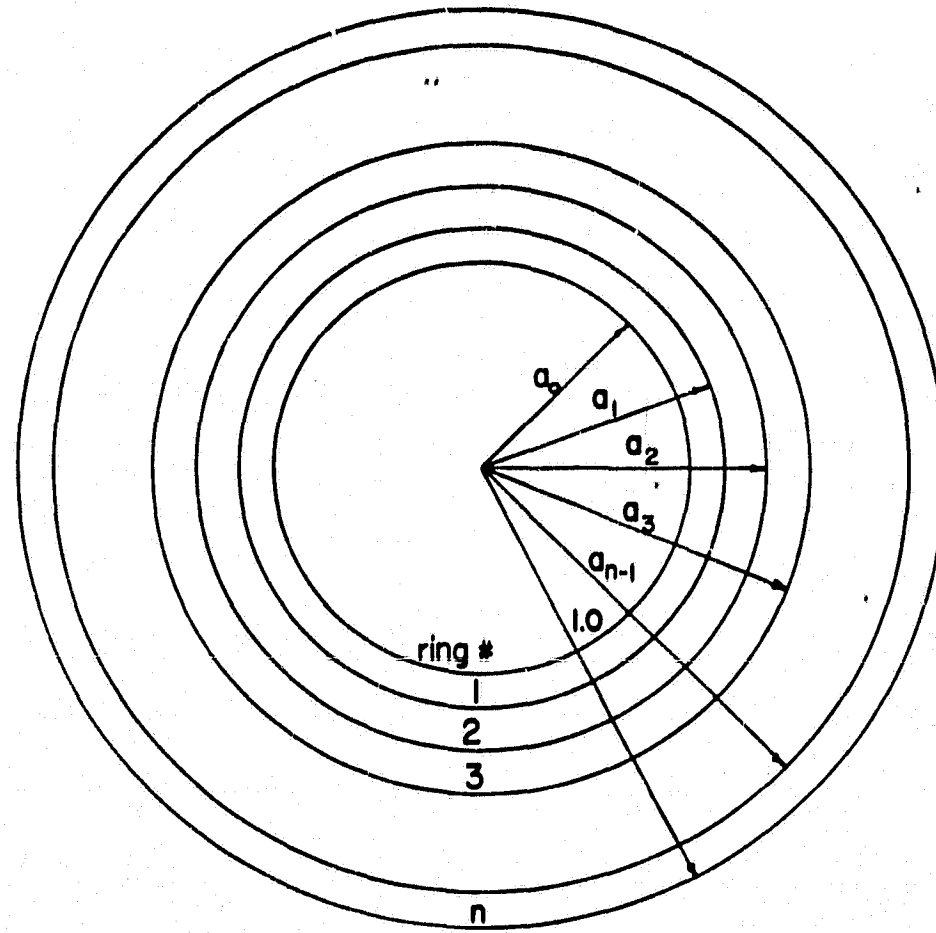


Figure II.3

Multiring Rotor Model. All rings are the same thickness
and may be either isotropic or orthotropic materials.

TABLE II.1 - LIST OF MATERIAL PROPERTIES¹

Material Name	E_x (10^6 psi)	E_θ (10^6 psi)	N	γ	$\nu_{r\theta}$	σ_{WTT} (10^3 psi)	σ_{WTC} (10^3 psi)	σ_{WRC} (10^3 psi)	σ_{WSH} (10^3 psi)
Segmented Iron	30.0	0.0	0.00	.286	.00	0.0	0.0	30.0	10.0
Celion 6000/Epoxy	1.3	19.4	3.72	.055	.35	264.0	162.0	24.8	12.0
Kevlar 49/Epoxy	0.8	5.0	3.72	.050	.34	200.0	40.0	20.0	8.7
Kevlar 29/Epoxy	0.7	11.0	3.71	.050	.34	200.0	40.0	20.0	8.7
E-Glass/Epoxy	1.3	5.7	2.09	.065	.30	160.0	90.0	6.0	12.0
901-S-Glass/Epoxy	1.3	6.3	2.20	.066	.30	219.0	120.0	6.0	12.0
S2-S-Glass/Epoxy	1.3	6.3	2.20	.066	.30	180.0	110.0	6.0	12.0
GY-70 (Graphite)/Epoxy	1.2	40.0	5.77	.060	.25	85.0	75.0	6.0	20.0
A-S (Graphite)/Epoxy	1.3	18.5	8.77	.055	.25	210.0	170.0	9.0	20.0
HTS (Graphite)/Epoxy	1.3	25.0	4.39	.056	.21	215.0	155.0	13.0	20.0
Boron/Epoxy	2.7	30.0	3.33	.072	.21	230.0	360.0	9.1	20.0
1SN1-400M Steel	30.0	30.0	1.00	.289	.26	260.0	260.0	260.0	130.0
1SN1-300N Steel	30.0	30.0	1.00	.289	.30	200.0	200.0	200.0	100.0
4340 Steel	30.0	30.0	1.00	.288	.32	130.0	130.0	130.0	65.0
1040 Steel	30.0	30.0	1.00	.288	.32	36.0	36.0	36.0	18.0
1020 Steel	30.0	30.0	1.00	.283	.30	25.0	25.0	25.0	12.0
2024-T85I Al	10.0	10.0	1.00	.283	.33	35.0	35.0	35.0	17.0
Iron (Mag Soft)	12.0	12.0	1.00	.283	.33	15.0	15.0	15.0	7.0

1 Nomenclature for Table II.1

E_x = radial (cross fiber) modulus of elasticity (10^6 psi)	σ_{WTT} = working stress in the tangential direction (10^3 psi)
E_θ = circumferential (along fiber) modulus of elasticity	σ_{WTC} = working stress in the tangential direction (10^3 psi) under compressive conditions
N = degree of orthotropism, $\sqrt{E_\theta/E_x}$	σ_{WRT} = working stress in the radial direction (10^3 psi) under tensile conditions
γ = weight density	σ_{WRC} = working stress in the radial direction (10^3 psi) under compressive conditions
$\nu_{r\theta}$ = Poisson's ratio of contraction in the radial direction due to extension in the tangential direction	σ_{WSH} = working stress under shear (10^3 psi)

Note: $\nu_{r\theta} = N \gamma r$

1. Rotation of the ring at constant angular velocity.
2. Interaction with adjoining rings due to rotational expansion.
3. Interference assembly of the rings.
4. Residual stresses due to curing.
5. Angular acceleration of the entire assembly.

The stress distribution for the entire flywheel is the summation of the above 5 stresses for each flywheel ring.

Of the 5 stress distributions given above, no. 3, interference assembly, is under the direct control of the designer. It can therefore be stated that it is the goal of the designer to choose an interference pressure set which will maximize the flywheel stored energy per unit weight (termed SED).

B. Interference Stresses

It will be instructive at this point to consider the hypothetical example of how interference stresses interact with rotational stresses in a simple 2 ring "pierced disk" rotor.

Shown in Figure II.4 is the stress distribution which occurs when 2 rings of the same material are interference assembled (no rotation). When the interference stress distribution is added to (i.e., superposed on) the rotational stress distribution the net result is as shown in Figure II.5. In Figure II.5 the stresses have been made nondimensional by the factor:

$$\rho_1 w^2 b^2 \text{ (units are psi)}$$

where:

ρ_1 = mass density for the first ring of the assembly (value is weight density in lb/in^3 divided by $g = 386 \text{ in/sec}^2$)

w = rotational speed (rad/sec)

b = outer radius of the flywheel(inches)

ORIGINAL PAGE IS
OF POOR QUALITY

INTERFERENCE ASSEMBLY

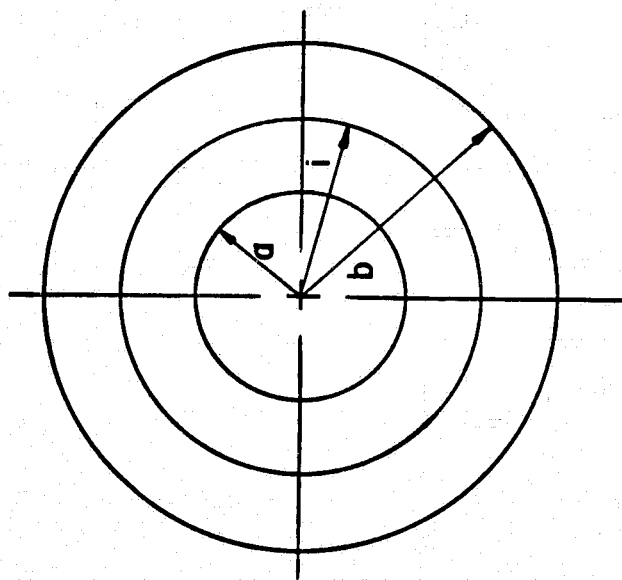
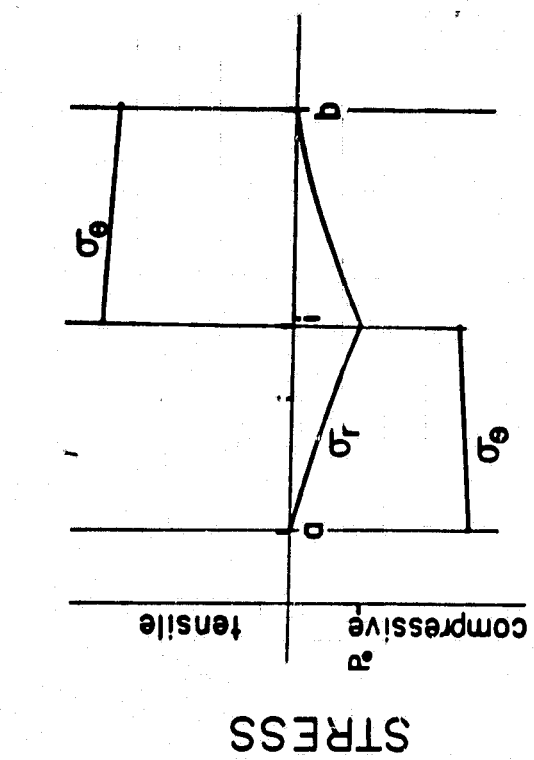


Figure II.4

Interference Stresses in a 2 Ring Rotor

STRESS VS. RADIUS

2 RING

ORIGINAL PAGE IS
OF POOR QUALITY

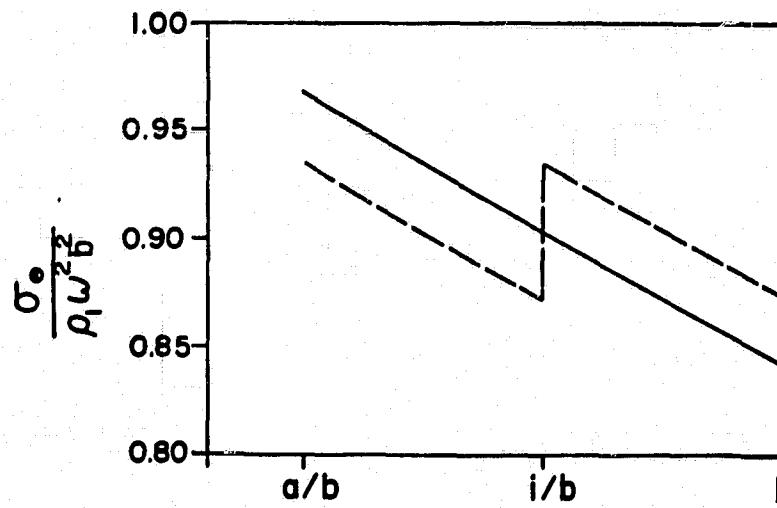
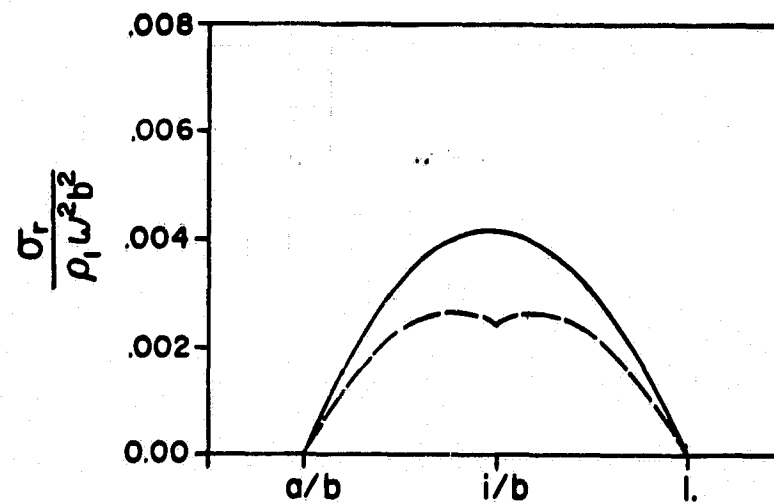


Figure II.5

Rotational Stresses in a 2 ring rotor. The dotted line shows the effect of interference assembly.

The solid line shown in each of the plots in Figure II.5 represents the stress distribution which occurs when the 2 rings are spun without any interference assembly present. The dotted lines show the stress distribution when the 2 rings are interference assembled and then spun. Has interference assembly actually helped? The answer is yes, because the largest value of nondimensional stress limits performance, and this value has been reduced when interference is applied between the rings. Consider the lower plot in Figure II.5. If the working tangential stress of the material, σ_θ , is constant, then the limiting value of $\sigma_\theta/\rho_1 w^2 b^2$ is = 0.97, with no interference present, and 0.94 with interference present. For a fixed value of b and σ_θ it is clear the interference assembled flywheel has a larger w . Since flywheels are characterized by the amount of kinetic energy per unit weight they achieve, the interference assembled flywheel will have a larger SED compared to a noninterference assembled one. Why? Because the flywheel is always limited by its rotational stresses and for a given σ_θ the interference assembled flywheel can rotate faster, and thus have a larger kinetic energy for the same flywheel weight.

C. Constraints

There are two principal constraints which limit the performance of the GSFC multiring flywheel. These are:

1. The flywheel must not fail.
2. The flywheel must not exceed a user specified displacement at the inner radius (to control the rotor/stator air gap).

The failure constraint is discussed in detail in Appendix 2. FLYANS allows the user to choose between the following 3 failure criterion:

1. modified TSAI-HILL
2. maximum STRESS
3. maximum STRAIN

and FLYANS will then return the limiting value of $\rho_1 w^2 b^2$ for the user selected geometry and materials. Extensive use of the FLYANS program by Dr. Kirk has shown that the TSAI-HILL failure criterion is generally the most conservative and it was therefore used for all work on this project. It should be noted that a prediction of flywheel performance based on one of the above failure theories is a prediction for the maximum or "burst" performance of the rotor.

The second constraint is on air gap growth and the FLYANS code applies this in addition to the failure criterion. Either a failure criterion or "inner radius displacement" always limits multiring rotor performance.

What about interference? Interference does not limit performance; it enhances it. FLYANS analyzes a user specified design assuming no interference and then asks if the user wishes to apply interference. If the user elects to apply interference, he is asked to either input the ring to ring interference pressure he desires or to permit the program to use its own algorithm to choose an interference pressure set. The interference pressure selection algorithm is documented in Appendix 1 and details may be found there. If the program selects the interference pressure set then the user must specify the maximum allowable radial interference (i.e., % INTERFERENCE = radial mismatch between 2 rings divided by the nominal radius of the rings). Typically 0.2 to 0.5% interference is used. The FLYANS code will then compute the "best" pressure set and will return the new SED and $\rho_1 w^2 b^2$ values. Typically the SED will increase 20% to 200% over the identical design without any interference. Finally, the FLYANS code returns the partial assembly pressures for each of the

rings. Rings are always added from the inside out, so knowing the partial assembly pressures and ring thickness, it is straightforward to calculate the assembly forces (this is exactly what FLYSIZE does).

D. Summary

The FLYANS code will analyze multiring flywheels including the presence of an iron inner ring. The required input parameters are summarized in Table II.2 and typical output parameters are shown in Table II.3. The code will select an interference pressure set which maximizes the specific energy density (SED) of the multiring rotor. When this code was applied to two 1600 Wh multiring flywheel designs for this project the SED went from 25 Wh/lb to 41 Wh/lb in one case, and from 19 to 42 Wh/lb in a second case. The detailed output for these two runs is presented in Section 2.3.

2.2. FLYSIZE - Flywheel Sizing Computer Code

A second computer code has been developed for this project and the program listing is shown in Appendix 3. The purpose of this code is to take output results of FLYANS and combine them with the specifics of a user design, in order to produce detailed information which can then be used to generate engineering drawings for each of the flywheel rings. The user supplied inputs are:

1. The number of rings in the wheel*
2. The outside radius of the wheel, (inches)
3. The inside radius ratios for each of the rings*
4. The calculated or specified % interference for each interface*
5. The user specified maximum inner displacement ratio*, (nondimensional, equal to actual displacement divided by flywheel outer radius)
6. The required stored energy, (Wh)

Table II.2

FLYANS INPUT PARAMETERS

1. Number of rings in the flywheel, (dimensionless)
2. Inner radius ratios of each ring, (dimensionless)
3. Flywheel materials, each specified by
 - a. Name and identification number
 - b. Orthotropic ratio, $\sqrt{E_\theta/E_r}$, where
 - E_θ = tangential direction modulus of elasticity, (psi)
 - E_r = radial direction modulus of elasticity, (psi)
 - c. Tangential modulus of elasticity, (psi)
 - d. Weight density, (lbs/in^3)
 - e. Working stress in tension in the tangential direction, (psi)
 - f. Working stress in compression in the tangential direction, (psi)
 - g. Working stress in tension in the radial direction, (psi)
 - h. Working stress in compression in the radial direction, (psi)
 - i. Shear working stress, (psi)
 - j. Material cost, (\$/lb)
 - k. Residual stress parameter, (dimensionless)
4. What material each ring is made from (chosen from the user supplied database in item 3).
5. The maximum inner radius displacement ratio (i.e. gap growth divided by flywheel outer radius).
6. The maximum permissible ring interference %.

Table II.3

FLYANS OUTPUT

1. Specific energy density (SED), (Wh/lb).
2. Volumetric energy density (VED), (Wh/ft³).
3. Limiting value of $\rho_1 \omega^2 b^2$, (psi).
4. Which ring limits performance.
5. Interference pressures at each ring interface
 - a. after complete assembly.
 - b. to assemble.

7. The limiting value of $\rho_1 w^3 b^2$, (psi)*
8. The calculated SED, (Wh/lb)*
9. The calculated VED, volumetric energy density, (Wh/ft³)*
10. The partial assembly pressures, (ksi)*
11. The weight densities for each of the flywheel rings*, (lb/in³)

The FLYSIZE code will then compute the following design values.

1. The inside and outside radius for each flywheel ring, (inches)
2. The radial mismatch at each ring interface, (inches)
3. The flywheel thickness, (inches)
4. The weight of each ring, (lbs)
5. The minimum conical taper which must be present on each ring to allow interference assembly, (degrees)
6. The maximum flywheel rotational speed, (rpm)
7. The total flywheel weight, (lbs)
8. The maximum inner radius displacement (air gap growth), (inches)
9. The partial assembly forces (assuming a 1-1/2° ring taper and 0.1 interface coefficient of friction), (lbs)

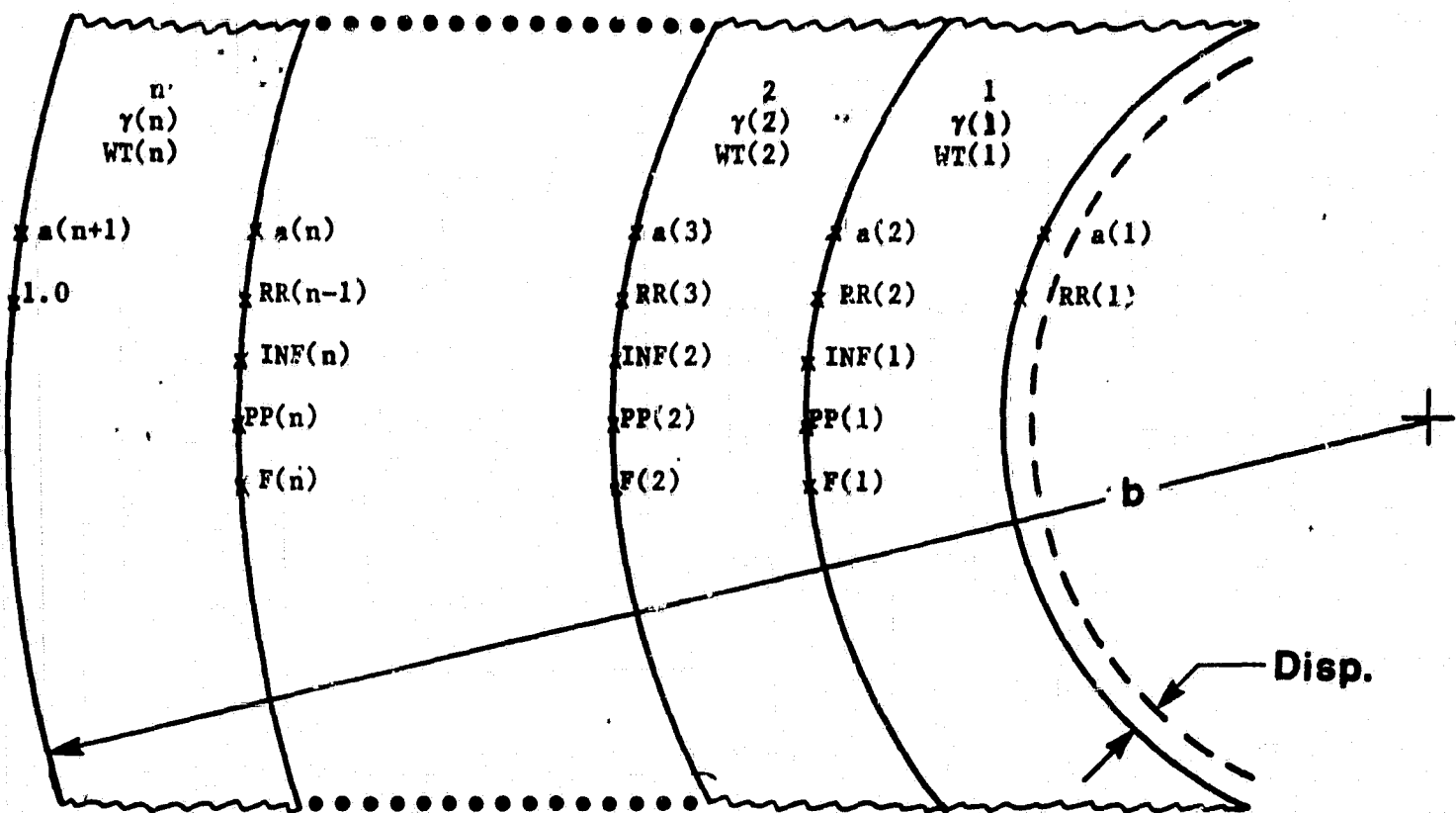
The calculation formulas which are used to generate the above outputs are explained in detail in Appendix 4. Shown in Table II.4 is a summary of the design parameters which are utilized or calculated by the FLYSIZE code. The symbols shown in this figure are consistent with those used in the FLYSIZE program (listed in Appendix 3) and will permit an easier understanding of FLYSIZE logic.

* Taken directly from the FLYANS run.

ORIGINAL PAGE IS
OF POOR QUALITY

Table II,4

FLYSIZE MULTIRING ROTOR PARAMETERS



SYMBOL TABLE

<u>SYMBOL</u>	<u>INPUT/OUTPUT</u>	<u>MEANING</u>
1, 2, ---n	I	Identification
$\gamma(1), \gamma(2) --- \gamma(n)$	I	Weight density
$WT(1), WT(2) --- WT(n)$	O	Weight
$a(1), a(2) --- a(n+1)$	O	Radius
$RR(1), RR(2) --- RR(n)$	I	Inside radius ratio
$INF(1), INF(2) --- INF(n)$	I	% Interference
$PP(1), PP(2) --- PP(n)$	I	Partial assy. pressure
$F(1), F(2) --- F(n)$	O	Partial assy. forces
b	I	Outer radius
DISP	I	Inner ring disp.

**The FLYSIZE code has been applied to two specific designs for this project
and the results will be presented in section 2.3.**

3. Results

Both the FLYANS and FLYSIZE computer codes were used to design two rotors for this project, and the design drawings for each are presented in Appendix 7. These two designs are identified as NASA-12 and NASA-20, and they represent the results which were obtained from running the FLYANS code over 40 times.

Shown in Table II.5 through II.8 are the FLYANS output for the NASA-12 and NASA-20 designs. The results shown in these 4 tables are summarized below.

1. Table II.5 shows the results for a 6 ring rotor with ID/OD = 0.5. This design is labeled NASA-12. The design is unoptimized and has no interference between rings. The SED (specific energy density) is 25.0 Wh/lb and this number includes the presence of an iron inner ring. Displacement of the inner radius (which is equal to the air gap growth due to rotation) is less than .006 times the outer radius of the flywheel.
2. Table II.6 shows the results for the NASA-12 design with interference between rings. The SED has been improved to 41.0 Wh/lb by the effect of prestressing (through interference). The inner radius displacement is still less than .006 times the outer radius of the flywheel.
3. Table II.7 shows the results for a 6 ring rotor with ID/OD = 0.4. This design is labeled NASA-20. The design is unoptimized and has no interference between rings. The SED is 18.5 Wh/lb and the inner radius displacement is less than .004 times the outer radius of the flywheel.
4. Table II.8 shows the results for the NASA-20 design with interference between rings. The SED has been improved to 41.9 Wh/lb and the inner

OPTIONAL FORM
OF FLOOR CRITICAL

RIN IDENTIFICATION = NASP-12
 RIN ON 123083 AT TIME = 172217
 SECOND OPTIMIZED CONFIGURATION
 MODIFIED TSAI-HILL FAILURE CRITERION

RING INDEX (J)	RATIO (ET/ER)	EJ/E1 RHOJ/RHO1	POISSON'S SONS STRESSES RATIO (KSI)	WORKING STRESSES (KSI)	INTERFERENCE PRESSURE (KSI) T	INTERFERING (DELTA EPSLN)	MATERIAL NAME AND COST	TESTVAL- PARAMETER
1	.560C	.100-UJS	.160+U01	* 100+C01	.000	1.66+U01TC 1.66+U01RT 1.66+U01RC 1.66+U01SH	6.21+005 -7.75+000	
						1.75+001 1.68+002		
2	.520L	.372+U01	.647+U12	* 192+C0C	* 350	2.64+U02TC 2.64+U02RT 2.64+U02RC 2.64+U02SH	1.02+002 2.29+000	
						2.48+U01TC 2.48+U01RT 2.48+U01RC 2.48+U01SH		
3	.600C	.372+U01	.647+U12	* 192+C0C	* 350	2.66+U02TC 2.66+U02RT 2.66+U02RC 2.66+U02SH	.94+001 2.20+001	
						2.80+U01TC 2.80+U01RT 2.80+U01RC 2.80+U01SH		
4	.760L	.372+U01	.647+U12	* 192+C0C	* 350	2.64+U02TC 2.64+U02RT 2.64+U02RC 2.64+U02SH	.90+001 2.16+001	
						2.80+U01TC 2.80+U01RT 2.80+U01RC 2.80+U01SH		
5	.850C	.372+U11	.647+U12	* 192+C0C	* 350	2.64+U02TC 2.64+U02RT 2.64+U02RC 2.64+U02SH	.83+001 2.08+000	
						2.80+U01TC 2.80+U01RT 2.80+U01RC 2.80+U01SH		
6	.910C	.372+U01	.647+U12	* 192+C0C	* 350	2.64+U02TC 2.64+U02RT 2.64+U02RC 2.64+U02SH	.73+001 1.98+000	
						2.80+U01TC 2.80+U01RT 2.80+U01RC 2.80+U01SH		
7								

Table II.5

ORIGINAL PAGE IS
OF POOR QUALITY

ETHETA1	= 3.0000-005 PSI
GFM1	= 2.8600-003 LBIN/IN ⁻³
INNER RAD DISP LIMIT	= 6.0000-003 X OUTER RADIUS
EX1 MOMENT/SLEPT VOL	= 1.0000-000 LBIN/IN ⁻²
SPEC ENERGY DENSITY	= 2.6986-001 WATT-HF/LB OR 1.9827-002 KJOULE/KG
ENERGY/UNIT PAT COST	= 1.1416-000 WATT-HF/DOLLAR
VOL ENERGY DENSITY	= 1.9844-003 WATT-HF/FT ⁻³ OR 2.5228-002 PEGA-J/M ⁻³
SPEC POWER DENSITY	= 2.0192-000 KWATT/LB OR 4.4516-000 KWATT/KG X (OUTER RADIUS IN METERS) ⁻¹
FLYWHEEL REV/MIN	= 7844.1 X (OUTER RADIUS IN METERS) ⁻¹
THE ENERGY DENSITY OF THE FLYWHEEL WAS LIMITED BY RING NUMBER 4 (RHO1)(OMEGA X B) ⁻² = 7.7484-005 PSI	

Table III.5 - Continued

ORIGINAL PAGE IS
OF POOR QUALITY

RLW IDENTIFICATION =NASA-12
RLW ON 123083 AT TIME = 172230

*****MAXIMIZED CONFIGURATION*****

MODIFIED TSAI-HILL FAILURE CRITERION

RING INFER. EJ/E1	RHO/J/RHO1 HEAT (EJ/ER)	POLY- SOST RATIO (KSI)	WORKING STRESSES (KSI)	USED P (KSI)	INTERFERENCE PRESSURE (KSI)	INTERFERING (DELTA EPSLN)	MATERIAL NAME AND COST	RESIDUAL STRESS PARAMETER .0U
1 .5500	.100-005	.100+C01	.000 1.00-0.00111 3.00+0.00144	1.02-0.04 -1.27+0.01			SEGMENTED IRON 5.00-001 \$/LBM	
2 .5500	.372+C01	.647+0.12	.192+0.0C .350 3.00+0.00277 7.00+0.00037	1.75-0.03 1.80-0.01			CELCION 6000/EPoxy 2.5C+C01 \$/LBM	-2.00-003
3 .6500	.372+C01	.647+0.12	.192+0.0C .350 3.00+0.00277 7.00+0.00037	1.48+0.02 1.52-0.03 -1.27+0.01	.00		CELCION 6000/EPoxy 2.5C+C01 \$/LBM	-2.00-003
4 .7500	.372+C01	.647+0.12	.192+0.0C .350 3.00+0.00277 7.00+0.00037	1.34+0.02 1.54+0.00 1.90-0.04 3.45-0.01			CELCION 6000/EPoxy 2.5C+C01 \$/LBM	-2.00-003
5 .8500	.372+C01	.647+0.12	.192+0.0C .350 3.00+0.00277 7.00+0.00037	1.58+0.02 1.54+0.00 1.90-0.04 3.45-0.01			CELCION 6000/EPoxy 2.5C+C01 \$/LBM	-2.00-003
6 .9500	.372+C01	.647+0.12	.192+0.0C .350 3.00+0.00277 7.00+0.00037	1.80+0.02 1.93+0.00 1.96+0.00 1.59+0.00			CELCION 6000/EPoxy 2.5C+C01 \$/LBM	-2.00-003

Table II.6

ORIGINAL PAGE IS
OF POOR QUALITY

THEMA1 = 3.0000-005 PSI
GAMMA1 = 2.8600-001 LBIN/IN⁻¹
INNER RAD DISP LIMIT = 6.0000-003 X OLTER RADIUS
RING INTERFER LIMIT = 3.0000-003 X MEAN RADIUS
X1 MOMENT/SLEPT VOL = 1.0000+000 LBIN/IN⁻²
SPEC ENERGY DENSITY = 4.1043+001 WATT-HF/LB OR 3.2573+072 KJ OULE/KG
ENERGY/UNIT PAT COST = 1.8752+000 WATT-HF/DOLLAR
VCL ENERGY DENSITY = 3.2602+003 WATT-HF/FT⁻³ OR 4.1446+002 MEGA-J/M³
SPEC POWER DENSITY = 2.5882+000 KWATT/LB OR 5.7059+000 KWATT/KG X (OUTER RADIUS IN METERS)⁻¹
FLYWHEEL REV/MIN = 10054.2 X (OUTER RADIUS IN METERS)⁻¹
THE ENERGY DENSITY OF THE FLYWHEEL WAS LIMITED BY RING NUMBER 5
(5M01)(GMEGA X B)**2= 1.2730+006 PSI
RING ADDED IS # 3 ASSY. PRESSURE = -3.927 KSI
RING ADDED IS # 4 ASSY. PRESSURE = -4.571 KSI
RING ADDED IS # 5 ASSY. PRESSURE = -4.455 KSI
RING ADDED IS # 6 ASSY. PRESSURE = -4.211 KSI

Table III.6 - Continued

ORIGINAL PAGE IS
OF POOR QUALITY

ALL IDENTIFICATION =NASD-20
RLM ON 12CE33 AT TIME = 172648

UNPUBLISHED COMMISSIONS

UNCLASSIFIED TSAIL-HILL-FALL 1988 CRIMES AGAINST CHILDREN

Table II.7

Table II.7 - Continued

ORIGINAL PAGE IS
OF POOR QUALITY.

SHETAT	=	3.00000-005 PSI
GAMMA1	=	2.86000-001 LBM/IN ⁻³
INNER RAD DISP LIMIT	=	4.00000-003 X OUTER RADIUS
EXT MOMENT/SLEPT VOL	=	1.00000-000 LB.F/IN ⁻²
SPEC ENERGY DENSITY	=	1.9483-001 WATT-HR/LB OR 1.4668-002 KJOUULE/KG
ENERGY/UNIT PAT COST	=	8.1427-001 WATT-HR/DOLLAR
VCL ENERGY DENSITY	=	1.5967-003 WATT-HR/FT ⁻³ OR 2.0299-002 MEGA-J/M ⁻³
-1-		
SPEC POWER DENSITY	=	1.6524-000 KWATT/LB OR 3.6430-000 KWATT/KG X (OUTER RADIUS IN METERS)
FLTWHEEL REV/MIN	=	6981.4 X (OUTER RADIUS IN METERS)
-1-		
THE ENERGY DENSITY OF THE FLYWHEEL WAS LIMITED BY RING NUMBER 4		
(RHO1)(OMEGA X B)**2 = 6.1378-005 PSI		

RIN IDENTIFICATION =MAS A-20
RLY ON 123-53 AT TIME = 172705
*****MAXIMIZED COMUNICATIONS*****

UNCLASSIFIED TS/SI-HULL FAILURE CRITERION

RING INNER DIA (J)	SHRT (ET/ER)	RHOJ/RH01	P015'S WORKING RATIO (KSI)	STRESS USED (KSI)	IN PREFERENCE TOLERATING (KSI)	IN PREFERENCE RADIAL (DELTA EPSLM)	MATERIAL NAME	RESIDUAL PARAMETER
1 .400	.103-0.05	.100+0.01	.000	1.00+0.011	1.06-0.005	-1.11+0.01	SEGMENTED IRON	.00
2 .4276	.372+0.01	.647+0.12	.192+0.0C	2.64+0.0211	2.64+0.021C	2.68+0.021RC	CELICN 6000/EPOXY	-2.00-0.03
3 .500	.372+0.01	.647+0.12	.192+0.0C	2.64+0.0211	2.64+0.021C	2.68+0.021RC	CELICN 6000/EPOXY	-2.00-0.03
4 .6356	.372+0.01	.647+0.12	.192+0.0C	2.64+0.0211	2.64+0.021C	2.68+0.021RC	CELICN 6000/EPOXY	-2.00-0.03
5 .900	.372+0.01	.647+0.12	.192+0.0C	2.64+0.0211	2.64+0.021C	2.68+0.021RC	CELICN 6000/EPOXY	-2.00-0.03
6 .9000	.372+0.01	.647+0.12	.192+0.0C	2.64+0.0211	2.64+0.021C	2.68+0.021RC	CELICN 6000/EPOXY	-2.00-0.03

Table III.8.

**ORIGINAL PAGE IS
OF POOR QUALITY**

ORIGINAL PAGE IS
OF POOR QUALITY

ELPHETA1 = $3.000J-605$ PSI
GPM/H1 = $2.860J-001$ LBH/IN \cdot 3
INNER RAD DISP LIMIT = $4.0000J-003$ X OUTER RADIUS
RING INTERFER LIMIT = $5.0000J-005$ X MEAN RADIUS
EXT MOMENT/SWEPT VOL = $1.0000J+000$ LBF/IN \cdot 2
SPEC ENERGY DENSITY = $4.1886J+001$ WATT-HR/LB OR $3.3238J+002$ KJOUULE/KG
ENERGY/UNIT WT COST = $1.8451J+000$ WATT-HR/DOLLAR
VCL ENERGY CENSITY = $3.6181J+003$ WATT-HR/FT \cdot 3 OR $4.3996J+002$ MEGA-J/M \cdot 3
SPEC POWER DENSITY = $2.4874J+000$ KWATT/LB OR $5.4838J+000$ KWATT/KG X (OUTER RADIUS IN METERS) \cdot
FLYWHEEL REV/MIN = $1050J.2$ X (OUTER RADIUS IN METERS) \cdot
THE ENERGY DENSITY OF THE FLYWHEEL WAS LIMITED BY RING NUMBER
 $(6J+0) (OMEGA X B) \cdot 2 = 1.3903J+006$ PSI
RING ADDED IS # 3 ASSY. PRESSURE = -8.456 KSI
RING ADDED IS # 4 ASSY. PRESSURE = -9.939 KSI
RING ADDED IS # 5 ASSY. PRESSURE = -7.572 KSI
RING ADDED IS # 6 ASSY. PRESSURE = -7.070 KSI

Table II.8 - Continued

radius displacement is still less than .004 times the outer radius of the flywheel.

One of the additional, and very informative, outputs from the FLYANS code are plots of residual and rotational stresses vs. radius ratio for each design being considered. These plots are shown in Appendix 6 for the following stresses:

1. Radial residual stress vs. radius ratio
2. Tangential residual stress vs. radius ratio
3. Radial stress (at max. speed) vs. radius ratio
4. Tangential stress (at max. speed) vs. radius ratio

and have been obtained for both the unoptimized and optimized NASA-12 and NASA-20 designs.

In order to apply the FLYANS results to a specific design it is necessary to specify the following parameters.

1. Total stored energy in Wh, a value of 1600 Wh is being used for this project.
2. The outer radius of the flywheel in inches, a value of 10 is being used in this project.

Once these values are specified, the FLYSIZE code can be run using the FLYANS output for each design being considered. When FLYSIZE is applied to the NASA-12 and NASA-20 designs the results are as shown in Tables II.9 through II.12. Based upon the results shown in these tables it is very convenient for the designer to choose the dimensions of each ring of the flywheel. The method used to select the ring diameters and tolerances is included in Appendix 5, and the detailed drawings for NASA-12 optimized and NASA-20 optimized are shown in Appendix 7 of this report.

NASA-12 UNOPTIMIZED 6 RING CELION 6000/EPOXY FLYWHEEL
RUN ON 12-26-1983 AT 11:06:55

RING NO. (--)	IN. R. RATIO (--)	INSIDE RADIUS (IN)	OUTSIDE RADIUS (IN)	RADIAL MISMATCH (IN)	% INT (10 ⁻³)	RING WEIGHT (LBS)	MIN. TAPER (DEG)
1	0.500	5.000	5.200			8.1	
2	0.520	5.200	6.000	0.000 2- 3	0.0 2- 3	6.9	0.0
3	0.600	6.000	7.000	0.000 3- 4	0.0 3- 4	10.0	0.0
4	0.700	7.000	8.000	0.000 4- 5	0.0 4- 5	11.5	0.0
5	0.800	8.000	9.000	0.000 5- 6	0.0 5- 6	13.0	0.0
6	0.900	9.000	10.000			14.6	
RING THICKNESS (INCHES).....				4.4			
RPM (ROT/MIN).....				30,880			
SED (WH/LB).....				25.0			
VED (WH/FT ³).....				1,984.4			
TOTAL STORED ENERGY (WH).....				1,600			
TOTAL FLYWHEEL WEIGHT (LBS) ...				64.0			
MAX. INNER RAD. DISP. (INCHES). 0.060							

PARTIAL ASSEMBLY		PRESSURES	FORCES
RING	3 ADDED TO PREVIOUS RINGS.....	0.0 KPSI	0.0 10 ³ LBS
RING	4 ADDED TO PREVIOUS RINGS.....	0.0 KPSI	0.0 10 ³ LBS
RING	5 ADDED TO PREVIOUS RINGS.....	0.0 KPSI	0.0 10 ³ LBS
RING	6 ADDED TO PREVIOUS RINGS.....	0.0 KPSI	0.0 10 ³ LBS

RING (--)	WEIGHT DENSITY (LB/IN ³)	RING (--)	WEIGHT DENSITY (LB/IN ³)
1	0.286	6	0.055
2	0.055		
3	0.055		
4	0.055		
5	0.055		

DATA FOR THIS RUN IS IN FILE B:RUN-12.DAT

Table II.9

ORIGINAL PAGE IS
OF POOR QUALITY

NASA-12 OPTIMIZED 6 RING CELION/EPOXY FLYWHEEL
RUN ON 12-26-1983 AT 11:07:40

RING NO. (--)	IN. R. RATIO (--)	INSIDE RADIUS (IN)	OUTSIDE RADIUS (IN)	RADIAL MISMATCH (IN)	% INT (10 ⁻³)	RING WEIGHT (LBS)	MIN. TAPER (DEG)
1	0.500	5.000	5.200			4.9	
2	0.520	5.200	6.016	0.016	2-3	3.0	2-3
3	0.600	6.000	7.018	0.018	3-4	3.0	3-4
4	0.700	7.000	8.021	0.021	4-5	3.0	4-5
5	0.800	8.000	9.024	0.024	5-6	3.0	5-6
6	0.900	9.000	10.000			9.9	
RING THICKNESS (INCHES)				2.7			
RPM (ROT/MIN)				39,581			
SED (WH/LB)				41.0			
VED (WH/FT ³)				3,260.2			
TOTAL STORED ENERGY (WH)				1,600			
TOTAL FLYWHEEL WEIGHT (LBS) ...				39.0			
MAX. INNER RAD. DISP. (INCHES) .				0.060			

PARTIAL ASSEMBLY		PRESSESSES	FORCES
RING 3	ADDED TO PREVIOUS RINGS.....	3.9 KPSI	43.7 10 ³ LBS
RING 4	ADDED TO PREVIOUS RINGS.....	4.5 KPSI	58.7 10 ³ LBS
RING 5	ADDED TO PREVIOUS RINGS.....	4.5 KPSI	66.7 10 ³ LBS
RING 6	ADDED TO PREVIOUS RINGS.....	4.2 KPSI	72.1 10 ³ LBS

RING (--)	WEIGHT DENSITY (LB/IN ³)	RING (--)	WEIGHT DENSITY (LB/IN ³)
1	0.286	6	0.056
2	0.055		
3	0.055		
4	0.055		
5	0.055		

DATA FOR THIS RUN IS IN FILE 3:RUN-12-0.DAT

Table II.10

ORIGINAL PAGE IS
OF POOR QUALITY

NASA-20 UNOPTIMIZED 6 RING CELION/EPOXY 6 RING FLYWHEEL
RUN ON 12-24-1983 AT 09:53:06

RING NO. (--)	IN. R. RATIO (--)	INSIDE RADIUS (IN)	OUTSIDE RADIUS (IN)	RADIAL MISMATCH (IN)	% INT (10 ⁻³)	RING WEIGHT (LBS)	MIN. TAPER (DEG)
1	0.400	4.000	4.200			8.1	
2	0.420	4.200	5.000	0.000 2- 3	0.0 2- 3	7.0	0.0
3	0.500	5.000	6.500	0.000 3- 4	0.0 3- 4	16.4	0.0
4	0.650	6.500	8.000	0.000 4- 5	0.0 4- 5	20.7	0.0
5	0.800	8.000	9.000	0.000 5- 6	0.0 5- 6	16.2	0.0
6	0.900	9.000	10.000			18.1	

ORIGINAL PAGE IS
OF POOR QUALITY

RING THICKNESS (INCHES) 8.5
RPM (ROT/MIN) 27,484
SED (WH/LB) 18.5
VED (WH/FT²) 1,596.7
TOTAL STORED ENERGY (WH) 1,600
TOTAL FLYWHEEL WEIGHT (LBS) ... 86.6
MAX. INNER RAD. DISP. (INCHES). 0.040

RING	PARTIAL ASSEMBLY	PRESURES	FORCES
RING 3	ADDED TO PREVIOUS RINGS.....	0.0 KPSI	0.0 10 ³ LBS
RING 4	ADDED TO PREVIOUS RINGS.....	0.0 KPSI	0.0 10 ³ LBS
RING 5	ADDED TO PREVIOUS RINGS.....	0.0 KPSI	0.0 10 ³ LBS
RING 6	ADDED TO PREVIOUS RINGS.....	0.0 KPSI	0.0 10 ³ LBS

RING (--)	WEIGHT DENSITY (LB/IN ³)	RING (--)	WEIGHT DENSITY (LB/IN ³)
1	0.286	6	0.055
2	0.055		
3	0.055		
4	0.055		
5	0.055		

DATA FOR THIS RUN IS IN FILE B:RUN-20.DAT

Table II.11

NASA-20 OPTIMIZED 6 RING CELION/EPOXY FLYWHEEL
RUN ON 12-26-1983 AT 09:02:16

RING NO. (--)	IN. R. RATIO (--)	INSIDE RADIUS (IN)	OUTSIDE RADIUS (IN)	RADIAL MISMATCH (IN)	% INT (10 ⁻³)	RING WEIGHT (LBS)	MIN. TAPER (DEG)
1	0.400	4.000	4.200			3.6	
2	0.420	4.200	5.025	0.025 2- 3	5.0 2- 3	3.1	0.6
3	0.500	5.000	6.533	0.033 3- 4	5.0 3- 4	7.2	0.8
4	0.650	6.500	8.040	0.040 4- 5	5.0 4- 5	9.1	0.9
5	0.800	8.000	9.045	0.045 5- 6	5.0 5- 6	7.1	1.1
6	0.900	9.000	10.000			8.0	
RING THICKNESS (INCHES).....				2.4			
RPM (ROT/MIN).....				41,372			
SED (WH/LB).....				41.9			
VED (WH/FT ³).....				3,618.1			
TOTAL STORED ENERGY (WH).....				1,600			
TOTAL FLYWHEEL WEIGHT (LBS) ...				38.2			
MAX. INNER RAD. DISP. (INCHES), 0.040							

PARTIAL ASSEMBLY		PRESSURES	FORCES
RING (--)	ADDED TO PREVIOUS RINGS.....	KPSI	10 ³ LBS
RING 3	ADDED TO PREVIOUS RINGS.....	8.5 KPSI	81.5 10 ³ LBS
RING 4	ADDED TO PREVIOUS RINGS.....	9.9 KPSI	124.6 10 ³ LBS
RING 5	ADDED TO PREVIOUS RINGS.....	7.6 KPSI	116.8 10 ³ LBS
RING 6	ADDED TO PREVIOUS RINGS.....	7.1 KPSI	122.7 10 ³ LBS

RING (--)	WEIGHT DENSITY (LB/IN ³)	RING (--)	WEIGHT DENSITY (LB/IN ³)
1	0.286	6	0.055
3	0.055		
4	0.055		
5	0.055		

DATA FOR THIS RUN IS IN FILE B:RUN-20-D.DAT

Table II.12

ORIGINAL PAGE IS
OF POOR QUALITY

4. Discussion

For a given form factor (ID/OD) rotor there are 2 principal advantages of using multiring construction versus winding the rotor as one continuous ring.

These are:

1. The residual stresses due to fabrication are known to be smaller for smaller size rings.
2. The individual rings of a multiring design can be interference assembled. The condition will significantly improve performance and is much better than building in rotor prestress through controlled winding tension.

The main disadvantage of multiring construction is that each ring interference must be bonded together upon assembly. This binding must be sufficiently strong so that the interference radial stresses (due to rotation) will not cause the outer rings to separate from the inner ones. Since the required strength of the interface bond is always less than (or equal to) the transverse strength of the graphite/epoxy, the same epoxy used in ring fabrication will accomplish the task of bonding the rings together. It can be concluded that the advantages of multiring fabrication outweigh the disadvantages and that the multiring construction with interference assembly represents the best manufacturing method or the NASA-12 optimized and NASA-20 optimized designs.

The NASA-12 optimized design will produce 41.0 Wh/lb at its maximum rotational speed of 39,581 rpm. This design has an inside diameter of 10 inches an outside diameter of 20 inches, and an axial thickness of 2.7 inches. It will store 1600 Wh of energy when it is running at maximum speed, and its air gap growth will not exceed .060 inches at 39,581 rpm. The design has an iron inner ring weighing 4.9 lbs and the total weight of the flywheel is 39.0

lbs. There are 6 rings in this design and rings 2 through 6 are Celion 6000/EPOXY (filamentry wound composite). There is light interference (.3%) between all Celion 6000/EPOXY rings and the assembly forces to press the rings together do not exceed 75,000 lbs.

The NASA-20 optimized design will produce 41.9 Wh/lb at its maximum rotational speed of 41,372 rpm. This design has an inside diameter of 8 inches, an outside diameter of 20 inches, and an axial thickness of 2.4 inches. It will store 1600 Wh of energy when it is running at its maximum speed, and its air gap growth will not exceed .040 inches at 41,372 rpm. The design has an iron inner ring weighing 3.6 lbs and the total weight of the flywheel is 38.2 lbs. There are 6 rings in this design and rings 2 through 6 are Celion 6000/EPOXY. There is heavy interference (.5%) between all Celion 6000/EPOXY rings but the assembly forces to press the rings together do not exceed 125,000 lbs.

It was generally observed that to control growth of the air gap it is desirable to decrease the inside diameter of the rotor. To control the stresses which result from this action it is necessary to increase ring prestressing through an increase in % interference between rings. To illustrate this point, had the NASA-20 design been limited to 0.3% interference between rings, it would develop only 35.2 Wh/lb versus the 41.9 Wh/lb which it will develop with 0.5% interference between rings.

It must be emphasized that the design values presented for NASA-12 and NASA-20 are for the flywheel pushed to its limiting failure speed. If the flywheel is operated at .707 of this limiting speed the maximum flywheel stresses will be 1/2 their failure values and the SED will be 1/2 of its limiting value. If it is required that the usable stored energy be 1600 Wh and

the flywheel is assumed to cycle between .707 of its limiting speed and .25 of its limiting speed, then the calculated flywheel thickness must be increased, in both the NASA-12 and NASA-20 designs, by a factor of 2.3. Obviously, then, when a flywheel is said to store 1600 Wh, it could only deliver this amount of energy if:

1. The flywheel is cycled from its maximum rotational speed to zero speed
2. The flywheel did not fail at its maximum rotational speed.

Clearly, the final rotor design for a magnetically suspended flywheel must proceed with consideration for the speed range of the motor/generator and the iron ring weight requirements for the magnetic suspension and motor/generator magnetic paths. The FLYANS/FLYSIZE tools used in this project are the best way to revise the rotor design as other system components evolve.

5. References

1. Kirk, J. A., Studer, P. A., and Evans, H. E., "Mechanical Capacitor," NASA TND-8185, March 1976.
2. Kirk, J. A., "Flywheel Energy Storage - Part I, Basic Concepts," International Journal of Mechanical Sciences, Vol. 19, 1977, pp. 223-231.
3. Kirk, J. A., and Studer, P. A., "Flywheel Energy Storage - Part II, Magnetically Suspended Superflywheel," International Journal of Mechanical Sciences, Vol. 19, 1977, pp. 233-245.
4. Michaelis, T. D., Schlieben, E. W. and Scott, R. D., "Design Definition of a Mechanical Capacitor," Final Report on NASA/GSFC contract NAS5-23650, May 1977.
5. Kirk, J. A., "Mechanical Capacitor - the Best Rim," Final Report on NASA/GSFC order S-40224-B, November, 1977.
6. Kirk, J. A., and Huntington, R. A., "Energy Storage - an Interference Assembled Multiring Superflywheel," Proceedings of the 12th IECEC Conference, Washington, D.C., September 2, 1977, pp. 517-524.
7. Kirk, J. A., and Huntington, R. A., "Stress Analysis and Maximization of Energy Density for a Magnetically Suspended Flywheel," ASME paper 77-WA/DE-24.

ORIGINAL PAGE IS
OF POOR QUALITY

8. Kirk, J. A., and Huntington, R. A., "Stress Redistribution for the Multiring Flywheel," ASME paper 77-WA/DE-26.
9. Huntington, R. A., "Stress Analysis and Maximization of Performance for a Multiring Flywheel," M.S. Thesis, University of Maryland, Mechanical Engineering Department, Jan. 1978. Thesis advisor: J. A. Kirk.
10. Ashton, J. E., Halpin, J. C., and Petit, P. H., Primer on Composite Materials: Analysis, Technomic Publishing Co., Stamford, Conn., 1969.

III. FABRICATION/ASSEMBLY

A. Materials.

Two candidate graphite epoxy materials exist for this application. These materials are:

Fiber

Celanese Celion 6000* or 12,000

Union Carbide Thornel 300, WYP6 1/0

The fiber should be without twist and have a matrix compatible sizing.

Epoxy

Shell EPON 826* with Jeffamine Chemical Company D230 Curative

NARMCO 5213

* Recommended for this task.

B. Techniques

1. Fabrication

Residual transverse and/or circumferential stresses should be held to a minimum. Prestressing using fiber tension has not proven practical. Either precompression of thin rings (via interference assembly) or a flexible urethane resin appears at present to be the best approach. Urethane resin use would require further study and testing before a practical matrix could be specified.

A controlled environment, such as room temperature and a relative humidity less than 50%, are desirable during winding. These conditions control variations in material properties. In addition, to assure quality materials, the resin should be stored carefully according to the manufacturer's recommendations and shelf life strictly adhered to. To verify the resin, a pad should be cast with each flywheel for subsequent testing.

Initial and final tie-off procedures as recommended in Lawrence Livermore Laboratory report UCRL-15437 should be adhered to wherever appropriate.

The cure and post cure cycles should be designed to optimize the properties of the resin and to minimize residual stresses. Usually, a heat-up cycle at a controlled rate to cure temperature followed by a cool down cycle also at a controlled rate can achieve both of these goals. Report UCRL-15437 page 11 thoroughly discusses this.

Fiber volume fraction (nominally 60-65%) should be controlled to within a $\pm 2\%$ tolerance. The void content should be maintained at less than 3%. These quantities should be checked at the inside, middle and the outside of each ring. The surface finish should be free of bubbles, pock marks, resin rich areas or exposed fibers.

2. Assembly

All composite rings should be tested both ultrasonically and radiographically before assembly. Only high quality rings should be included in a multiring configuration. Subsequent flaw detection should also be administered in order to assure no fracturing occurred during assembly.

Assembly procedures as specified on the assembly drawing must be strictly followed. Each ring pair should be static balanced for mating assembly and overall static balance will be obtained by removing material from the inner ring only.

C. Drawings

The drawing package is found in Appendix 7 and contains drawings for two different ID/OD ratios. The sponsor will include the appropriate package for the design selected to be built.

D. Candidate Fabricators

The demise of the Department of Energy program in Mechanical Energy Storage Technology (MEST) has reduced the number of possible candidate flywheel fabricators to only two. They are:

Lord Corporation (A.J. Hannibal)

1635 West 12th Street

P. O. Box 10039

Erie, PA 16514-0039

and

Hercules Corporation (P. Ward Hill)

Aerospace Division

P.O. Box 98

Magna, Utah 84044

At present, the strongest candidate from the standpoints of technical capability, interest and corporate commitment is the Lord Corporation.

E. Testing

Over the past several years two experimental facilities have been active in testing composite material flywheels. These are:

1. The Oak Ridge Flywheel Evaluation Laboratory, located at the Oak Ridge Y-12 plant near Knoxville, Tennessee.
2. The Applied Physics Laboratory of Johns Hopkins University in Laurel, Maryland.

Both facilities have been funded by the Department of Energy and both have been significantly dismantled as a result of DOE no longer funding a flywheel effort. In addition, both facilities were built with the sole intention of testing shaft driven flywheels. Therefore, a major portion of their

experimental equipment consisted of a high speed air turbine and air supply source, neither of which is required for the GSFC design.

Our current assessment of GSFC spin testing requirements would indicate that the following experimental equipment would be required to evaluate a GSFC magnetically suspended flywheel design:

1. An air tight enclosure having a volume of at least 7 ft³ (3 feet in diameter by 1 foot high).
2. A containment ring to surround the flywheel system.
3. One or more optical viewing ports to permit cameras to view the enclosure interior.
4. Instrumentation to measure pressure, temperature, wheel runout, wheel wobble, etc.
5. An air flushing system to exhaust epoxy and composite material fumes from the enclosure.
6. A capture device which will restrain the spinning rotor so it does not destroy the suspension or motor/generator electronics if the rotor decouples.
7. Vacuum equipment to pump the enclosure to 10⁻² TORR or better.
8. Remote viewing and data collection capabilities.
9. Controllers for the motor/generator electronics to either run at a constant speed or cycle between two reference speeds for fatigue testing.

Our best estimate is that while some of the facilities of the two laboratories may still be available and applicable to GSFC requirements, it is not cost effective to adapt them for GSFC testing.

IV. SPECIFICATION FOR COMPOSITE FLYWHEEL RING-ROTOR

Introduction

The objective of this task is to fabricate, assemble and static test a multiring rotor for the NASA/GSFC "Spacecraft Flywheel Power System" program. Previous studies by NASA/GSFC showed the merits of considering Inertial Energy Storage as a possible viable alternative to electrochemical or fuel cell power storage devices for long life, high cycle rate, extended use, space applications. These studies showed that a magnetically suspended ring rotor, made of filament wound construction, containing an integral ironless armature motor-generator rotor, operating in an evacuated hermetically sealed enclosure should be an efficient means for space energy storage use. This effort addresses the first systems element, the "Filament Wound" rotor.

Scope

The scope of this phase of the program includes fabrication, assembly and static testing of the filament wound multiring rotor. Analysis has established the best fiber/epoxy materials and the method of prestressing of multiring elements to maximize energy storage capacity.

Requirements

A. Size

1. Assembly

OD - 20.000" +0.010"

ID - 8.000" +0.010"

or 10.000" +0.010"

W - 2.700" +0.005"

or 2.400" +0.005"

2. Components

Rings No. 1, 1A

See drawings No. 7-1 & 7-1A in Appendix 7

Rings No. 2, 2A

See drawings No. 7-2 & 7-2A " "

Rings No. 3, 3A

See drawings No. 7-3 & 7-3A " "

Rings No. 4, 4A

See drawings No. 7-4 & 7-4A " "

Rings No. 5, 5A

See drawings No. 7-5 & 7-5A " "

Rings No. 6, 6A

See drawings No. 7-6 & 7-6A " "

Note:

Mandrel cylindricity control is critical. Each mandrel will have the taper stated on the appropriate drawing with a 15% tolerance allowable. This must be strictly adhered to in order to meet the assembly load requirements.

B. Material Selection

Fiber

Celanese Celion 6000 graphite fiber will be used.

Epoxy

Shell EPON 826 with Jeffamine Chemical Company D230 curative will be used.

Mixing will be as prescribed by the manufacturer.

C. Processing

Wrap Lay-Up

1. Tensioning

Fiber tensioning should be controlled to minimize residual transverse and/or circumferential stresses. It is desirable to strive for a zero residual stress winding technique.

2. Temperature

Winding will take place in a clean "dust-free" area with room temperature controlled to $75^{\circ}\text{F} \pm 10^{\circ}\text{F}$. Relative humidity will be controlled to be less than 50%.

3. Resin

Resin will be stored carefully according to the manufacturer's recommendations and shelf life strictly adhered to. To verify resin, a pad should be cast with each mix for subsequent testing.

4. Fiber Tie-Off

Initial and final tie-off procedures as recommended in UCRL-15437 will be adhered to.

D. Cure Method

The cure method and post cure cycle shall be designed to optimize the properties of the resin and to minimize residual stresses. A heat-up cycle at a controlled rate to 230°F followed by a cool down cycle also at a controlled rate can achieve both of these goals. See page 11 of UCRL-15437 for control rates. An oven with a good commercial temperature controller will be adequate for this operation.

E. Finishing

The fiber volume fraction shall be controlled to within a tolerance of $\pm 2\%$. Void content shall be maintained at less than 3%. The surface finish shall be free of bubbles, pock marks, resin rich areas or exposed fibers. The machined outside diameter of each ring shall be smooth and free of loose fiber ends.

F. Assembly

Drawing Nos. 7-7 and 7-7A (Appendix 7) cover assembly of the ring-rotor. Assembly procedure stated must be followed implicitly. Only composite rings that passed both ultrasonic and radiographic inspection will be used. Ring alignment must be controlled during the "nesting" process. Press anvil and ram faces must be parallel and smooth to prevent surface damage of the rings. After each ring is assembled, the sub-assembly will be tested ultrasonically and radiographically and certified before moving on to the next assembly procedure. The completed assembly will be tested and certified (see Section 4).

G. Testing

1. Fiber

A certificate of physical and mechanical properties shall be included with each spool of graphite fiber. Only materials that exceed the minimum manufacturer's requirements will be used.

2. Epoxy

Pads taken from each batch mixed (see Section III - Resin) will be tested in accordance with the manufacturer's recommendations to insure that conformance to specifications has been met.

3. Rings

Fiber volume fraction and void content shall be checked at the inside, middle and outside of each ring.

4. Ring Assembly

All composite rings shall be tested both ultrasonically and radiographically before assembly. Only high quality rings shall be included for multiring assembly. Subsequent flaw detection shall be administered during the subassembly build-up to assure that no fracturing occurred during the assembly process.

H. Balancing

Prior to assembly of rings each ring should be static balanced and oriented so, upon assembly, any imbalance compensates that which exists in other rings. After complete assembly final static balance will be achieved by removal of material from the inside of the inner ring. Final static balance will be 300 micro grams or less.

V. SUMMARY

The design definition of a composite fiber ring rotor has been completed. Two specific designs have been included with this report, both capable of storing a maximum energy of 1600 Wh. Both designs account for the presence of a iron inner ring and both utilize Celion 6000/EPOXY as the composite material for the fiber composite rings.

The first design is identified as NASA-12 and consists of a total of 6 rings with the flywheel having an ID/OD ratio of 0.5. The first ring is iron and the remaining 5 rings are interference assembled Celion 6000/EPOXY. The projected maximum Specific Energy Density (SED), for the interference assembled flywheel, is 41 Wh/lb (90.2 Wh/kg) and 25 Wh/lb (55.0 Wh/kg) for the identical design assembled without interference. The air gap growth, from zero to full speed, will not exceed .060 inches.

The second design is identified as NASA-20 and also consists of a total of 6 rings, with the flywheel having an ID/OD ratio of 0.4. The first ring is iron and the remaining 5 rings are interference assembled Celion 6000/EPOXY. The projected maximum SED is 42 Wh/lb (92.4 Wh/kg), for the interference assembled flywheel, and 19 Wh/lb (41.8 Wh/kg) for the identical geometry assembled without interference. The air gap growth, from zero to full speed, will not exceed .040 inches.

The major differences between NASA-12 and NASA-20 are in the level of interference which is built into the ring. NASA-12 is designed for 0.3% maximum ring to ring interference while NASA-20 has 0.5%. NASA-20 has a smaller ID/OD ratio and thus a smaller maximum air gap growth. Both designs appear equally viable but before either is built it is recommended that two of

the Celion 6000/EPOXY rings, from the NASA-20 design, be fabricated, strain gaged, and pressed together. Details of this recommendation may be found in Section VI.

In addition to producing 2 specific designs, this project has also demonstrated the usefulness of two computer codes, FLYANS (FLYwheel ANalySis) and FLYSIZE (FLYwheel SIZE), for efficiently carrying out multiring rotor design - including the presence of an iron inner ring. Since the rotor design may have to be modified as the motor/generator and magnetic suspension evolves, the computer codes will allow this to be done as easily as possible. In addition, both codes are available for use in projecting the types of future composite material properties which will most benefit the GSFC magnetically suspended flywheel.

A review of the spin test requirements for the GSFC system indicates existing experimental facilities will not be applicable. Two of the most active facilities, Oak Ridge and Johns Hopkins University Applied Physics Laboratory, have been effectively dismantled due to their loss of DOE funding. Even if these facilities were fully functional, the unique capabilities of the GSFC system (i.e. to spin its own rotor) effectively eliminate the need for a major item in these facilities, namely the high speed air turbine. It would thus appear that a new spin test facility, which takes advantage of the experience gained from the DOE program, would be most cost effective for NASA/GSFC.

VI. RECOMMENDATIONS

The results presented in this report show that interference assembly of rotor rings will be required to achieve competitive energy densities with shaft driven flywheel designs. It is suggested that 2 rings (Number 5 and Number 6) of the NASA-20 design be built, instrumented with strain gages, and then pressed together. The experimental results can be compared to the theoretical predictions in order to enhance our understanding of pressing assembly performance. After these 2 rings have been assembled, they can be disassembled, and ring No. 5 machined to generate .3% interference (making it identical to ring Number 5 in the NASA-12 design). The rings can then be instrumented and pressed together again, and results can be compared to theoretical predictions. Finally, the rings can be disassembled and then radially cut in order to determine the residual stresses present in each ring. This test sequence requires only 2 rings and will provide the greatest information return for the cost invested.

In characterizing the composite ring-rotor, the iron ring was treated as a uniform profile mass load. Before a practical rotating assembly can be built, the iron ring must be defined in detail to identify the magnetic suspension portion of the assembly. In addition, the inner composite ring must be further defined to accommodate the ironless armature portion of the motor/generator. This also includes provisions for the magnet assembly.

Both of these refinements will necessitate recalculating the stress patterns and analytically determining the true operating characteristics of this design. While it is felt that the new calculations will not seriously de-rate the ring-rotors defined in this study, one must know what the actual operating capacity of this design is before test hardware is built.

Completion of this follow-on effort will result in a detailed definition of the rotating assembly. This approach is a necessary and logical sequence in pursuit of a total energy storage system design.

VII. APPENDICES

- 1. Reference Paper for FLYANS Code**
- 2. Failure Analysis**
- 3. FLYSIZE Listing**
- 4. FLYSIZE Formulas**
- 5. Ring Tolerances**
- 6. Stress Plots**
- 7. Drawings**

APPENDIX 2

FAILURE ANALYSIS

from

Huntington, R. A., M. S. Thesis, "Stress
Analysis and Maximization of Performance
for a Multiring Flywheel," University of
Maryland, Mechanical Engineering
Department, Jan. 1978. Thesis advisor:
Dr. J. A. Kirk.

To determine the performance of the multiring flywheel, it has been stated that a suitable failure criterion must be applied to the stress distribution. This appendix will present several failure criteria, including the maximum stress, maximum strain, Tsai-Hill, and Tsai-Wu failure theories [1, 2-5]*. Their development, applications, and limitations will also be presented along with their specific application to the multiring flywheel.

A simple test for the determination of a failure stress is a uniaxial tensile test in which a specimen is continuously loaded until rupture. The results of this test may be applied directly to a design situation in which uniaxial loads along a known direction are found. However, virtually all real situations involve stress states which are biaxial or triaxial with both normal and shear stress components. Since it would be very impractical, if not impossible, to perform a failure test for every combination of stress which may be foreseen, it becomes necessary to develop a failure criterion, based on a limited number of experiments, to predict if any arbitrary stress state will cause material failure. This prediction of failure stress has been studied in isotropic materials since the nineteenth century. Two widely used criteria, the Treska and von Mises, have emerged from these studies. Both assume that failure is induced solely by the action of shear stresses. The von Mises criterion further defines the distortional energy - the strain energy not associated with dilatation - as a parameter which reaches a critical value at failure. Modifications of both of these criteria (for isotropic materials) have been proposed to eliminate original restrictions [6-8]. Also, a

* Denotes references at back of this Appendix.

generalization of the von Mises criterion has been proposed by Hill [3] for slightly anisotropic metals. However, the materials considered for the multiring flywheel consist of both isotropic metals and orthotropic metals and orthotropic composites. Therefore, either one very general or several individual failure criteria are necessary to meet the requirements of the multiring flywheel. Two of the failure theories to be discussed, the Tsai-Hill and Tsai-Wu criteria, meet this requirement of generality since they both reduce to the von Mises failure theory for isotropic materials. The other failure criteria to be discussed should not be applied to isotropic materials, although it may be applied to pseudo-isotropic composite laminates.

The complexities of failure prediction for a composite material is easily portrayed by a brief discussion of the stress states in an isotropic versus an orthotropic materials under an arbitrary loading. For an isotropic material, the state of stress may be transformed at will to any convenient reference plane (usually the principle stress or maximum shear directions) without change in material properties. However, if the stress state of the composite is transformed, both the elastic properties and material strengths vary. While the variations of elastic properties follow the transformation of a fourth rank tensor, the transformation of strength is not well known. Therefore, a failure criterion for a composite material must relate all components of stress to a plane of symmetry in which strength properties are well known. This adds to the number of parameters necessary to characterize a failure surface. A failure theory for composites is further complicated by the variety of modes of failure which exist. The three major modes are fiber fracture, matrix cracking and delamination [9]. Therefore, it is necessary that the criterion predict

stress limits for several failure modes. However, it is not necessary to actually predict the mode of failure which will occur under a given loading.

Maximum Stress Criterion

The maximum stress failure criterion assumes that failure will occur in a composite material when any one of the stress components exceeds a critical value [2]. Each component of stress is considered independently from the others and all of the critical stress values are independent. This failure criterion is given by the following equation set:

$$\begin{aligned} -\sigma_r^C &< \sigma_r < \sigma_r^T \\ -\sigma_\theta^C &< \sigma_\theta < \sigma_\theta^T \\ -\tau_{r\theta}^S &< \tau_{r\theta} < \tau_{r\theta}^S \end{aligned} \quad (2.1)$$

where: $\sigma_r^C, \sigma_r^T, \sigma_\theta^C, \sigma_\theta^T, \tau_{r\theta}^S$ are the uniaxial compressive, tensile and shear strengths.

If any of the inequalities given by Eqn. 2.1 are violated, failure is postulated to occur. This is a very simple criteria to use and mainly because of this, it is often used to predict failure of composite materials. There are, however, several major restrictions on the general application of this method. The first of these requires that the components of stress be transformed to the material symmetry axes. But for the multiring flywheel, the stress distributions are given in the r-θ plane while this is also the assumed plane of material symmetry. Therefore, this restriction does not limit application for the multiring. The most important restriction on the

application of this criterion is simply its accuracy. This is demonstrated by Figure 2.1, which is a plot of predicted and experimentally determined failure stresses versus the angle between the line of action of a uniaxial load and the fiber orientation of the composite material. It should be noted that the loading axis uses a logarithmic scale so that the apparently small deviations represent large errors in the criterion. It should also be noted that this failure criterion predicts discontinuities in the failure strength, associated with changing failure modes, while the experimental data shows smooth variations.

Maximum Strain Criterion

The maximum strain failure criterion is very similar to the maximum stress criterion in application. The only major difference between these criteria is the assumption that a critical value of strain limits material strength rather than a critical value of stress (as with the maximum stress criterion). These strain values may be transformed to stress terms by application of Hooke's Law yielding the following equation set which describes this failure criterion in the case of plane stress:

$$\begin{aligned} -\sigma_r^c &< \sigma_r - \frac{\nu_{r\theta}}{N^2} \sigma_\theta < \sigma_r^T \\ -\sigma_\theta^c &< \sigma_\theta - \nu_{r\theta} \sigma_r < \sigma_\theta^T \\ -\tau_{r\theta}^s &< \tau_{r\theta} < \tau_{r\theta}^s \end{aligned} \quad (2.2)$$

where: σ_r^c etc. have been previously defined.

Comparison of Eqns. 2.1 and 2.2 shows that the only difference between these failure criteria is the poisson effects between the normal stress components. Along with their similarities, these criteria share identical

ORIGINAL PAGE IS
OF POOR QUALITY

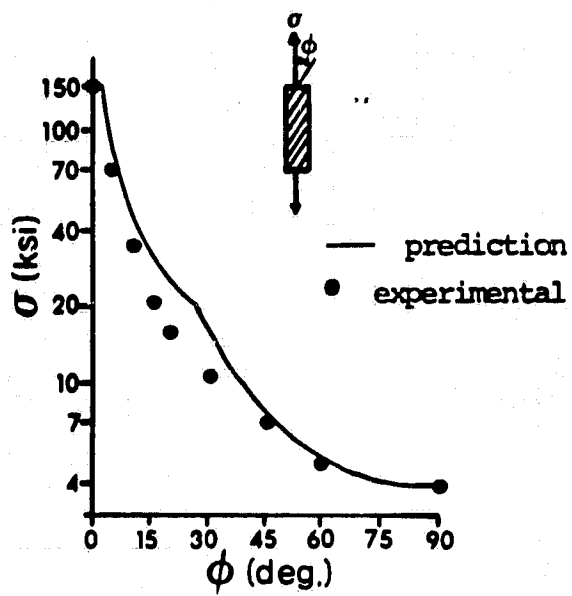


Figure 2.1 Maximum stress failure criterion prediction of composite off-axis strength (after ref. 2)

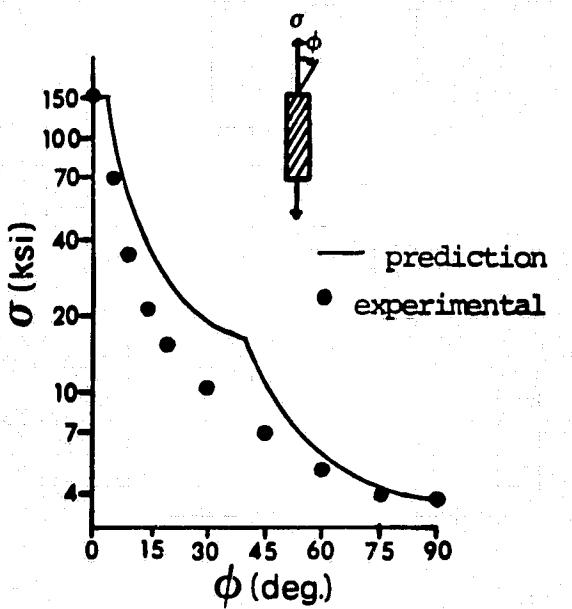


Figure 2.2 Maximum strain failure criterion prediction of composite off-axis strength (after ref. 2)

restrictions (i.e.: stress components must be transformed to material symmetry axes and inaccurate predictions of failure stress). The latter of these is shown by Figure 2.2 which is a plot of predicted and experimentally determined failure stress similar to Figure 2.1. Again large errors are seen in the predicted failure stress over a wide range of loading orientation.

Tsai-Wu Criterion

The preceding failure criteria each have several inadequacies which impair their agreement with experimental data and their application. An obvious method of improving data fit is to increase the number of independent parameters in the criterion. The next failure criterion to be discussed, the Tsai-Wu theory [5, 10, 11], achieves this with a tensorial failure theory which relates linear and quadratic stress components. The basic postulate is that there exists a failure surface with an equation of the form:

$$F_i \sigma_i + F_{ij} \sigma_i \sigma_j = 1 \quad i,j = 1,2,\dots,6 \quad (2.3)$$

where: F_i = 2nd rank tensor of strength parameters

F_{ij} = 4th rank tensor of strength parameters

These strength tensors will obey known tensor transformations for coordinate changes and are assumed to be symmetric. The former demonstrates that it is now possible to determine the strength properties of an anisotropic material in an arbitrary plane once the terms of the strength tensor are established. This is a major advantage of this failure theory although this feature is not needed to analyze multiring flywheel failure. It may be noted

that the linear stress terms allow for variations in the tensile and compressive strengths while the quadratic terms define a closed ellipsoidal failure surface which intersects each stress axis provided that the following stability relations [5] are satisfied

$$F_{ij}^2 \leq F_{ii} F_{jj} \quad (2.4)$$

where: repeated indices are NOT summations

The failure theory, as represented thus far, is applicable to general anisotropic materials with triaxial loading; however, the multiring flywheel deals with specially orthotropic materials under plane stress loadings. For this case, Eqn. 2.3 may be expanded, yielding:

$$F_1 \sigma_r + F_2 \sigma_\theta + F_6 \tau_{r\theta} + F_{11} \sigma_r^2 + 2F_{12} \sigma_r \sigma_\theta + F_{22} \sigma_\theta^2 + F_{66} \tau_{r\theta}^2 = 1 \quad (2.5)$$

Using Eqn. 2.5, the F's may now be evaluated with experimental data. All but F_{12} may be found by uniaxial tensile and compressive testing and assuming that the positive and negative pure shear strengths are equal, the F's become:

$$\begin{aligned} F_{11} &= \frac{1}{\sigma_r^T \sigma_r^C} & F_1 &= \frac{\sigma_r^C - \sigma_r^T}{\sigma_r^T \sigma_r^C} \\ F_{22} &= \frac{1}{\sigma_\theta^T \sigma_\theta^C} & F_2 &= \frac{\sigma_\theta^C - \sigma_\theta^T}{\sigma_\theta^T \sigma_\theta^C} \\ F_{66} &= \left(\frac{1}{\tau_{r\theta}^S}\right)^2 & F_6 &= 0 \end{aligned} \quad (2.6)$$

The stress interaction term, F_{12} , must be determined with a combined stress loading arrangement. A great deal of work has been carried out to determine optimal tests for this parameter [5, 10, 11]; however, conclusive

results have not been presented in these references. This identifies a significant disadvantage of this failure theory since information which may determine F_{12} is not generally available for the composite materials being considered for the multiring flywheel. To examine the effect of variations of F_{12} on the predicted performance of a flywheel rotor, F_{12} is defined using Eqns. 2.4 and 2.6 as:

$$F_{12} = -C \sqrt{\frac{1}{\sigma_x^T \sigma_x^C} + \frac{1}{\sigma_\theta^T \sigma_\theta^C}} \quad (2.7)$$

where: $-1 \leq C \leq 1$ for stability conditions

Figure 2.3 shows the effect of variations of F_{12} , within these stability limits, on the predicted SED of a single ring flywheel ($a_0 = .75$). Since the maximum prediction is three times greater than the minimum, it is obvious that the SED, and other performance parameters, is very sensitive to change in F_{12} .

Despite this disadvantage, the Tsai-Wu failure, the Tsai-Wu failure theory has good agreement with experimental data if F_{12} is properly selected. This is demonstrated by Figure 2.4 which shows predicted and experimental data for off-axis strength tests on a boron-epoxy composite. Despite this improvement in accuracy over the previously discussed failure theories, the lack of information needed to determine F_{12} prevents the further use of this failure. However, an additional failure criterion, the Tsai-Hill theory [1, 2-4], which is similar to the Tsai-Wu theory, will be discussed next.

Tsai-Hill Criterion

The Tsai-Hill criterion is a generalization of the von Mises yield criterion for isotropic materials. It was first proposed by Hill in 1948 [3]

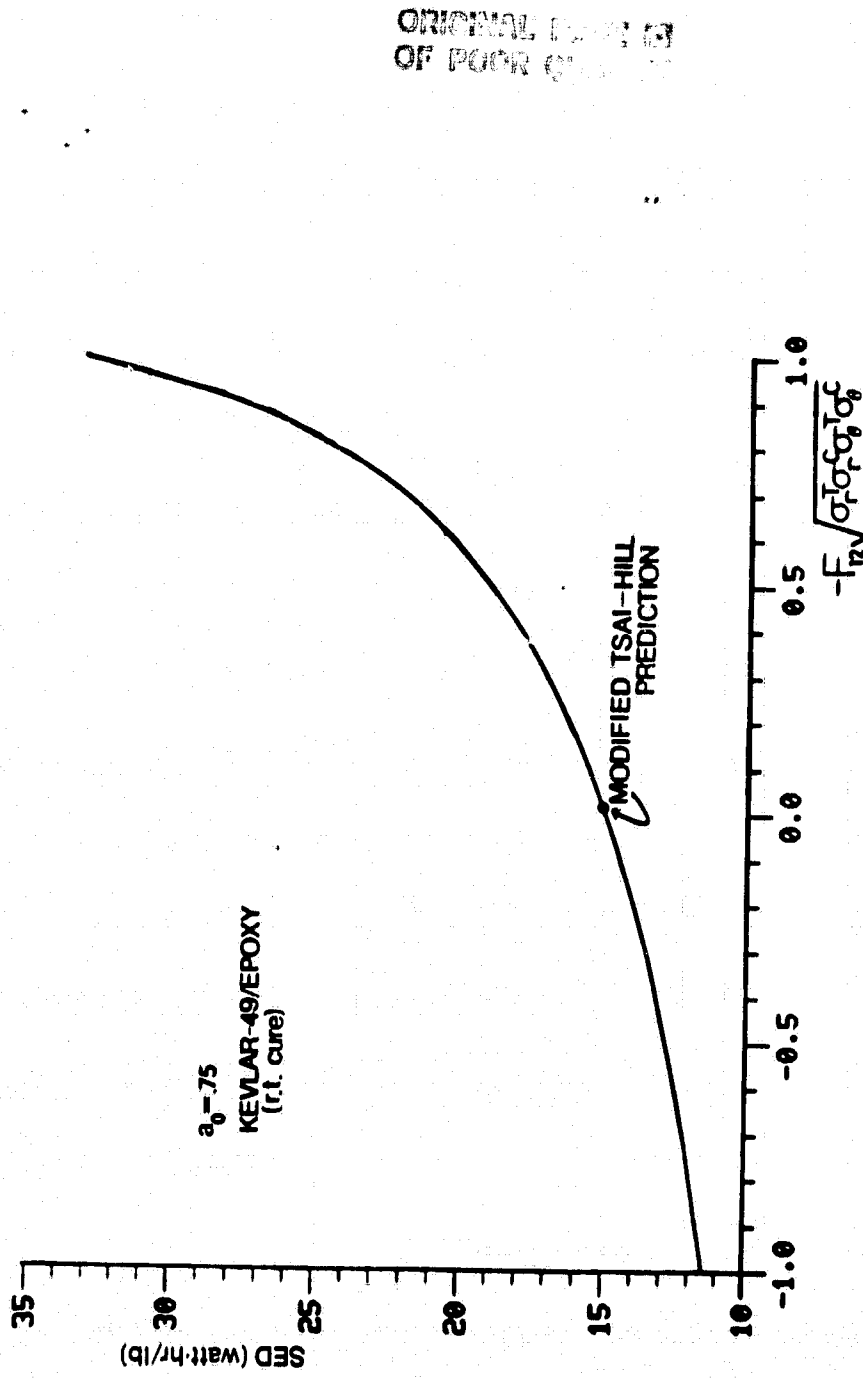


Figure 2.3 Effect of variations of F_{12} on the predicted SED of a single ring flywheel

ORIGINAL PAGE IS
OF POOR QUALITY

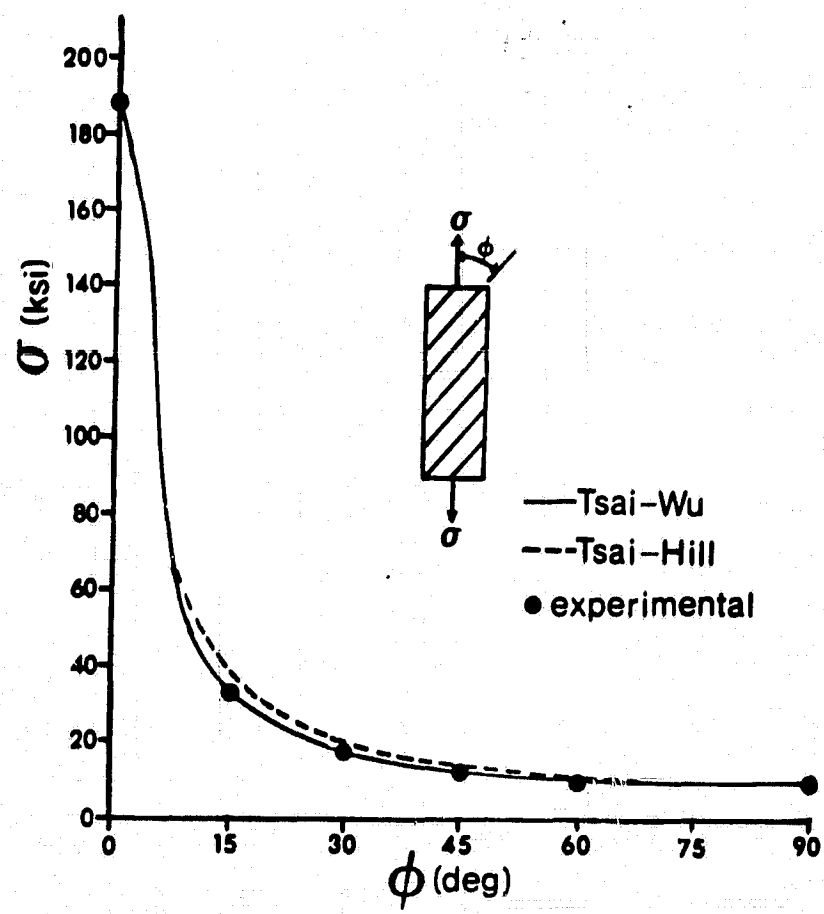


Figure 2.4 Tsai-Wu and Tsai-Hill failure criteria predictions of Boron/Epoxy off-axis strength (after ref. 11)

for slightly anisotropic metals and latter adapted (1965) to composite materials by Tsai [4]. As described in these references, the criterion contains only quadratic stress terms. However, linear terms have been added to allow for variations in the tensile and compressive strengths. The resulting criterion, which will be termed the modified Tsai-Hill criterion, is identical to Eqn. 2.5 with the F's defined by Eqn. 2.6. However, this criterion contrasts the Tsai-Wu in that the interaction term F_{12} is not independent of the other strength parameters. For the materials considered in this project, $2F_{12} = -F_{12}$. Therefore, the parameter C from Eqn. 2.7 becomes:

$$C = \frac{1}{2} \sqrt{\frac{\sigma_r T_\theta C}{\sigma_\theta T_r C}} \quad (2.8)$$

For filamentary wound composite or isotropic materials, it is obvious that C is within the stability requirements given by Eqn. 2.7. The agreement of the modified Tsai-Hill failure criterion with experimental data is shown in Figure 2.4. Also, the value of C given by Eqn. 2.8 for the previously cited single ring flywheel has been indicated on Figure 2.3. It is easily seen that the agreement with experiment is not as good as is seen for the Tsai-Wu theory. However, this sacrifice of some accuracy is necessary to eliminate the problem of determining F_{12} for the Tsai-Wu theory. Therefore, the modified Tsai-Hill criterion will be used instead of the Tsai-Wu theory for the multiring flywheel. However, the development of the remaining theory will be general enough to allow a simple transition back to the Tsai-Wu criterion if F_{12} values become available in the future for the materials considered in this study.

References (for Appendix 2)

1. Ashton, J.E., Halpin, J.C., Petit, P.H., Primer on Composite Materials: Analysis, Technomic, Stanford, Conn., 1969.
2. Jones, R.M., Mechanics of Composite Materials, McGraw-Hill, New York, 1975
3. Hill, R., "A Theory of the Yielding and Plastic Flow of Anisotropic Metals," Proc. Royal Society (London) A, Vol. 193 (1948).
4. Tsai, S.W., "Strength Characteristics of Composite Materials," NASA CR-224, 1965.
5. Tsai, S.W. and Wu, E.M., "A General Theory of Strength for Anisotropic Materials," J. Composite Materials, Vol. 5 (1971), p. 58.
6. Hoffman, O., "The Brittle Strength of Orthotropic Materials," J. of Composite Materials, Vol. 1 (1967), p. 200.
7. Mohr, O., "Welche Umstände bedingen die Elastizitätsgrenze und den Bruch eines Materials," Z.V.D. Ingenieure, 1900, p. 1524.
8. von Mises, R., "Mechanik der plastischen Formänderung von Kristallen," Z. Angew. Math. Mech., Vol. 8 (1928), p. 161.
9. Mehan, R.L. and Mullin, J.V., "Analysis of Composite Failure Mechanisms Using Acoustic Emissions," J. Composite Materials, Vol. 5, (1971), p. 266.
10. Wu, E.M., "Optimal Experimental Measurements of Anisotropic Failure Tensors," J. Composite Materials, Vol. 6 (1972), p. 472.
11. Pipes, R.B. and Cole, B.W., "On the Off-Axis Strength Test for Anisotropic Materials," J. Composite Materials, Vol. 7 (1973), p. 246.

APPENDIX 3

FLYSIZE LISTING

(This program is written for an IBM PC using BASIC.)

B:FLYSIZE.BAS -- printed on 12-26-1983 at 11:19:28 -- Page 1

```
10'-----FLYSIZE-----  
20 DIM A(15), F(10),RMM(15),GAMMA(15),LABEL$(15)  
30 DIM PROMPT3$(5),PROMPT7$(10),RR(15),INF(15),PF(15),GAMMAS$(10),PHIDI(10)  
40 SCREEN 2 :KEY OFF  
50 WIDTH 80  
60 CLS  
70'-----INPUT USER DATA-----  
80 GOSUB 5000  
90'-----NOW DO COMPUTATIONS-----  
100'-----CALCULATE RING THICKNESS-----  
110 PI=3.14159  
120 T =1728*KE/(PI*B^2*VED)  
130'-----CALCULATE WHEEL RPM-----  
140 RPM=107.61*(SQR(RHOOMEGBABG0/GAMMA(1)))/B  
150'-----CALCULATE NOMINAL RING RADIUS VALUES-----  
160 FOR I =1 TO N+1  
170 A(I) = RR(I)*B  
180 NEXT I  
190'-----CALCULATE PARTIAL ASSEMBLY FORCES-----  
200'-----AND MINIMUM TAPER ANGLE FOR EACH RING PAIR-----  
210 MU=.1  
220 PHID=1.5  
230 CONV=PI/180!  
240 PHIR=PHID%CONV  
250 FOR I =2 TO N-1  
260 F(I)=2*PI*A(I)*T*PF(I)*(MU*TAN(PHIR))  
270 PHIDI(I) = ATN(INF(I)*.001*A(I)/T)/CONV  
280 NEXT I  
290'-----CALCULATE RADIAL MISMATCH-----  
300 FOR I=2 TO N-1  
310 RMM(I) = INF(I) * A(I) * .001  
320 NEXT I  
330 RMM(0)=0  
340 RMM(N)=0  
350'-----CALCULATE RING WEIGHTS-----  
360'-----THE WEIGHT DENSITIES FOR THE RINGS ARE GAMMA(1) THRU GAMMA(N)-----  
370'-----THE WEIGHT DENSITIES ARE READ IN AS USER DATA-----  
380 WTOTAL = 0  
390 FOR I = 1 TO N  
400 RINGAREA = PI * (A(I+1)^2 - A(I)^2)  
410 RINGVOL = T * RINGAREA  
420 WT(I) = RINGVOL * GAMMA(I)  
430 WTOTAL = WTOTAL + WT(I)  
440 NEXT I  
450'-----END OF COMPUTATIONAL LOOP-----  
460 REM  
470 REM  
480 REM  
490'-----OUTPUT THE RESULTS-----  
500 GOSUB 7000  
510 END  
5000'-----INPUT & FILE CREATION SUBROUTINE-----  
5005'-----INPUT IS FROM THE KEYBOARD OR FROM A USER SPECIFIC FILE-----  
5010'-----THE USER FILE IS BIRUN-XXXX.DAT AND MUST BE ALREADY AVAILABLE ON-
```

ORIGINAL PAGE IS
OF POOR QUALITY

B:FLYSIZE.BAS -- printed on 12-26-1983 at 11:19:30 -- Page 2

```
5015 ' -----DRIVE B. IF THE INPUT IS SPECIFIED FROM THE KEYBOARD A USER-----  
5020 ' -----FILE OF THE SAME FORM WILL BE CREATED ON DRIVE B, AND THE INPUT-----  
5025 ' -----DATA WILL BE WRITTEN THERE.  
5030 CLS  
5035 LOCATE 2,5  
5040 PRINT "WILL YOU INPUT FROM <F>ILE"  
5045 LOCATE 3,5  
5050 PRINT " OR <K>EYBOARD"  
5055 LOCATE 5,5  
5060 PRINT "ENTER F OR K ";  
5065 A$=INKEY$  
5070 IF A$="" GOTO 5065  
5075 IF A$="K" OR A$="k" THEN FLAG% = 1: GOTO 5090  
5080 IF A$="F" OR A$="f" THEN FLAG% = 2: GOTO 5090  
5085 GOTO 5065  
5090 IF FLAG% = 2 GOTO 5105  
5095 LOCATE 7,5  
5100 PRINT "A FILE WILL BE CREATED FOR YOUR INPUT DATA ON DRIVE B:"  
5105 LOCATE 8,5  
5110 PRINT "THE NAME OF FILE IS B:RUN-XXXX.DAT"  
5115 LOCATE 9,5  
5120 PRINT "XXXX SHOULD BE AN INTEGER BETWEEN 0 AND 9999"  
5125 LOCATE 11,5  
5130 INPUT; "ENTER XXXX NOW"; ID$  
5135 FILENAME$ = "B:RUN-" + ID$ + ".DAT"  
5140 IF A$="K" OR A$="k" THEN OPEN FILENAME$ FOR OUTPUT AS #2  
5145 IF A$="F" OR A$="f" THEN OPEN FILENAME$ FOR INPUT AS #1  
5150 PROMPT0$ = "ENTER A RUN TITLE UP TO 80 CHARACTERS LONG"  
5155 PROMPT1$ = "NUMBER OF RINGS"  
5160 PROMPT2$ = "ENTER RADIUS RATIO FOR EACH RING INTERFACE"  
5165 PROMPT3$(0) = "INSIDE RADIUS RATIO"  
5170 PROMPT3$(1) = "OUTER RADIUS RATIO(MUST=1.0)"  
5175 PROMPT4$ = "ENTER INTERFERENCE FOR EACH RING INTERFACE"  
5180 PROMPT5$ = "ENTER THE PARTIAL ASSEMBLY PRESSURES"  
5185 PROMPT7$(1) = "FLYWHEEL OUTER RADIUS(IN)"  
5190 PROMPT7$(2) = "STORED ENERGY(WH)"  
5195 PROMPT7$(3) = "RHO1(OMEGA*KB)**2(PSI)"  
5200 PROMPT7$(4) = "SED(WH/LB)"  
5205 PROMPT7$(5) = "VED(WH/FT**3)"  
5210 PROMPT7$(6) = "NON-DIM. DISP. LIMIT(10^-3)"  
5215 ' -----INPUT AN 80 CHARACTER(MAX) DESCRIPTIVE RUN TITLE-----  
5220 LOCATE 14,5 :PRINT PROMPT0$  
5225 LOCATE 15,1 :IF FLAG% = 1 THEN INPUT RUNTITLE$ ELSE INPUT #1,RUNTITLE$  
5230 IF FLAG% = 1 THEN WRITE #2,RUNTITLE$  
5235 CLS  
5240 ' -----INPUT NUMBER OF RINGS-----  
5245 LOCATE 1,36 :PRINT PROMPT1$  
5250 LOCATE 1,51 :IF FLAG% = 1 THEN INPUT N ELSE INPUT #1,N  
5255 IF FLAG% = 1 THEN WRITE #2,N  
5260 ' -----INPUT RING RADIUS RATIOS-----  
5265 LOCATE 2,10 :PRINT PROMPT2$  
5270 FOR I = 1 TO N  
5275 LOCATE I+2,32  
5280 IF I=1 THEN PRINT PROMPT3$(0)
```

B:FLYSIZE.BAS -- printed on 12-26-1983 at 11:19:32 -- Page 3

```
5285 IF I>1 THEN PRINT USING "RING ### TO ##"; I-1; I
5290 LOCATE I+2,51
5295 IF FLAG% = 1 THEN INPUT RR(I) ELSE INPUT #1,RR(I)
5300 IF FLAG% = 1 THEN WRITE #2,RR(I)
5305 NEXT I
5310 '-----INPUT OUTER RADIUS RATIO, MUST EQUAL 1.0-----
5315 LOCATE I+2,20 :PRINT PROMPT3$(1)
5320 LOCATE I+2,51
5325 IF FLAG% = 1 THEN INPUT RR(N+1) ELSE INPUT #1,RR(N+1)
5330 IF FLAG% = 1 THEN WRITE #2,RR(N+1)
5335 '-----INPUT RING TO RING INTERFERENCE-----
5340 LOCATE 14,8 :PRINT PROMPT4$
5345 FOR I = 2 TO N-1
5350 LOCATE I+14,1
5355 PRINT USING "INTERFERENCE RING ### TO RING #### (10^-3 IN/IN)"; I; I+1
5360 LOCATE I+14,51
5365 IF FLAG% = 1 THEN INPUT INF(I) ELSE INPUT #1,INF(I)
5370 IF FLAG% = 1 THEN WRITE #2,INF(I)
5375 NEXT I
5380 CLS
5385 '-----INPUT MISC. VALUES-----
5390 FOR I = 1 TO 6
5395 LOCATE I+4,25 :PRINT PROMPT7$(I)
5400 LOCATE I+4,55 :IF FLAG% = 1 THEN INPUT VAR(I) ELSE INPUT #1, VAR(I)
5405 IF FLAG% = 1 THEN WRITE #2, VAR(I)
5410 NEXT I
5415 B = VAR(1)
5420 KE = VAR(2)
5425 RHOOMEGABSO = VAR(3)
5430 SED = VAR(4)
5435 VED = VAR(5)
5440 DISP = VAR(6)*B*9.799999E-04
5445 CLS
5450 '-----INPUT PARTIAL ASSEMBLY PRESSURES-----
5455 LOCATE 1,14 :PRINT PROMPT5$
5460 FOR I = 2 TO N-1
5465 LOCATE I+1,20
5470 PRINT USING "PP RING ### ADDED TO ALL PRIOR RINGS (KSI)"; I+1
5475 LOCATE I+1,63
5480 IF FLAG% = 1 THEN INPUT PP(I) ELSE INPUT #1, PP(I)
5485 IF FLAG% = 1 THEN WRITE #2, PP(I)
5490 NEXT I
5495 '-----INPUT THE RING WEIGHT DENSITIES IN LB/IN^3-----
5500 CLS
5505 LOCATE 3,20 :PRINT "ENTER THE WEIGHT DENSITY OF EACH RING"
5510 LOCATE 4,5 :PRINT "IF PRESENT RING & ALL FOLLOWING RINGS HAVE THE SAME DENS
ITY ENTER 'S'"
5515 FOR I=1 TO N
5520 LOCATE I+5,5
5525 PRINT USING "ENTER DENSITY FOR RING ### (LB/IN^3)"; I;
5530 IF FLAG% = 1 THEN INPUT GAMMAS$(I) ELSE INPUT #1,GAMMAS$(I)
5535 IF FLAG% = 1 THEN WRITE #2,GAMMAS$(I)
5540 ISTAR = I
5545 IF GAMMAS$(I) = "S" OR GAMMAS$(I) = "s" THEN 5565
```

5550 GAMMA(I) = VAL(GAMMA\$(I))
5555 NEXT I
5560 GOTO 5585
5565 '-----SETS ALL SUBSEQUENT RINGS TO SAME DENSITY IF S ENTERED-----
5570 FOR I=ISTAR TO N
5575 GAMMA(I)=VAL(GAMMA\$(ISTAR-1))
5580 NEXT I
5585 LOCATE I+6,10 :PRINT "*****END OF USER INPUT*****"
5590 CLOSE #1
5595 IF FLAG%>=1 THEN CLOSE #2
5600 RETURN
7000 '-----OUTPUT SUBROUTINE-----
7005 LABEL\$(1)="RING THICKNESS(INCHES)"
7010 LABEL\$(2)="RPM(ROT/MIN)"
7015 LABEL\$(3)="SED(WH/LB)"
7020 LABEL\$(4)="VED(WH/FT^3)"
7025 LABEL\$(5)="TOTAL STORED ENERGY(WH)"
7030 LABEL\$(6)="TOTAL FLYWHEEL WEIGHT(LBS)"
7035 LABEL\$(7)="MAX. INNER RAD. DISP.(INCHES)"
7040 CLS
7045 LOCATE 8,14
7050 PRINT "ENTER THE FIRST LETTER FOR ONE OF THE FOLLOWING CHOICES"
7055 LOCATE 12,23
7060 PRINT "<S>CREEN.....OUTPUT TO SCREEN"
7065 LOCATE 14,23
7070 PRINT "<E>ND.....END THE PROGRAM"
7075 LOCATE 17,27
7080 PRINT "YOUR CHOICE";
7085 A\$ = INKEY\$
7090 IF A\$="S" OR A\$="s" GOTO 7105
7095 IF A\$="E" OR A\$="e" THEN END
7100 IF A\$="" GOTO 7085
7105 OPEN "SCRN;" FOR OUTPUT AS #1 :GOTO 7110
7110 CLS
7115 LOCATE 1,40-LEN(RUNTITLE\$)/2
7120 PRINT RUNTITLE\$
7125 LOCATE 2,27
7130 PRINT #1, "RUN ON ";DATE\$;" AT ";TIME\$;
7135 LOCATE 3,3
7140 PRINT #1,"RING" TAB(9) "IN. R." TAB(18) "INSIDE" TAB(27) "OUTSIDE" TAB(40)
"RADIAL" TAB(56) "%" TAB(64) "RING" TAB(75) "MIN."
7145 LOCATE 4,4
7150 PRINT #1,"NO." TAB(10) "RATIO" TAB(18) "RADIUS" TAB(27) "RADIUS" TAB(39) "M
ISMATCH" TAB(55) "INT" TAB(63) "WEIGHT" TAB(74) "TAPER"
7155 LOCATE 5,3
7160 PRINT #1,"(--)" TAB(10) "(-)" TAB(19) "(IN)" TAB(28) "(IN)" TAB(41) "(IN)"
TAB(53) "(10^-3)" TAB(64) "(LBS)" TAB(74) "(DEG)"
7165 LOCATE 6,1
7170 PRINT #1, STRINGS(80,45);
7175 K = 6
7180 FOR I = 1 TO N
7185 LOCATE I+K,3 :PRINT #1, USING "####"; I
7190 LOCATE I+K,10 :PRINT #1, USING "#.###"; RR(I)
7195 LOCATE I+K,18:PRINT #1, USING "####.###"; A(I)

7200 LOCATE I+K,27:PRINT #1, USING "###.##";A(I+1)+RMM(I)
7205 IF I=1 THEN GOTO 7230
7210 LOCATE I+K,39:IF I<N THEN PRINT #1, USING "#.##";RMM(I)
7215 LOCATE I+K,45:IF I<N THEN PRINT #1, USING "#_##";I;I+1
7220 LOCATE I+K,52:IF I<N THEN PRINT #1, USING "#.#";INF(I)
7225 LOCATE I+K,56:IF I<N THEN PRINT #1, USING "#_##";I,I+1
7226 LOCATE I+K,75:IF I<N THEN PRINT #1, USING "#.#";PHIDI(I)
7230 LOCATE I+K,63
7235 PRINT #1, USING "###.##";WT(I)
7250 NEXT I
7255 L = 6
7260 LOCATE I+L,14:K=1:GOSUB 10000
7265 LOCATE I+L,45:PRINT #1, USING "###.##";T
7270 LOCATE I+L+1,14:K=2:GOSUB 10000
7275 LOCATE I+L+1,45:PRINT #1, USING "###.##";RPM
7280 LOCATE I+L+2,14:K=3:GOSUB 10000
7285 LOCATE I+L+2,45:PRINT #1, USING "###.##";SED
7290 LOCATE I+L+3,14:K=4:GOSUB 10000
7295 LOCATE I+L+3,45:PRINT #1, USING "###.##";VED
7300 LOCATE I+L+4,14:K=5:GOSUB 10000
7305 LOCATE I+L+4,45:PRINT #1, USING "###.##";KE
7310 LOCATE I+L+5,14 :K=6:GOSUB 10000
7315 LOCATE I+L+5,45 :PRINT #1, USING "###.##";WTOTAL
7320 LOCATE I+L+6,14 :K=7:GOSUB 10000
7325 LOCATE I+L+6,45 :PRINT #1, USING "#.##";DISP
7330 GOSUB 11000
7335 CLS
7340 LOCATE 1,15
7345 PRINT "PARTIAL ASSEMBLY" PRESSURES FORCES"
7350 M=0
7355 FOR I=2 TO N-1
7360 LOCATE I+M,4
7365 CAPTION\$="RING #### ADDED TO PREVIOUS RINGS"
7370 PRINT USING CAPTION\$; I+1;
7375 PRINT STRING\$(40-LEN(CAPTION\$),46);
7380 LOCATE I+M,41 :PRINT USING "###.##";PP(I)
7385 LOCATE I+M,49: PRINT "kPSI"
7390 LOCATE I+M,53 :PRINT USING ".....# ##.## 10^3 LBS";F(I);
7395 NEXT I
7400 ISTAR=I+M
7405 COL% =1 : ROW% =0
7410 CAPTION1\$=" RING WEIGHT DENSITY"
7415 CAPTION2\$=" (--) (LB/IN^3)"
7420 LOCATE ISTAR+1,COL%
7425 PRINT CAPTION1\$
7430 LOCATE ISTAR+2,COL%
7435 PRINT CAPTION2\$
7440 LOCATE ISTAR+3,COL% :PRINT STRING\$(25,45);
7445 IF N>5 THEN LOCATE ISTAR+1,40:PRINT CAPTION1\$
7450 IF N>5 THEN LOCATE ISTAR+2,40:PRINT CAPTION2\$
7455 IF N>5 THEN LOCATE ISTAR+3,40:PRINT STRING\$(25,45);
7460 FOR I=1 TO N
7465 IF I>5 THEN COL% =40 :ROW% =5
7470 LOCATE ISTAR+3+I-ROW%,COL%

ORIGINAL PAGE IS
OF POOR QUALITY

7475 PRINT USING " ##"; I
7480 LOCATE ISTAR+3+I-ROW%,COL% +15
7485 PRINT USING "#.##"; GAMMA(I)
7490 NEXT I
7495 IF N>5 THEN ENDREF%=ISTAR+10
7500 IF N<5 THEN ENDREF%=ISTAR + N + 5
7505 LOCATE ENDREF%,15
7510 PRINT "DATA FOR THIS RUN IS IN FILE ";FILENAME\$
7515 GOSUB 11000
7520 CLOSE #1
7525 GOTO 7000
10000 '-----OUTPUT FORMATTING SUBROUTINE-----
10020 PRINT LABEL\$(K); STRING\$(30-LEN(LABEL\$(K)),46);
10030 RETURN
11000 '-----PAUSE SUBROUTINE-----
11010 LOCATE 25,5
11030 PRINT "PRESS ANY KEY TO CONTINUE--SHIFT/PRTSC FOR A COPY";
11040 FOR I=1 TO 1000 :NEXT I
11050 FOR I=1 TO 79: LOCATE 25,I :PRINT " ";:NEXT I
11060 B\$ = INKEY\$
11070 IF B\$="" THEN 11060
11080 RETURN

ORIGINAL PAGE IS
OF POOR QUALITY

APPENDIX 4

FLYSIZE FORMULAS

4-1 Calculation of Taper Angle

Shown in Figure 4.1 is a schematic diagram showing the cross section of two rings, Ring (I) and Ring (I+1), which are to be assembled using pressing force $F(I)$. In order to permit these 2 rings to be press assembled, it is necessary that point A lie inside (i.e. towards the center line) of point B. To calculate the minimum value of ϕ which will permit this, assume that point A and point B are directly above each other, and further assume that the following information is known for these 2 rings:

T = ring axial thickness, (inches)

$INF(I)$ = % interference between ring (I) and (I+1), (dimensionless)

$A(I)$ = nominal radius of the interface between ring (I) and (I+1), (inches).

It then follows from the definition of % interference that:

$$RMM(I) = INF(I) * A(I)$$

where:

$RMM(I)$ = radial mismatch between Ring (I) and (I+1).

Then, it can be seen that $\phi(I)$, the taper angle, should be selected so that:

$$\phi(I) \geq \tan^{-1} (RMM(I)/T) \quad (4-1)$$

FLYSIZE calculates the taper angle for each interfering ring pair using the equality in equation (4-1) and provides the results in a printed design report for the subject flywheel. In general the angle $\phi(I)$ is less than 1.5 degrees for up to 0.5% interference.

ORIGINAL PAGE IS
OF POOR QUALITY.

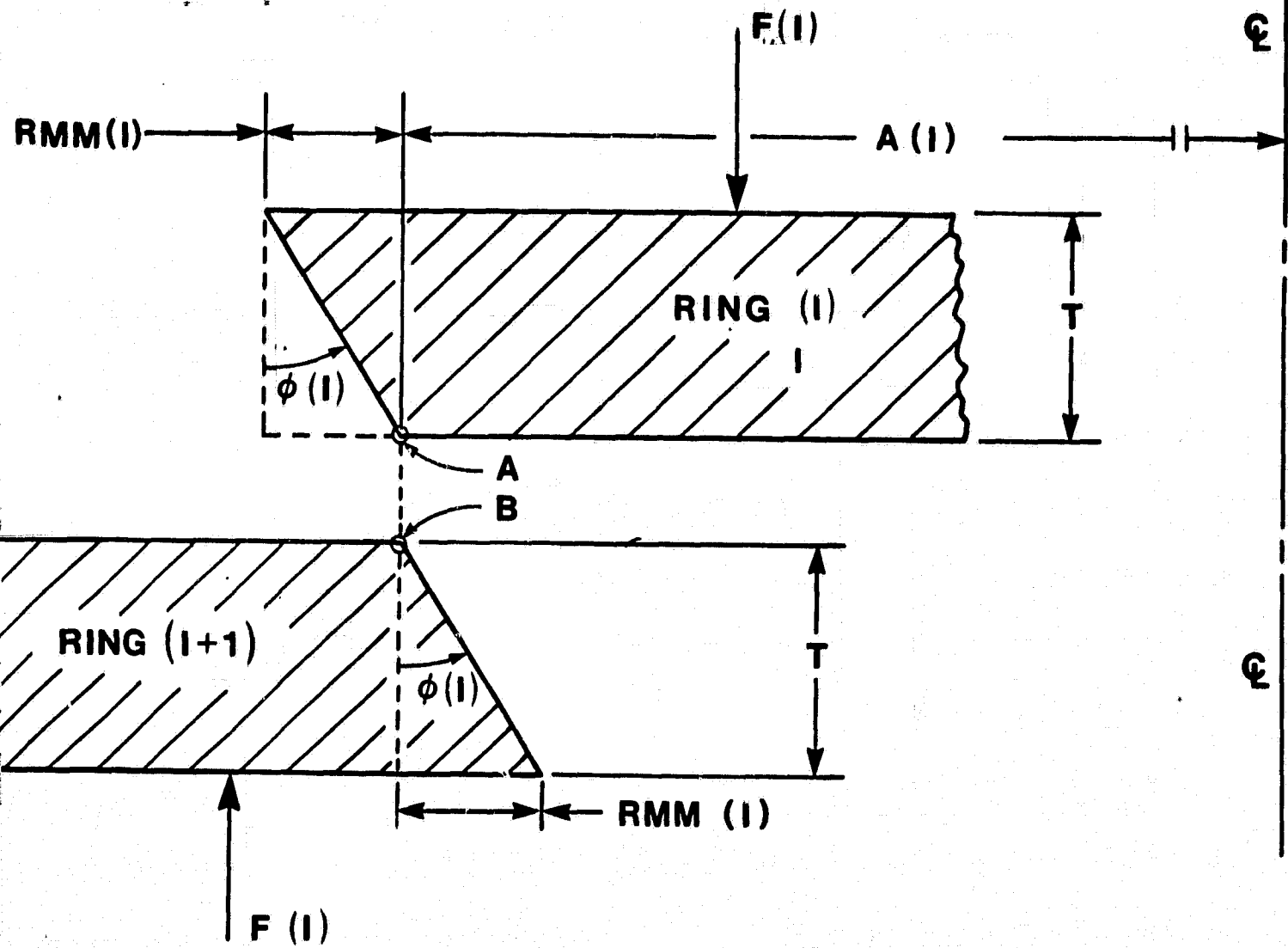


Figure 4.1

Schematic diagram of 2 rotor rings. These rings are to be assembled using pressing force $F(I)$.

4-2 Calculation of Assembly Forces

Show in Figure 4.2 is a schematic diagram of the pressing forces ($F(I)$) which acts on Ring (I). Since the Rings (I) and (I+1) are tapered the pressing force will be a maximum at the point where the two rings are flush with each other. Assume that at this point the following information is known:

$P(I)$ = partial assembly pressure between Ring (I) and (I+1), (psi)

μ = 0.1, coefficient of friction between the two rings. This value is taken as a constant for FLYSIZE and assumes the rings are put together using epoxy as an effective lubricant.

$\tau(I)$ = $\mu * P(I)$, interfacial shear stress between the two rings, (psi).

Since the forces are in equilibrium it is known that:

$$\sum_z \text{Forces} = 0$$

Therefore:

$$\begin{aligned} F(I) &= \tau(I) * \text{AREA}(I) \cos \phi + P(I) \text{AREA}(I) \sin \phi \\ &= \text{AREA}(I) (\tau(I) \cos \phi + P(I) \sin \phi) \end{aligned} \quad (4-2)$$

where:

$\text{AREA}(I)$ = surface area of the interface between the two rings, (in^2)

ϕ = 1.5° , assumed to be constant for all rings, (degrees)

The expression for $\text{AREA}(I)$ is obtained assuming that the line segment T - A is revolved about the center line of the ring. Therefore:

$$\text{AREA}(I) = 2 * \pi * (T/\cos \phi) * (A(I) + RMM(I)/2), (\text{in}^2) \quad (4-3)$$

In practice $RMM(I)$ is at least 2 orders of magnitude less than $A(I)$, so equation (4-3) simplifies to:

$$A(I) = 2 * \pi * (T/\cos \phi) * A(I), (\text{in}^2) \quad (4-4)$$

If equation (4-4) is substituted into equation (4-2), then:

ORIGINAL PAGE IS
OF POOR QUALITY

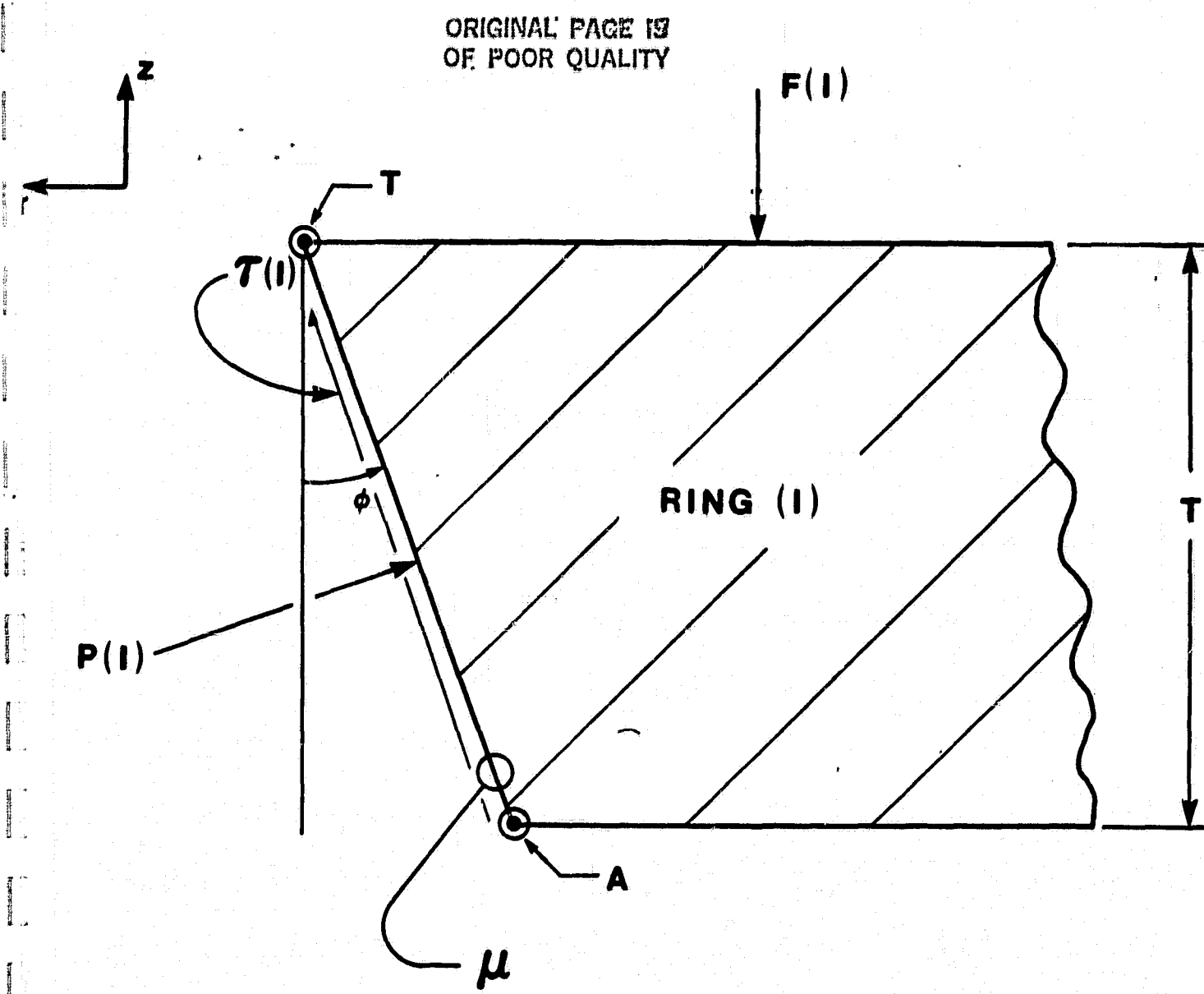


Figure 4.2

Schematic diagram of the pressing force
and interface stresses acting on Ring (I)

$$F(I) = 2 * \pi * (T/\cos \phi) * A(I) * (\mu * P(I) \cos \phi + P(I) * \sin \phi)$$

$$F(I) = 2 * \pi * A(I) * T * P(I) * (\mu + \tan \phi), \text{ (lbs)} \quad (4-5)$$

FLYSIZE calculates the assembly force between Rings (I) and (I+1) using equation (4-5). The actual pressures ($P(I)$) used by FLYSIZE are the partial assembly pressures required to add Ring (I+1) to all previously assembled rings. This means that the force calculated using equation (4-5) will be the partial assembly force required to add Ring (I+1) to all the previously assembled rings. Note that multiring assembly always starts from the inside ring outward, and that the first 2 rings which are press assembled are rings 2 and 3. Ring 1 is always segmented iron and requires no interference assembly.

Practically this means that it is added last and simply bonded into place.

4-3 Calculation of Ring Thickness

To calculate the ring thickness (T), assume that the following information is known:

KE = the required total stored energy in the flywheel, (Wh)

VED = the volumetric energy density of the subject flywheel, (Wh/ft³)

b = flywheel outer radius, (inches)

Since $VED = KE/(\pi b^2 T)$ by definition then:

$$T = 1728 * KE/(\pi * b^2 * VED), \text{ (inches)} \quad (4 - 6)$$

where the constant 1728 converts ft³ to in³.

FLYSIZE calculates the ring thickness using equation (4-6).

4-4 Calculation of Maximum Wheel RPM

To calculate the maximum wheel rpm assume that the following information is known:

$\rho_1 \omega^2 b^2$ = a known value from the FLYANS code, (psi); call this K

ρ_1 = mass density of the ring (1); equal to weight density ($\gamma(1)$) of ring (1) divided by g (386 in/sec²)

b = outer radius of the flywheel (inches)

Since ω is the angular rotational speed (radians/sec), it is equal to the rpm (N) as:

$$\omega = \frac{(2)(\pi)}{60} (N) \quad (4-7)$$

If equation (4-7) is applied to $\rho_1 \omega^2 b^2 = K$ then:

$$N = \frac{(60)}{(2)(\pi)(b)} \sqrt{K/\rho_1} \quad (4-8)$$

simplifying

$$N = \frac{(60)}{(2)(\pi)(b)} \sqrt{386} (\sqrt{K/\gamma(1)}) \quad (4-9)$$

$$N = \frac{187.61}{b} \sqrt{\frac{K}{\gamma(1)}} , \text{ (rpm)} \quad (4-10)$$

FLYSIZE calculates the flywheel rpm using equation (4-10).

4-5 Calculation of Miscellaneous Values

To calculate the nominal ring radius ($A(I)$) values, assume the following information is known:

$RR(I)$ = Inside radius ratios for Ring (I), (dimensionless)

b = outside radius of flywheel, (inches)

Then:

$$A(I) = RR(I) * b \quad (4-11)$$

FLYSIZE computes the inside radius of each ring using equation (4-11). If there is no interference between rings the outside radius of Ring (I) is equal to the inside radius of Ring (I+1), namely $A(I+1)$. If there is interference then the outside radius of Ring (I) is equal to the nominal inside radius of the next Ring ($A(I+1)$) plus the radial mismatch ($RMM(I)$) between Ring (I) and (I+1). Recall that $RMM(I)$ has previously been discussed in section 4-1.

To calculate the weight of each ring assume that the following information is known:

$A(I)$ = nominal inside radius of ring (I), (inches)

$A(I+1)$ = nominal outside radius of ring (I), (inches)

$\gamma(I)$ = weight density for ring (I), (lb/in^3)

Then:

$$WT(I) = RINGVOL * \gamma(I) \quad (4-12)$$

where:

$RINGVOL$ = volume of ring (I), RING AREA * T, (in^3)

$RINGAREA$ = $\pi * (A(I+1)^2 - A(I)^2)$

T = ring thickness, (inches)

FLYSIZE calculates the weight of each ring using equation (4-12), and then adds up all the ring weights to obtain the total weight of the rotor.

To calculate the maximum inner radius displacement (i.e. gap growth) of the flywheel, assume that the following information is known:

b = flywheel outer radius, (inches)

IRDR = inner radius displacement ratio, (dimensionless)

Since:

$$\text{IRDR} = \frac{gg}{b}$$

Then:

$$gg = (\text{IRDR}) * b \quad (4-13)$$

where:

gg = air gap growth or displacement of inner flywheel radius from 0 speed to maximum speed, (inches)

FLYSIZE calculates the maximum air gap growth using equation (4-13).

APPENDIX 5

Determining Ring Dimensions Using FLYSIZE Results

As an example of the procedure used to select ring dimensions and tolerances, consider the design NASA-12, rings 3 and 4, as previously shown in Table II.10. The dimensions of the two rings are summarized below:

Ring	Inside Radius	Outside Radius	Radial Mismatch
(--)	(inches)	(inches)	(inches)
3	6.000	7.018	0.018
4	7.000	8.021	

First the radius of each ring is converted to a diameter and a tolerance of $\pm .001$ inches is assigned to the diameter. Thus:

$$\text{O.D. (ring 3)} = 14.036 \pm .001 \text{ inches}$$

$$\text{I.D. (ring 4)} = 14.000 \pm .001 \text{ inches}$$

Using these specifications the maximum and minimum radial interference at the 3-4 interface can be obtained and is:

$$\text{max. radial interference} = 0.019 \text{ inches}$$

$$\text{min. radial interference} = 0.017 \text{ inches}$$

This variation in interference is considered acceptable and will not degrade performance. It is now necessary to choose a tolerance on the ring taper angles so that the design interference will be acceptable after assembly is completed.

Consider the drawing shown in Figure 5.1, showing the interface between rings 3 and 4. The nominal taper angle, $\phi(\text{nom})$, must be selected so that point B on ring 3 lies to the inside of point A' on ring 4. A value of $\phi(\text{nom}) = 1^\circ$ will accomplish this for all rings in the NASA-12 design so it will be used.

It is mandatory that the tolerances on the interface taper angle, ϕ , be selected so that the interference between the top of ring 3 (point A) and the

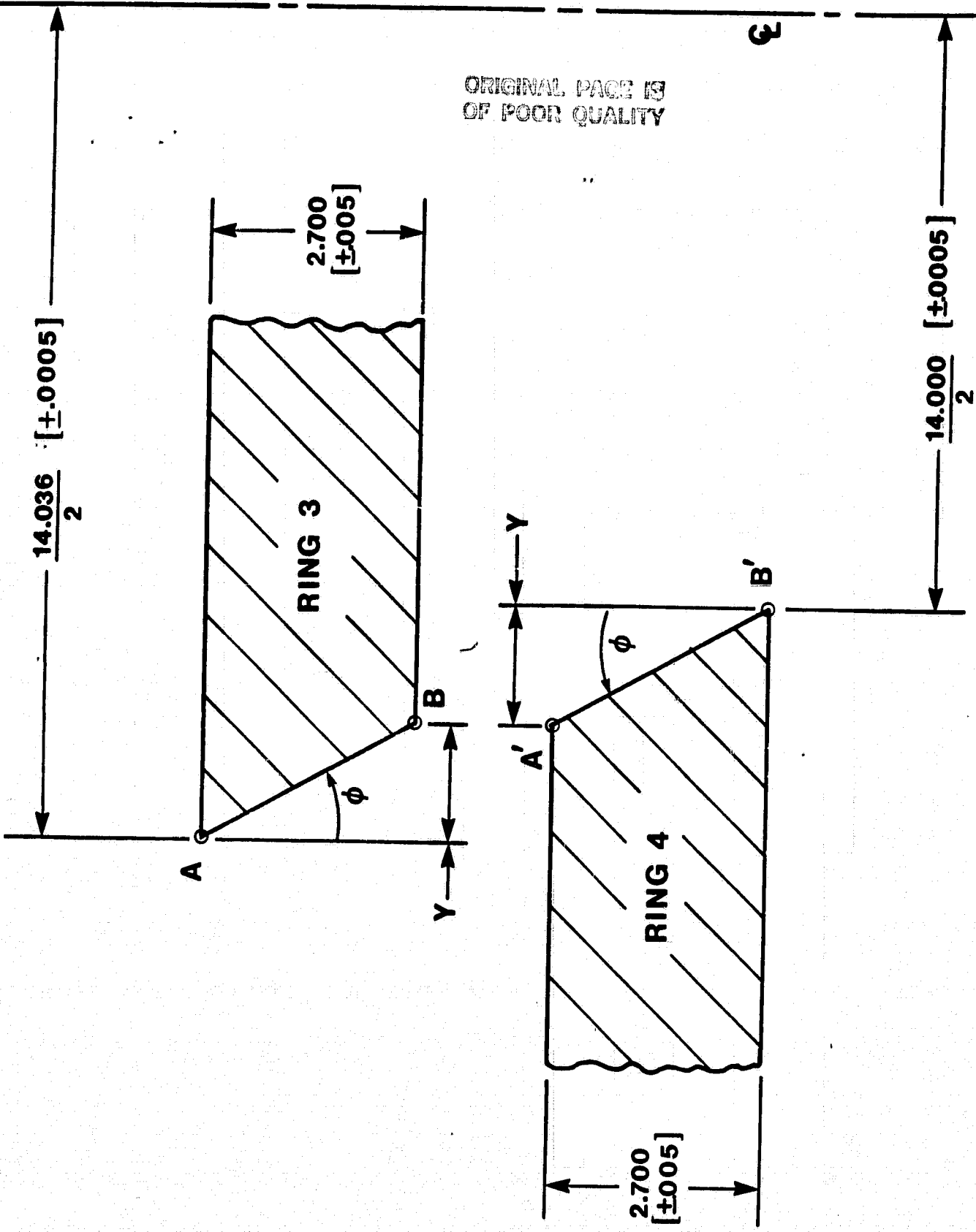


Figure 5.1
Ring 3 and Ring 4 interface in the NASA design

top of ring 4 (point A') be "close to" the interference between the bottom of ring 3 (point B) and the bottom of ring 4 (point B'). This means that the nominal value of dimension Y must not vary by more than $\pm .0005$ inches between ring 3 and ring 4. Assuming the $\phi(\text{nom})$ is 1 degree, then:

$$Y(\text{nom}) = 2.7 * \tan(1^\circ) = 0.0471 \text{ inches}$$

Thus:

$$Y(\text{max}) = 0.0471 + .0005 = .0476$$

$$Y(\text{min}) = 0.0471 - .0005 = .0466$$

and:

$$\tan \phi(\text{max}) = Y(\text{max})/2.7$$

$$\phi(\text{max}) = 1.01$$

$$\tan \phi(\text{min}) = Y(\text{min})/2.7$$

$$\phi(\text{min}) = 0.99$$

The tolerance on ϕ is therefore ± 0.01 degrees.

Practically, this means that the interface between rings 3 and 4 must be measured and then machined to assure that the diameter of the top of ring 3 is within ± 0.0005 of the diameter of the top of ring 4. And, the diameter of the bottom of ring 3 is within ± 0.0005 of the bottom of ring 4.

APPENDIX 6

**Plots of Stress vs. Radius Ratio for
NASA-12 and NASA-20 Rotor Designs**

CHART NO. 65
OF PAPER QUALITY

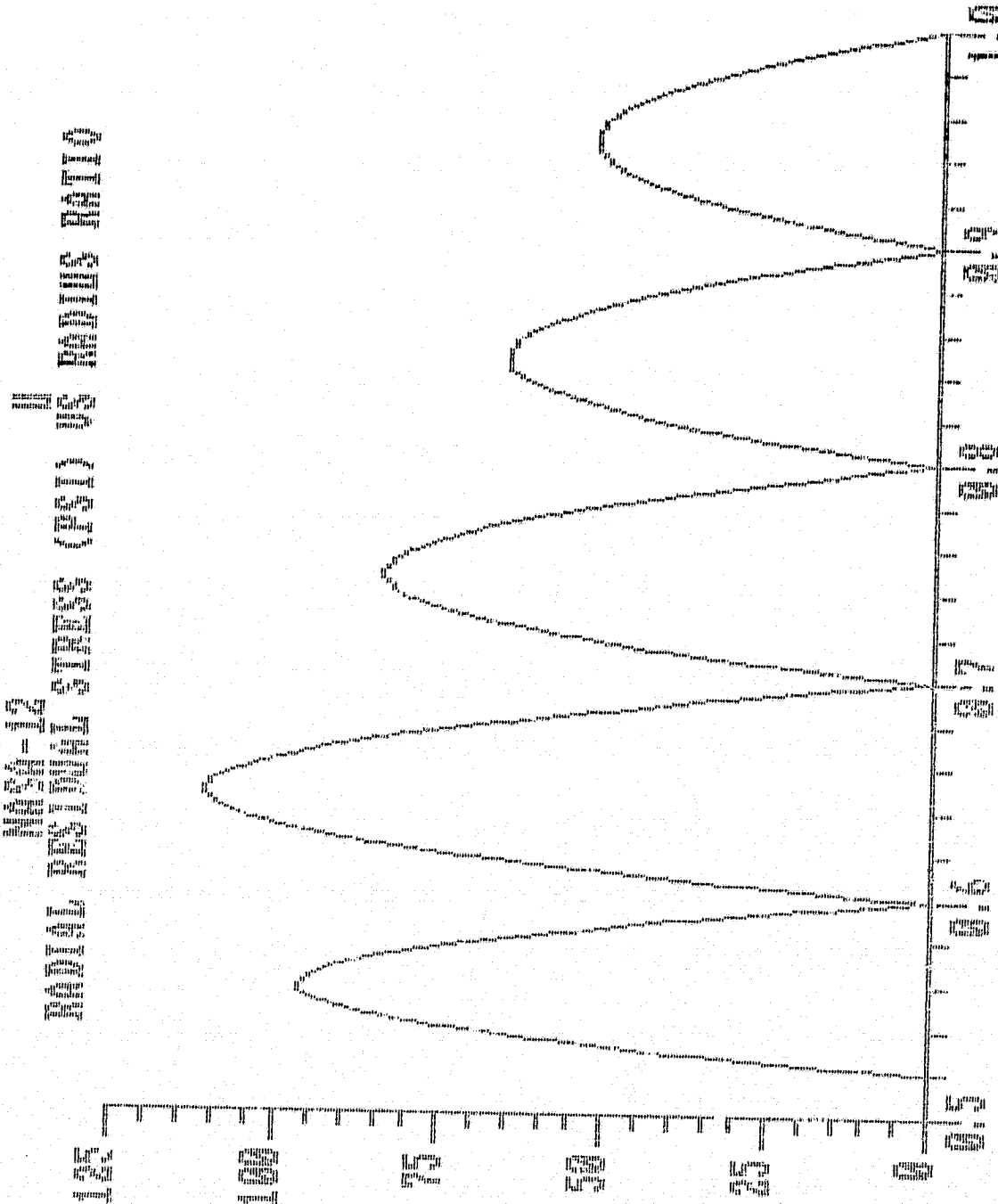


Fig. 6-1A

ORIGINAL PAGE IS
OF POOR QUALITY

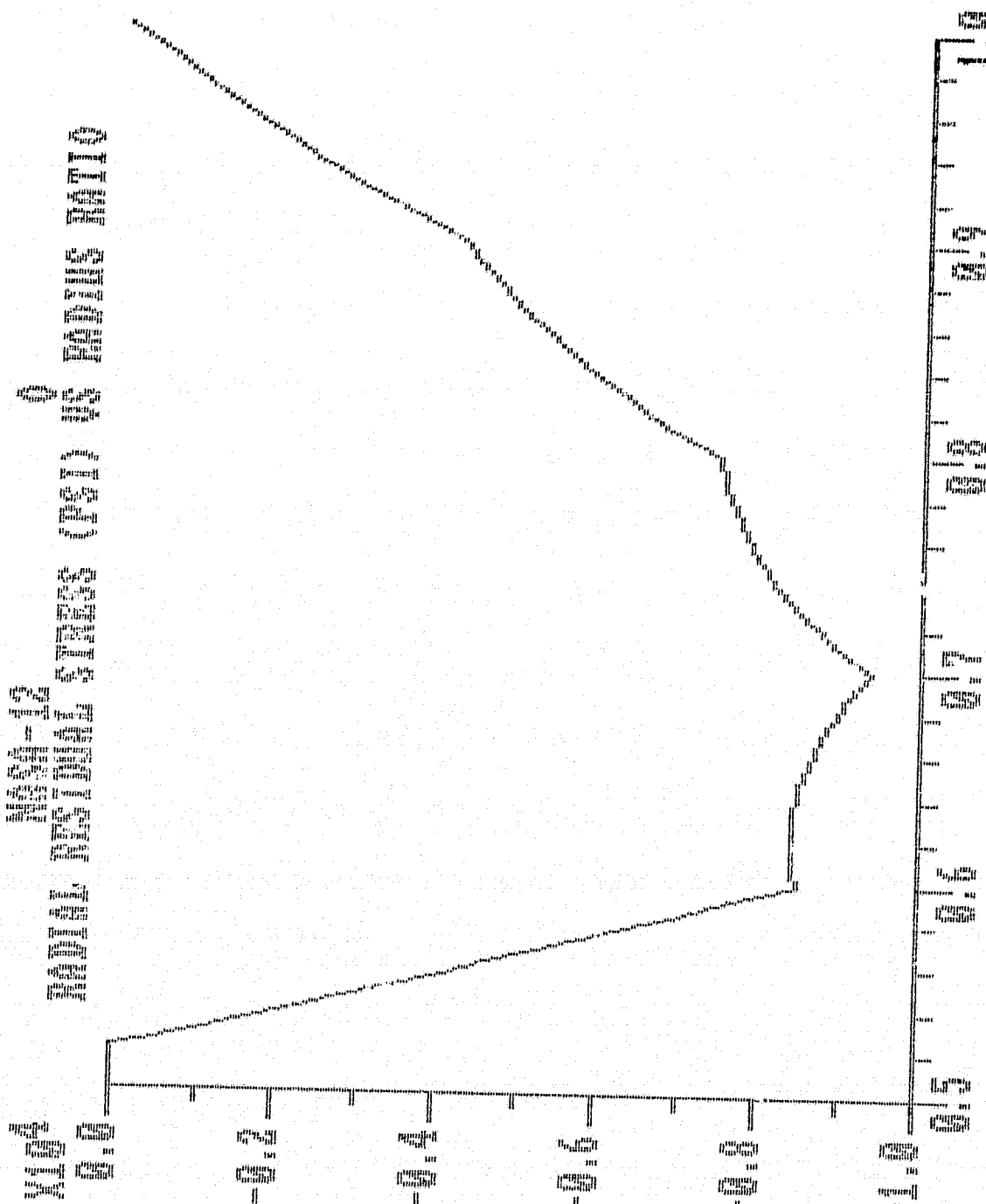


Fig. 6-1B

ORIGINAL PAGE IS
OF POOR QUALITY

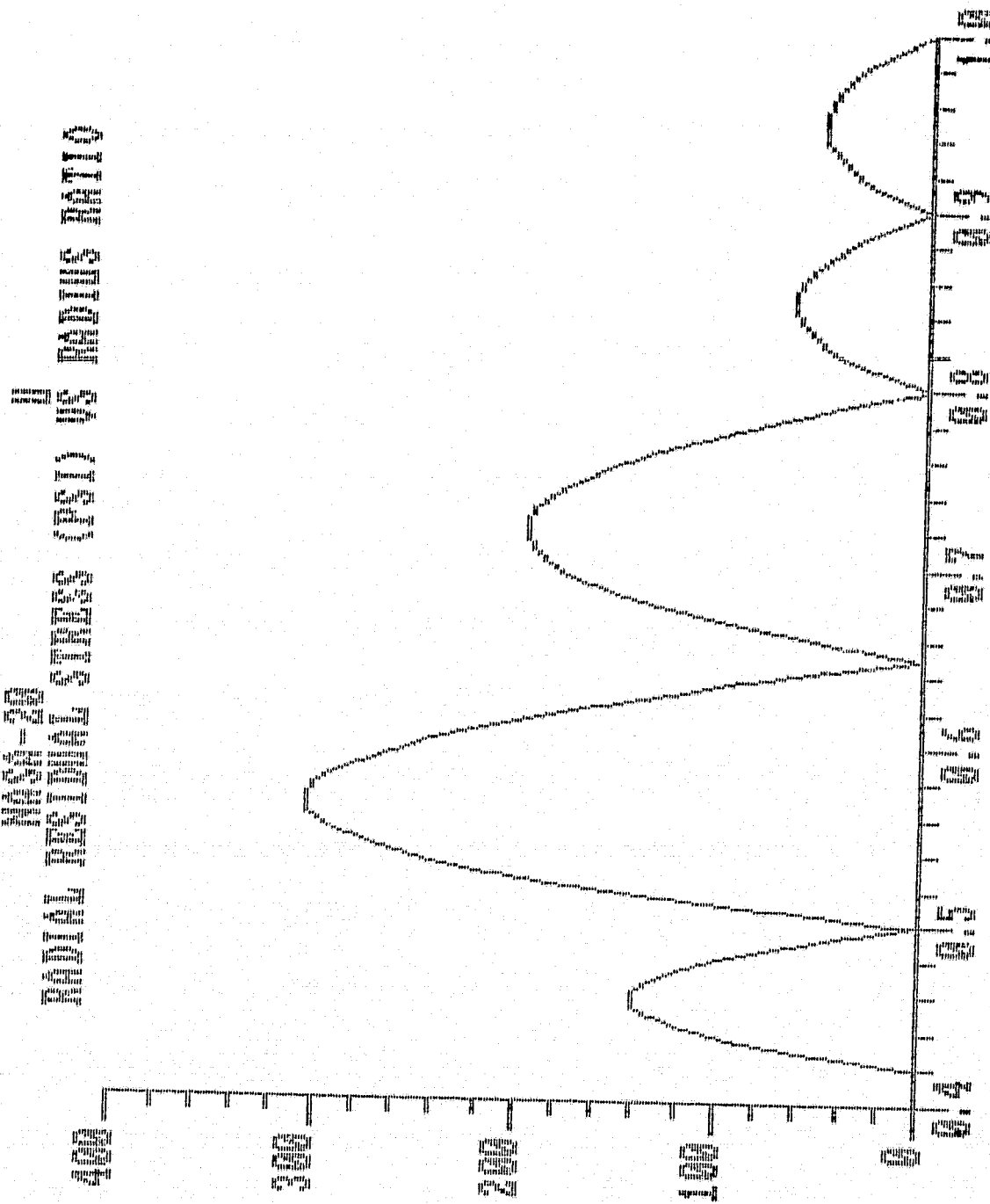


Fig. 6-1C

ORIGINAL PAGE IS
OF POOR QUALITY

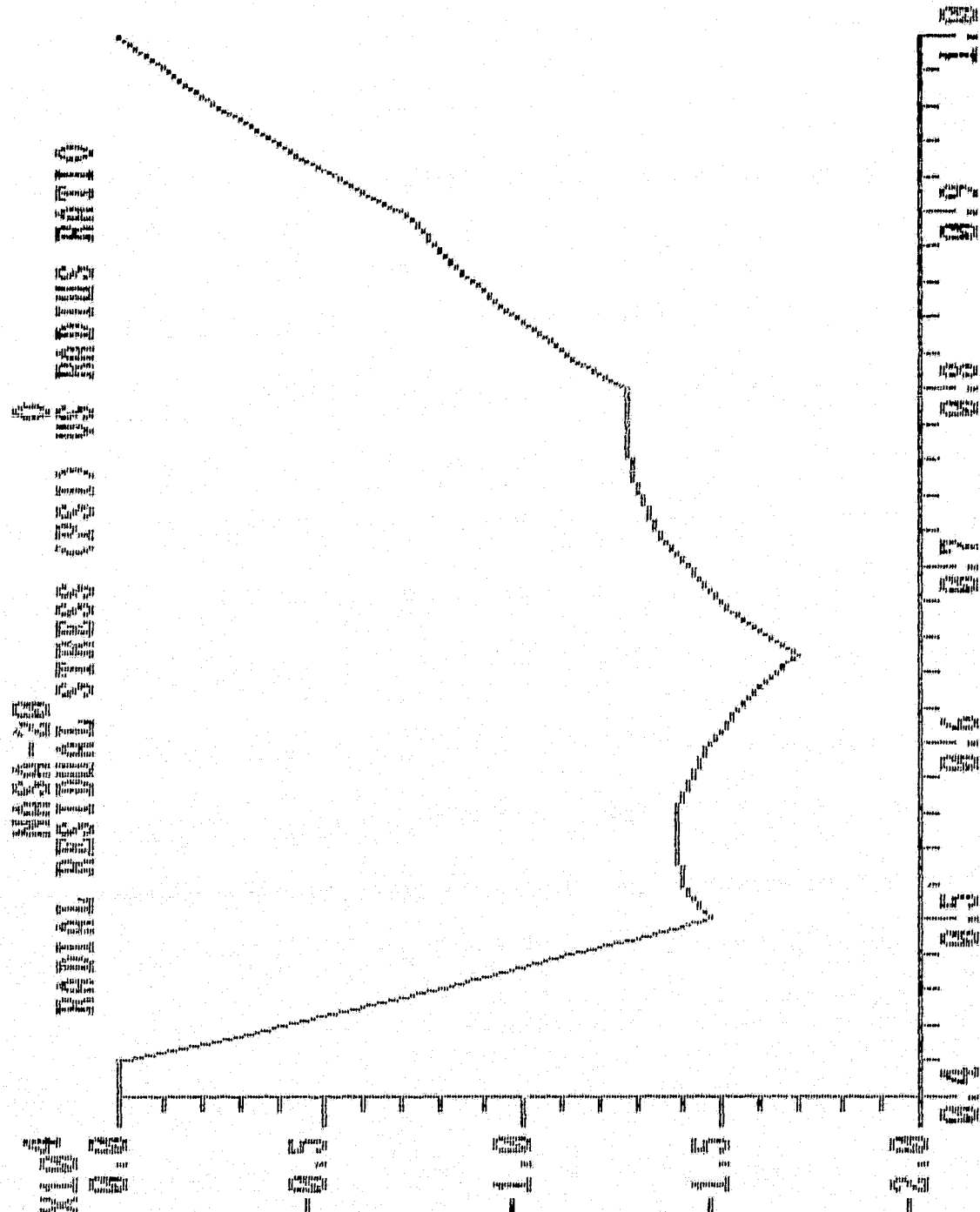


Fig. 6-1D

ORIGINAL PAGE IS
OF POOR QUALITY

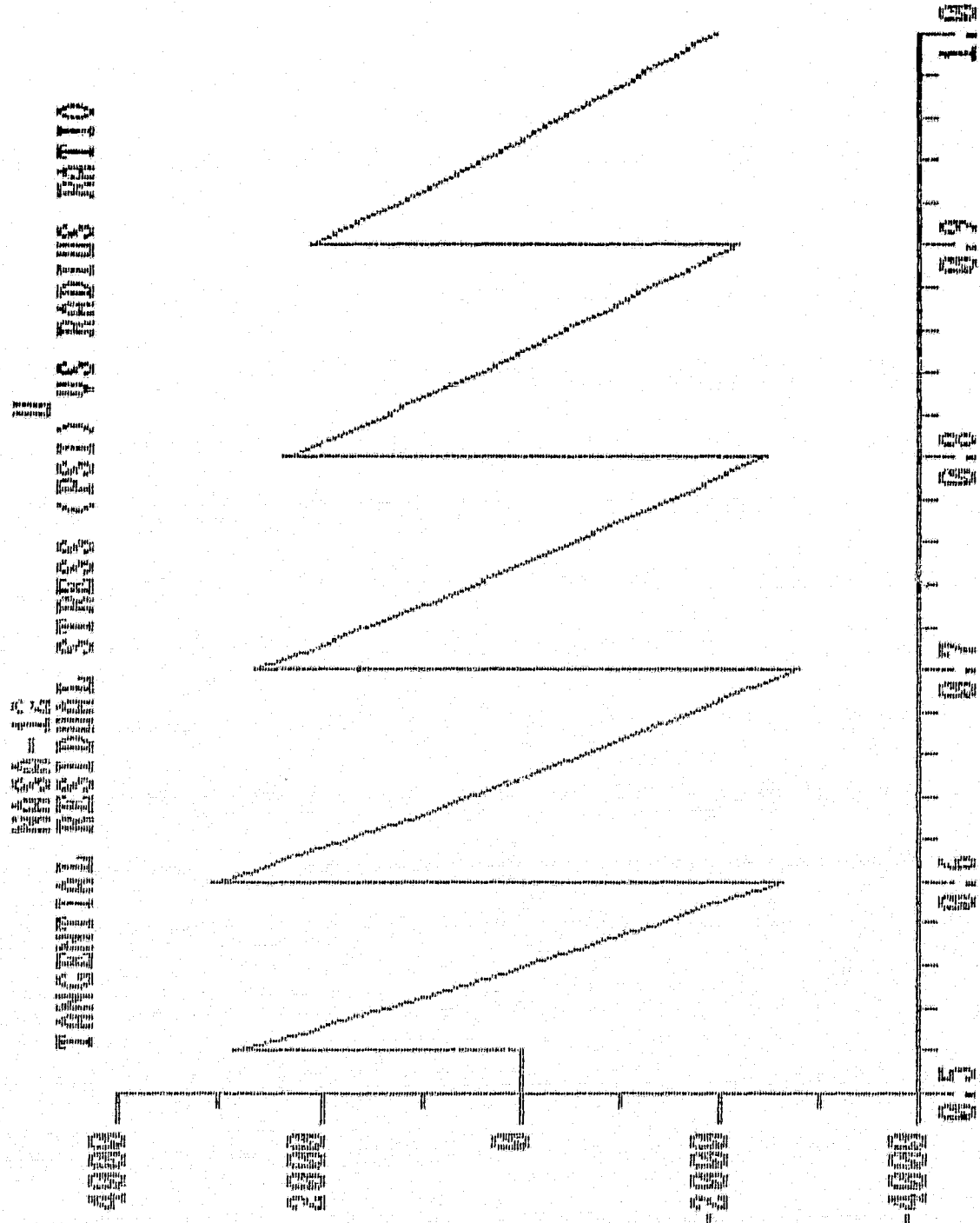


Fig. 6-2A

ORIGINAL PAGE IS
OF POOR QUALITY

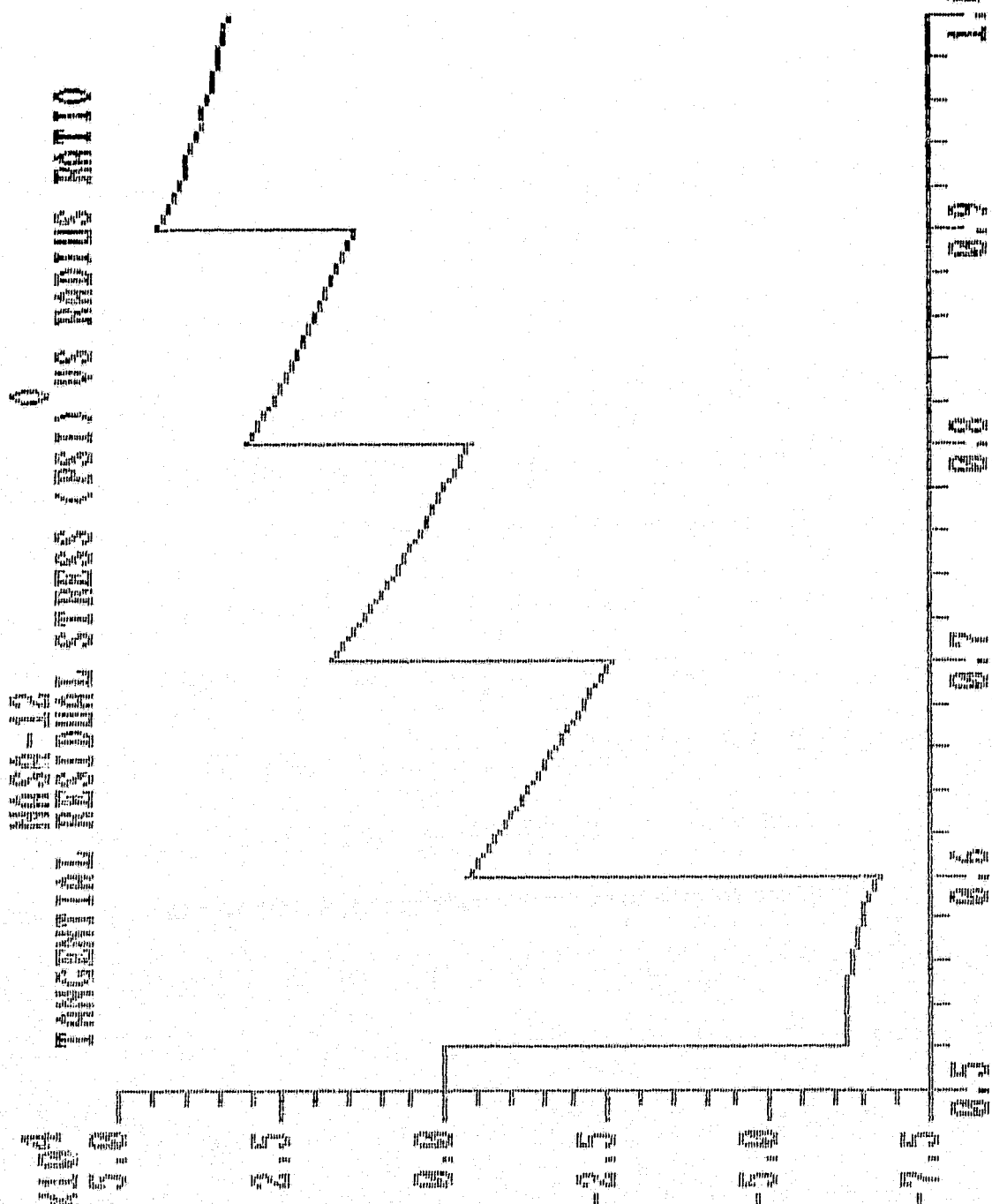


Fig. 6-28

C-2

ORIGINAL PAGE IS
OF POOR QUALITY

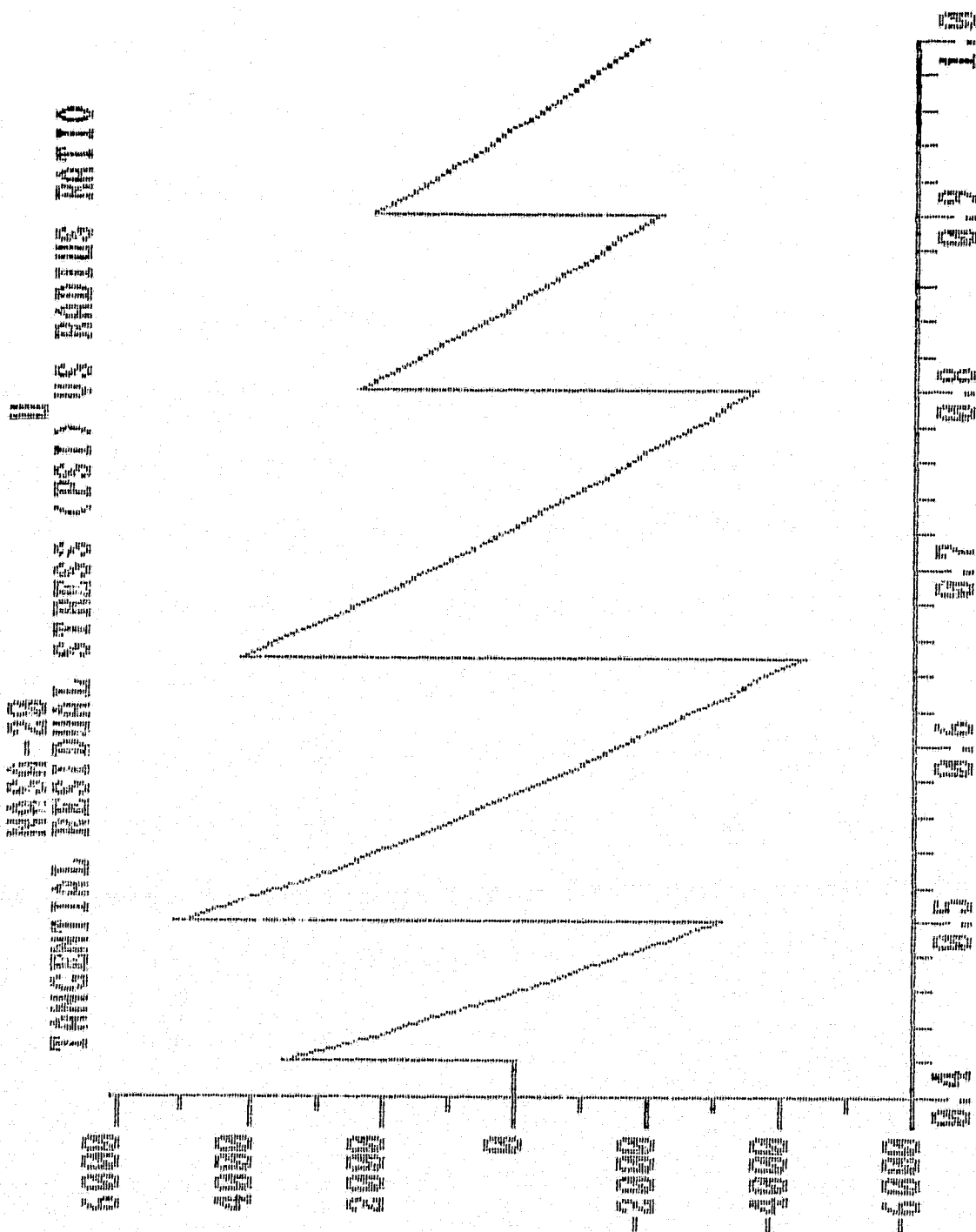


Fig. 6-2C

ORIGINAL PAGE IS
OF POOR QUALITY

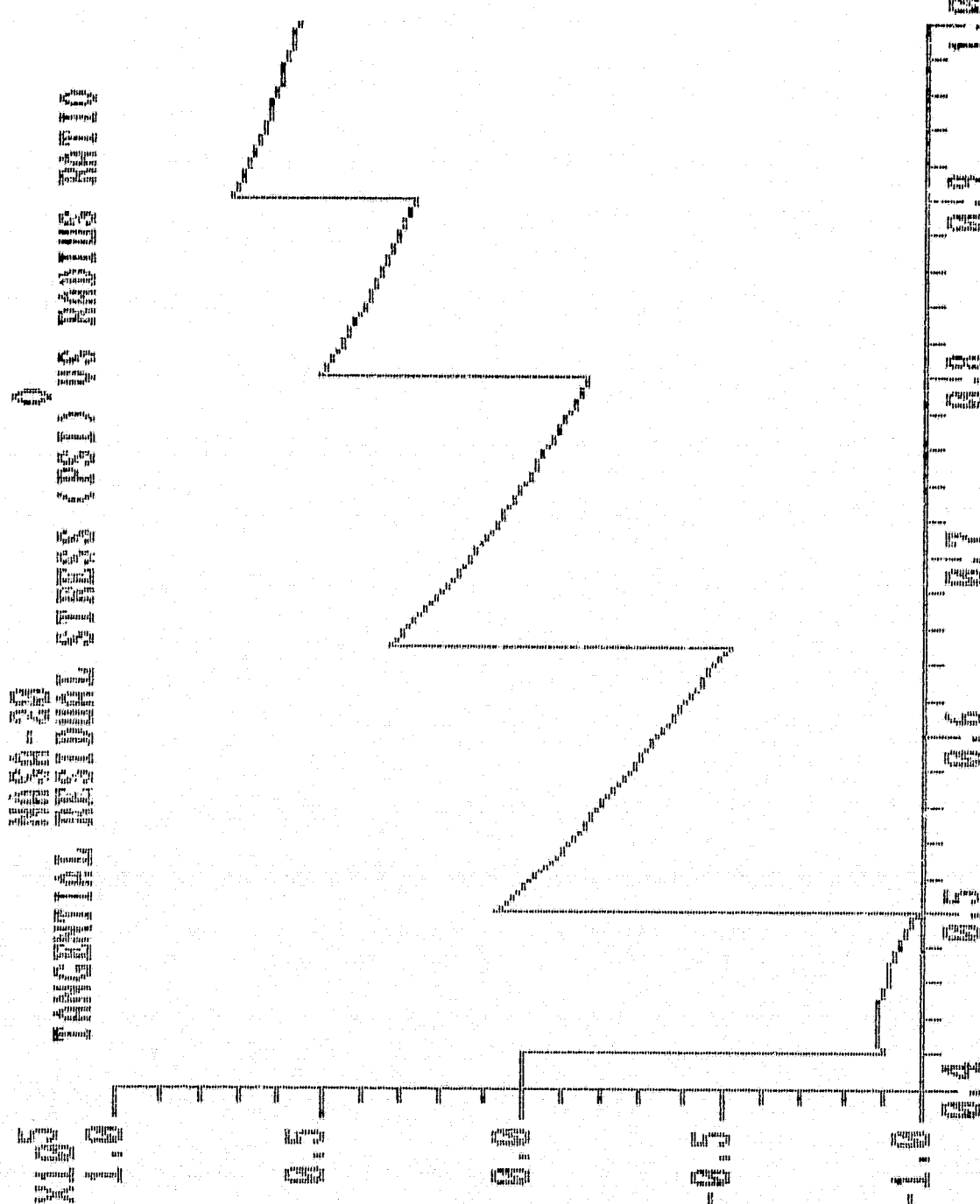


Fig. 6-2D

ORIGINAL PAGE IS
OF POOR QUALITY.

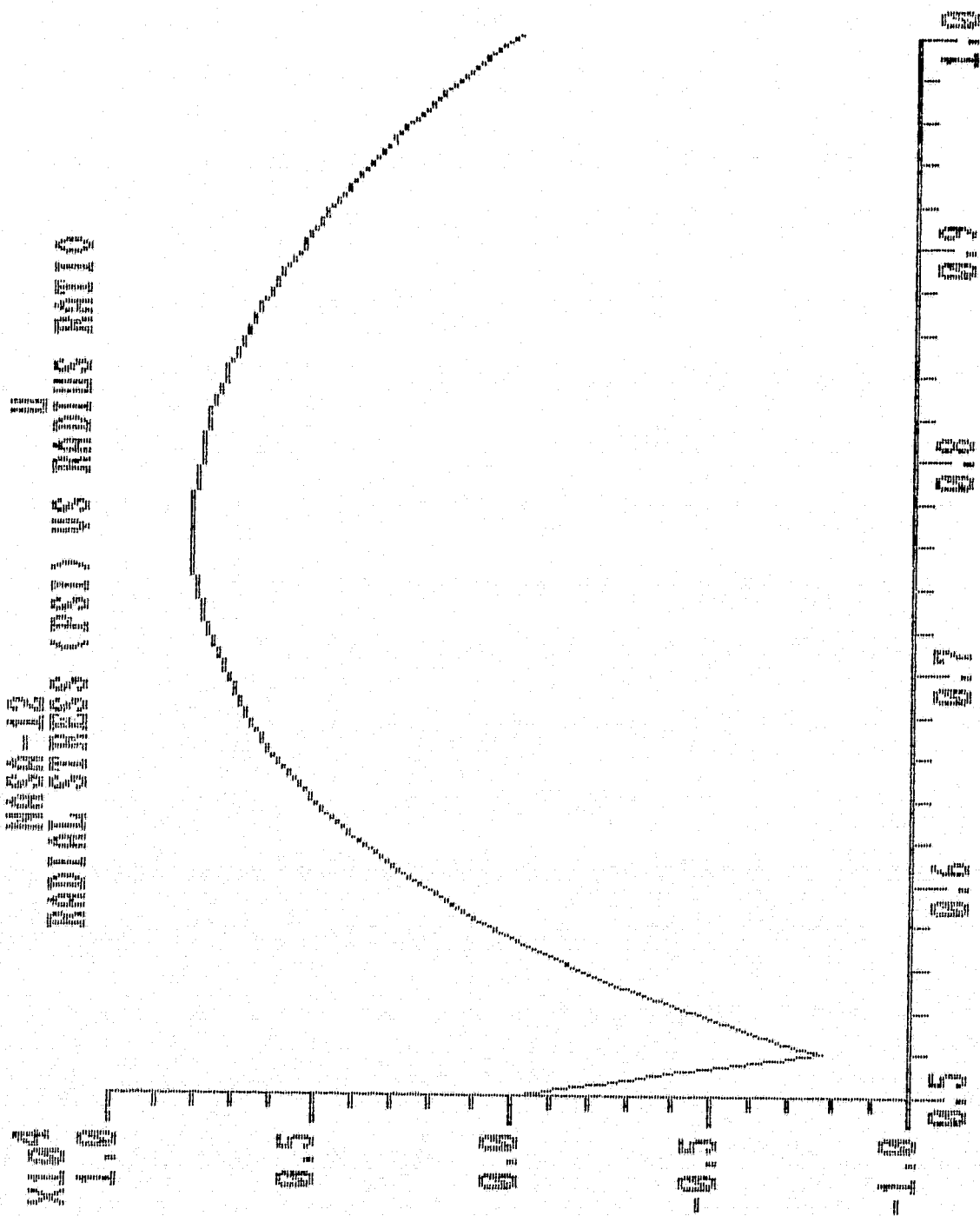


Fig. 6-3A

ORIGINAL PAGE IS
OF POOR QUALITY

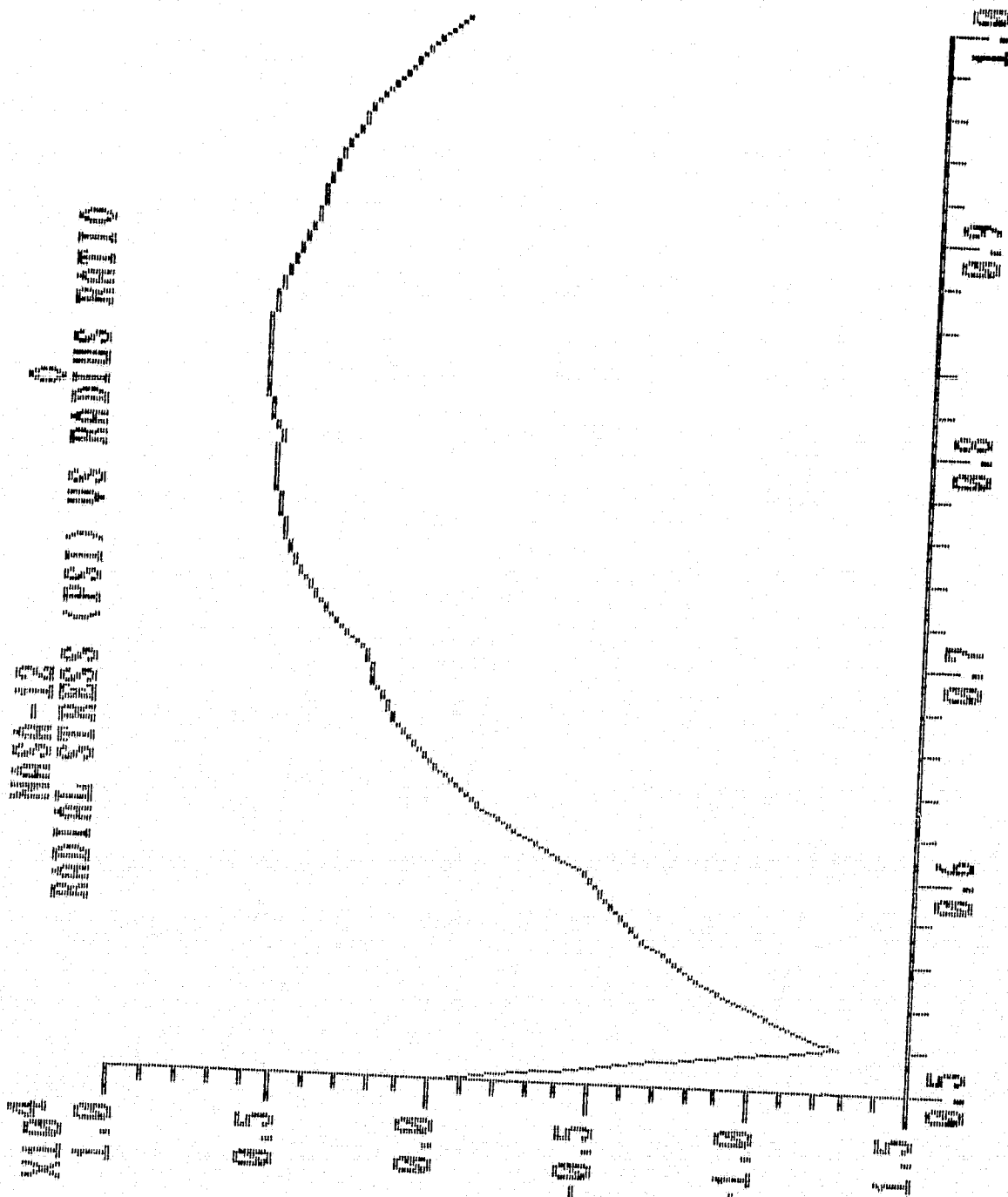
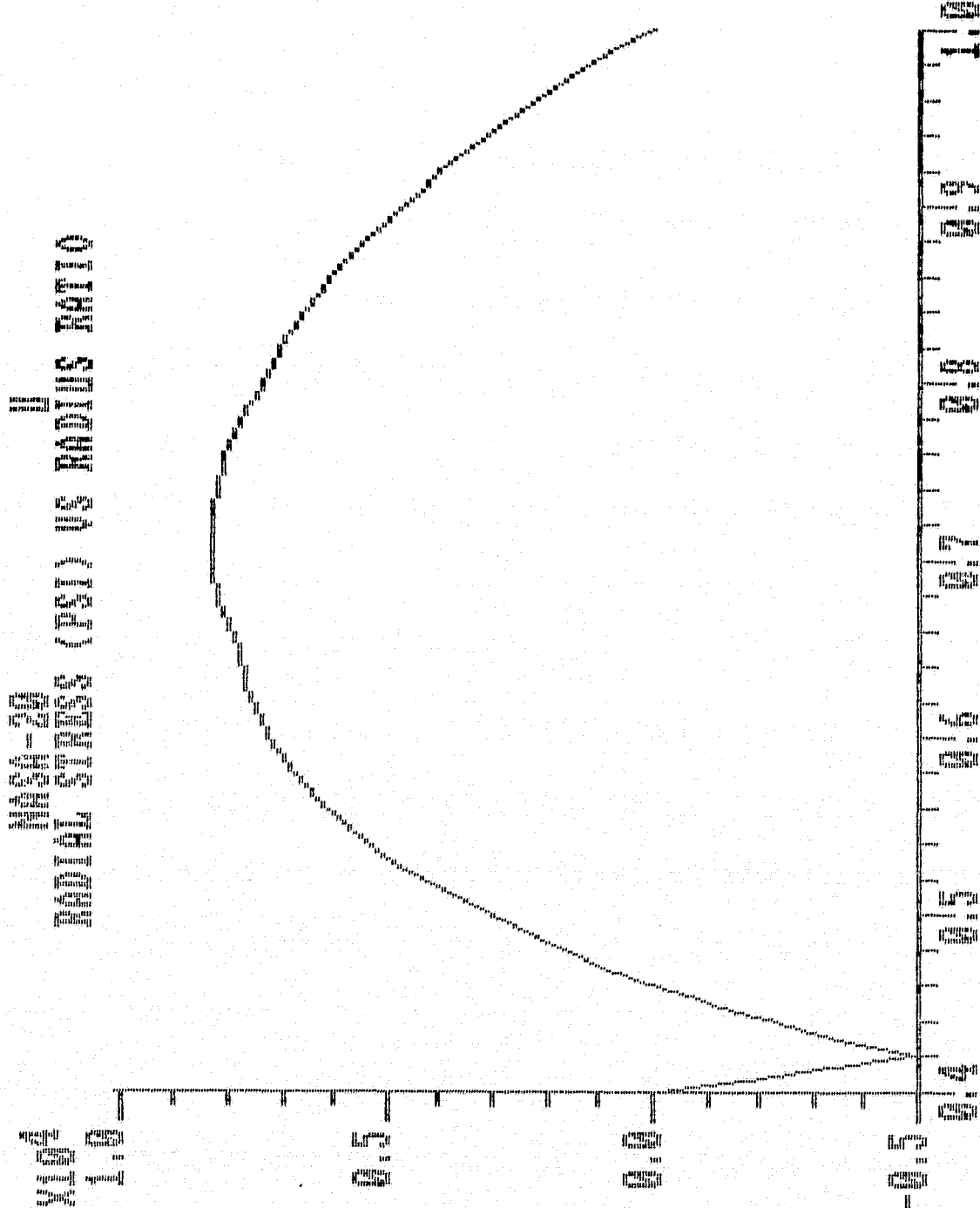


Fig. 6-3B

ORIGINAL PAGE IS
OF POOR QUALITY

Fig. 6-3C



ORIGINAL PAGE IS
OF POOR QUALITY

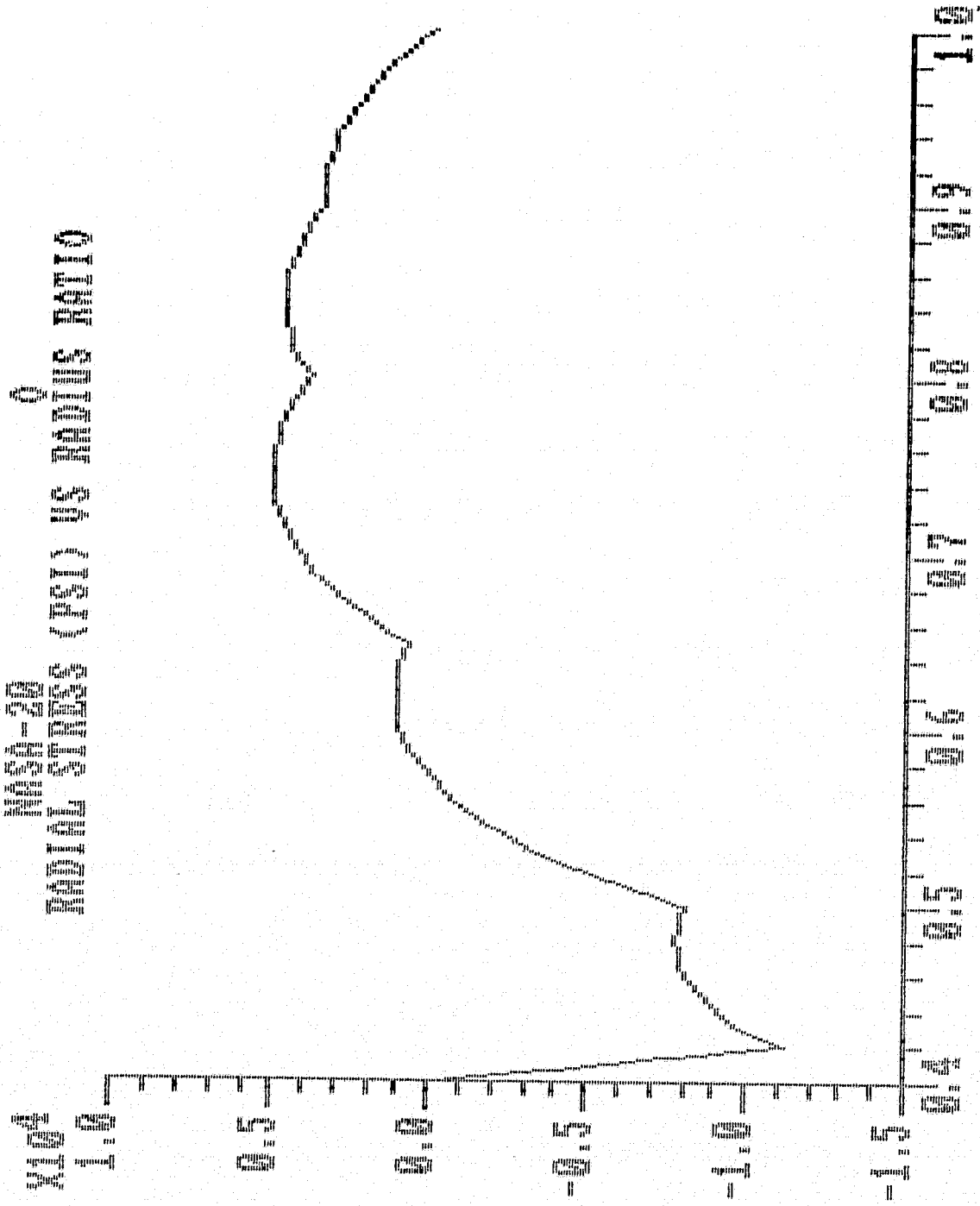


Fig. 6-3D

**ORIGINAL PAGE IS
OF POOR QUALITY**

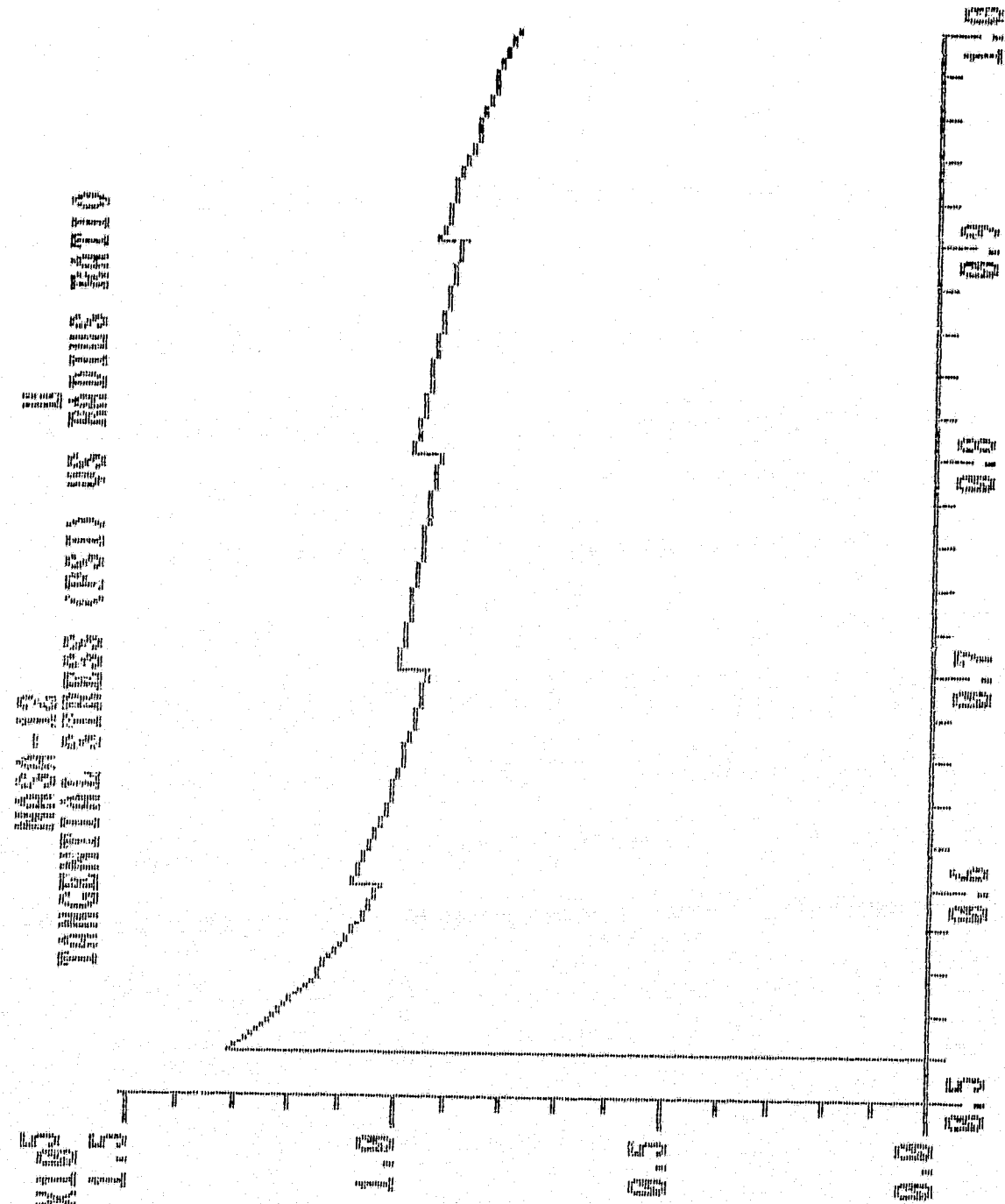


Fig. 6-4A

ORIGINAL PAGE IS
OF POOR QUALITY

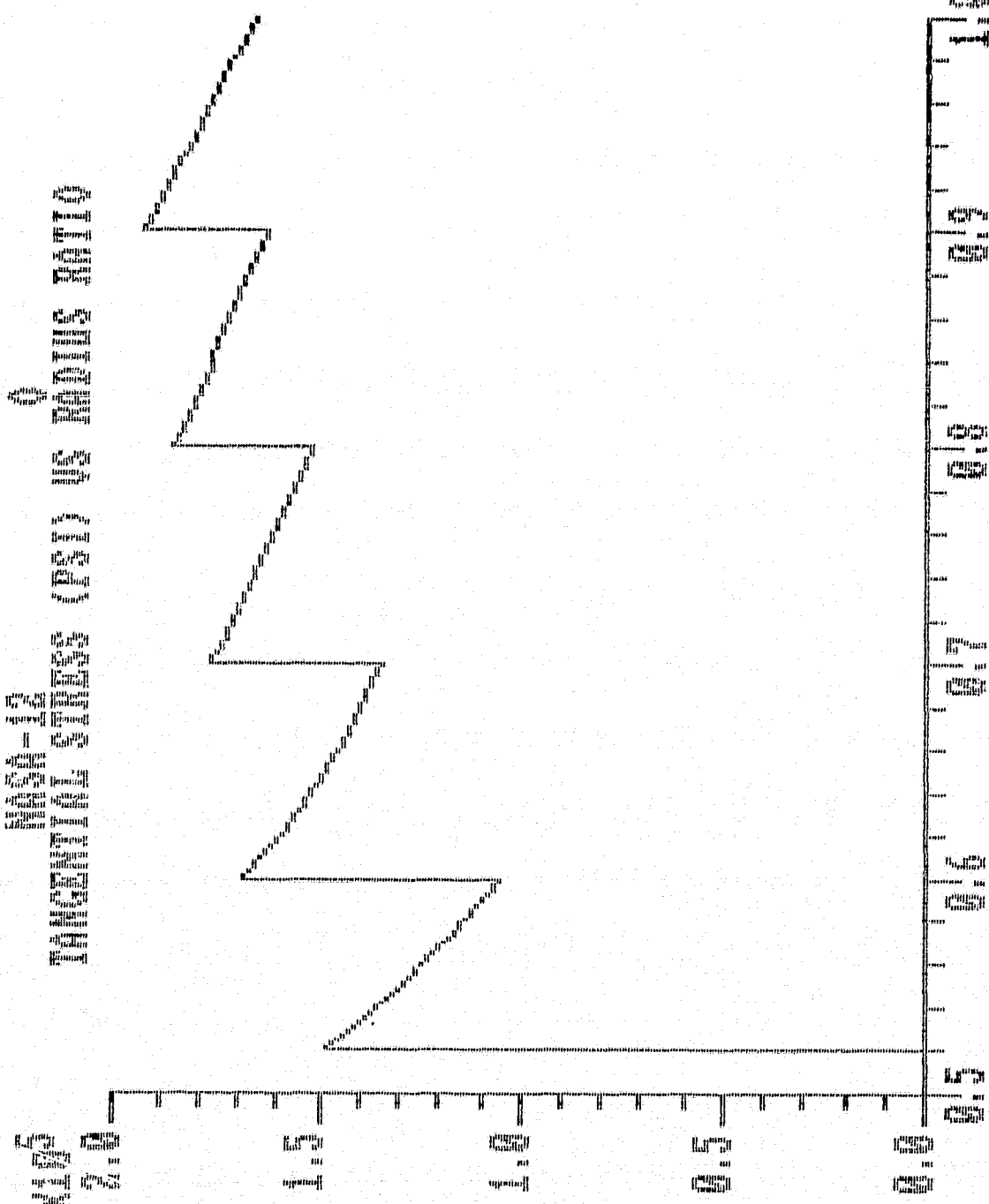


Fig. 6-4B

ORIGINAL PAGE IS
OF POOR QUALITY

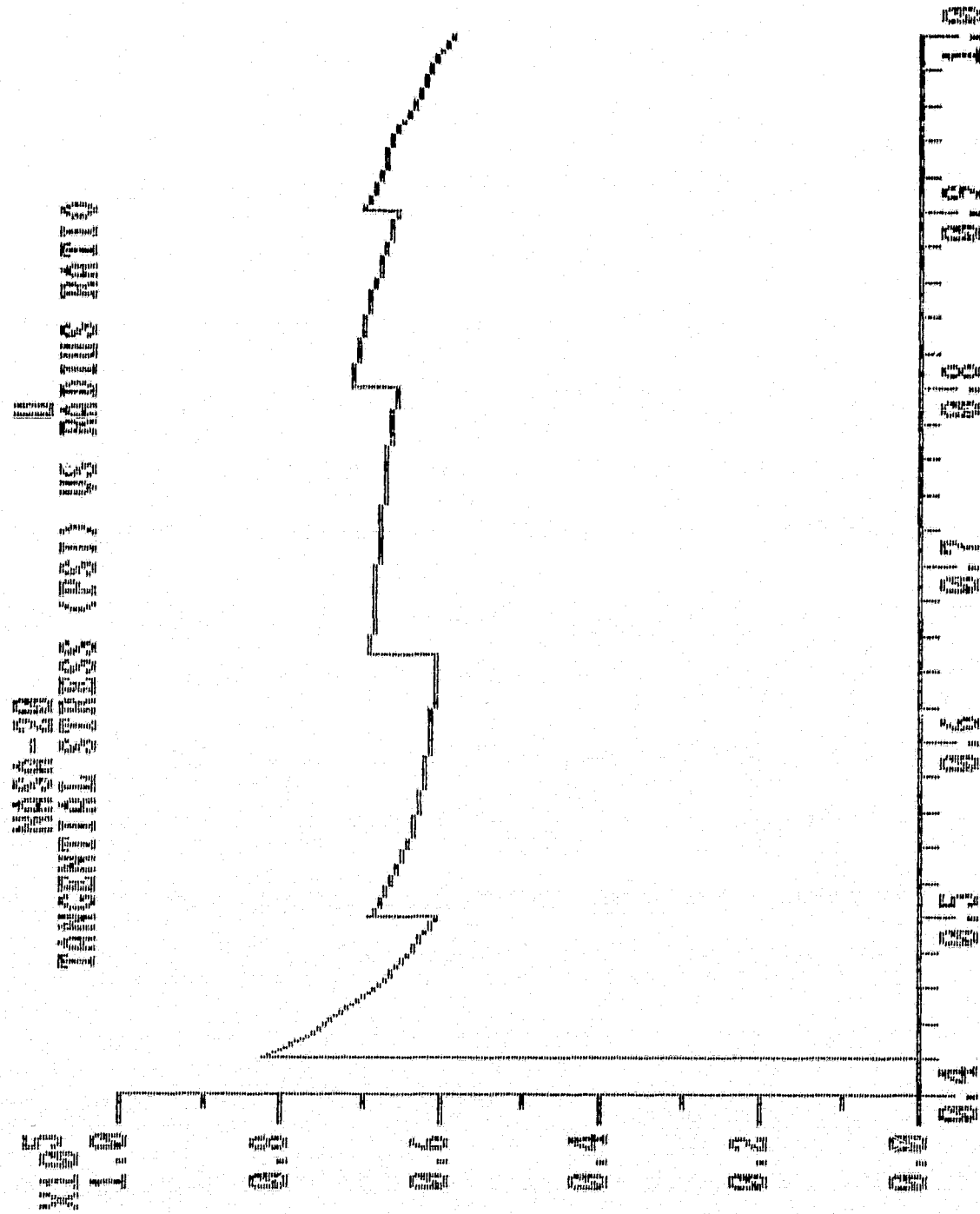


Fig. 6-4C

**ORIGINAL NOISE IS
OF POOR QUALITY**

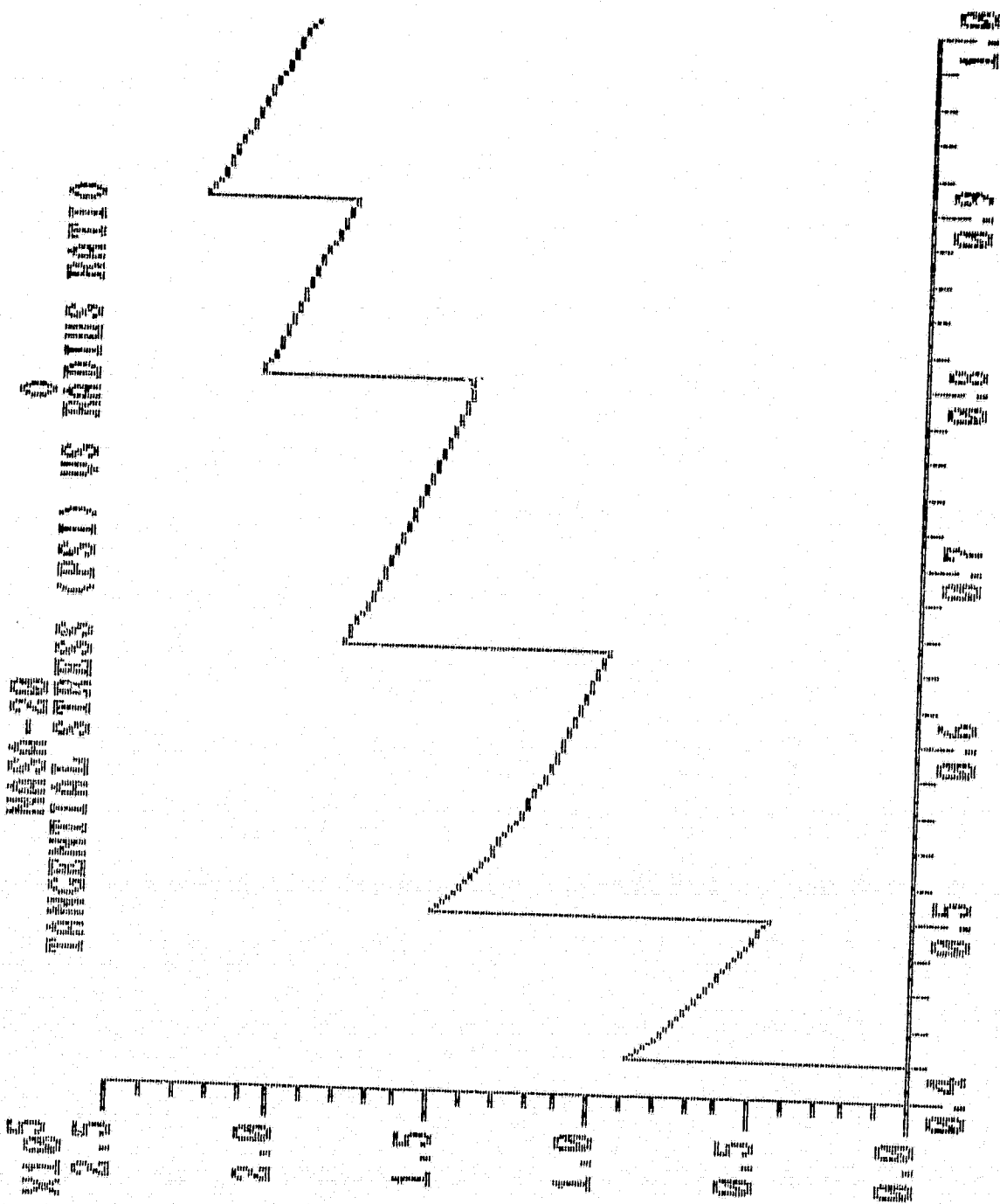


Fig. 6-40

APPENDIX 7

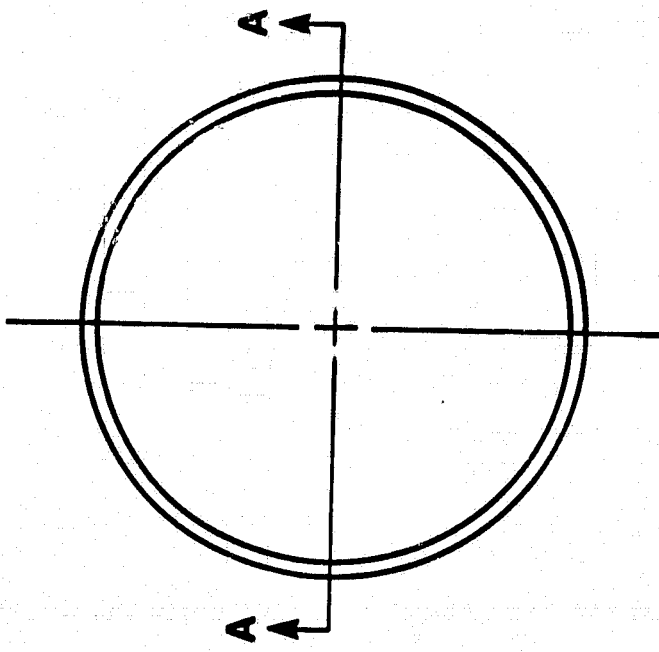
Engineering and Assembly Drawings for

NASA-12 and NASA-20

6 ring flywheel rotor designs

ORIGINAL PAGE IS
OF POOR QUALITY

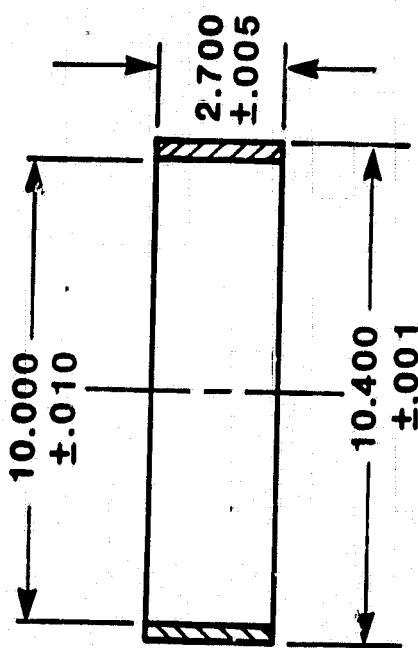
Drawing 7-1



Note: 1. Approximate ring
weight = 4.9 lbs.

2. This ring is added after
all others have been
assembled. Its exact
design has not been
determined as part of
this project.

Name	NASA-12
Name	Ring 1
Material	Segmented Iron
Date	12-30-83
Scale	1:4
Tol., Unless spec.	
Angles ± 0.1 , Dim. $\pm .001$	
Designer	JAK
Draftsman	JTS

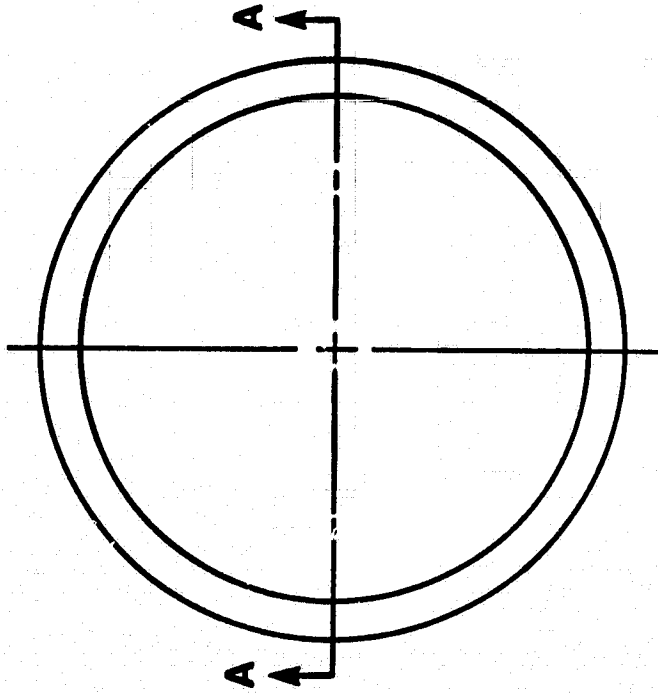


Section A-A

Drawing 7-2

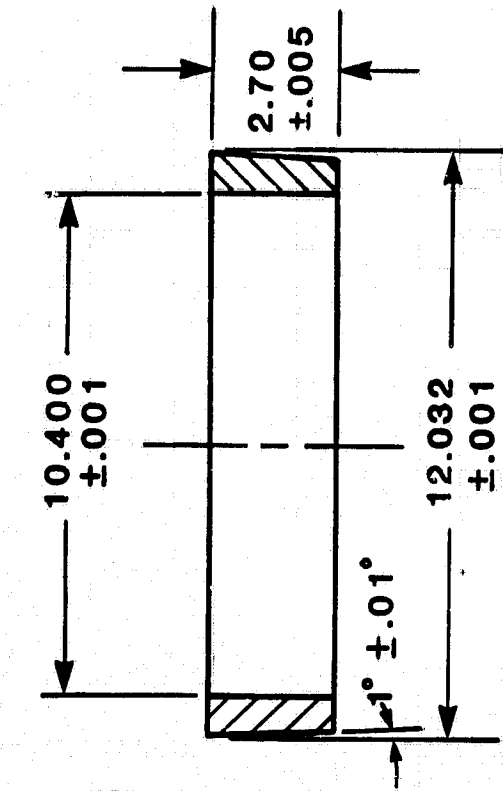
Note: Approximate ring weight = 4.2 lbs.

ORIGINAL PAGE IS
OF POOR QUALITY



Name	NASA-12
Name	Ring 2
Material	Cellon 6000/Epoxy
Date	12-30-83
Scale	Quarter
Tol., Unless Spec.	Angles ± 0.1 Dim. $\pm .001$
Designer	J A K
Drafterman	J T S

Taper angles
not to scale



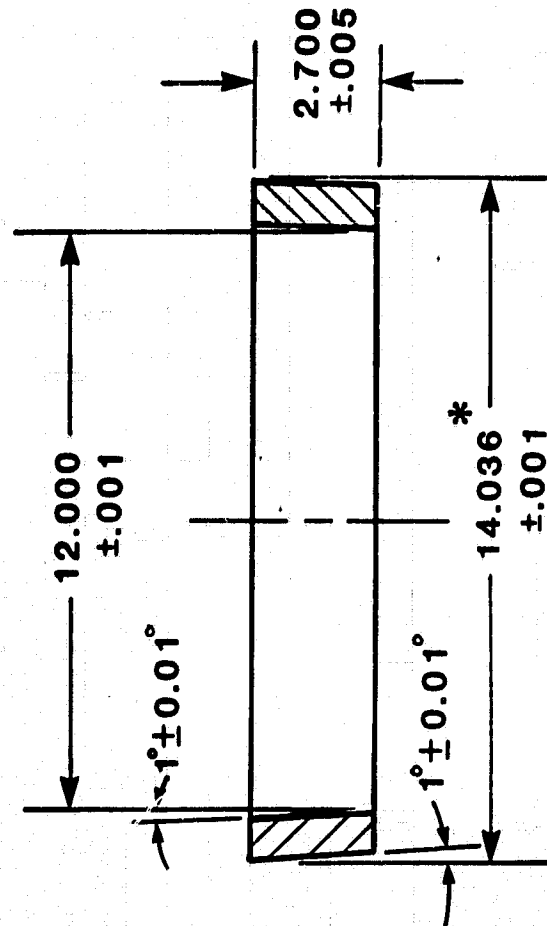
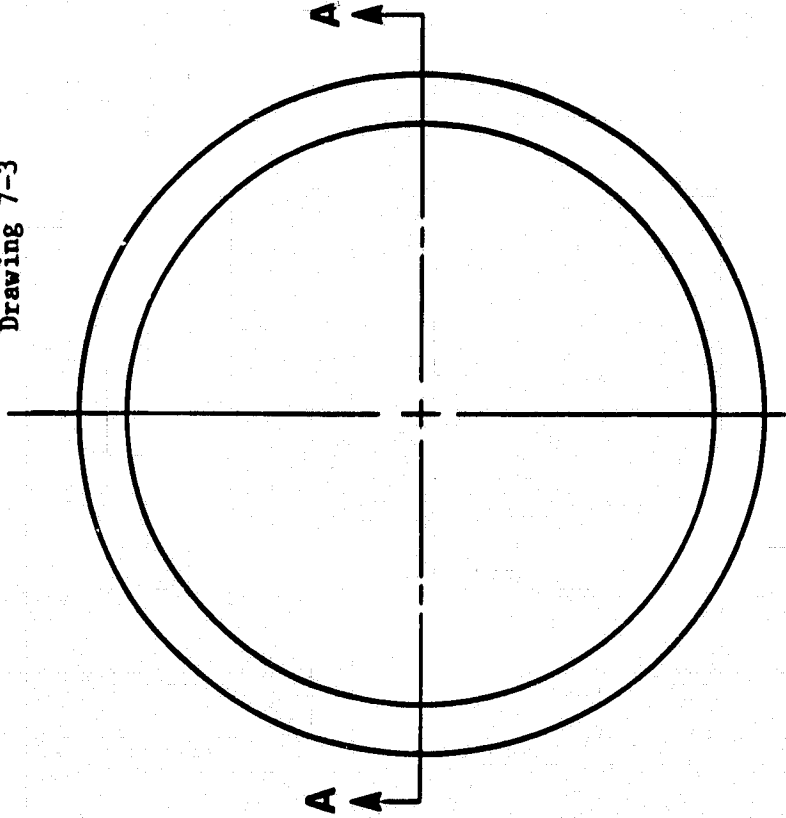
Drawing 7-3

Note: Approximate ring weight = 6.1 lbs.

* Machine after assembly

ORIGINAL PAGE IS
OF POOR QUALITY

Name	NASA-12
Name	Ring 3
Material	Celion 6000/Epoxy
Date	12-30-83
Scale	1:4
Tol., Unless spec.	Angles $\pm 0.1^\circ$, Dim. $\pm .001$
Designer	J A K
Draftsman	J T S



Section A-A

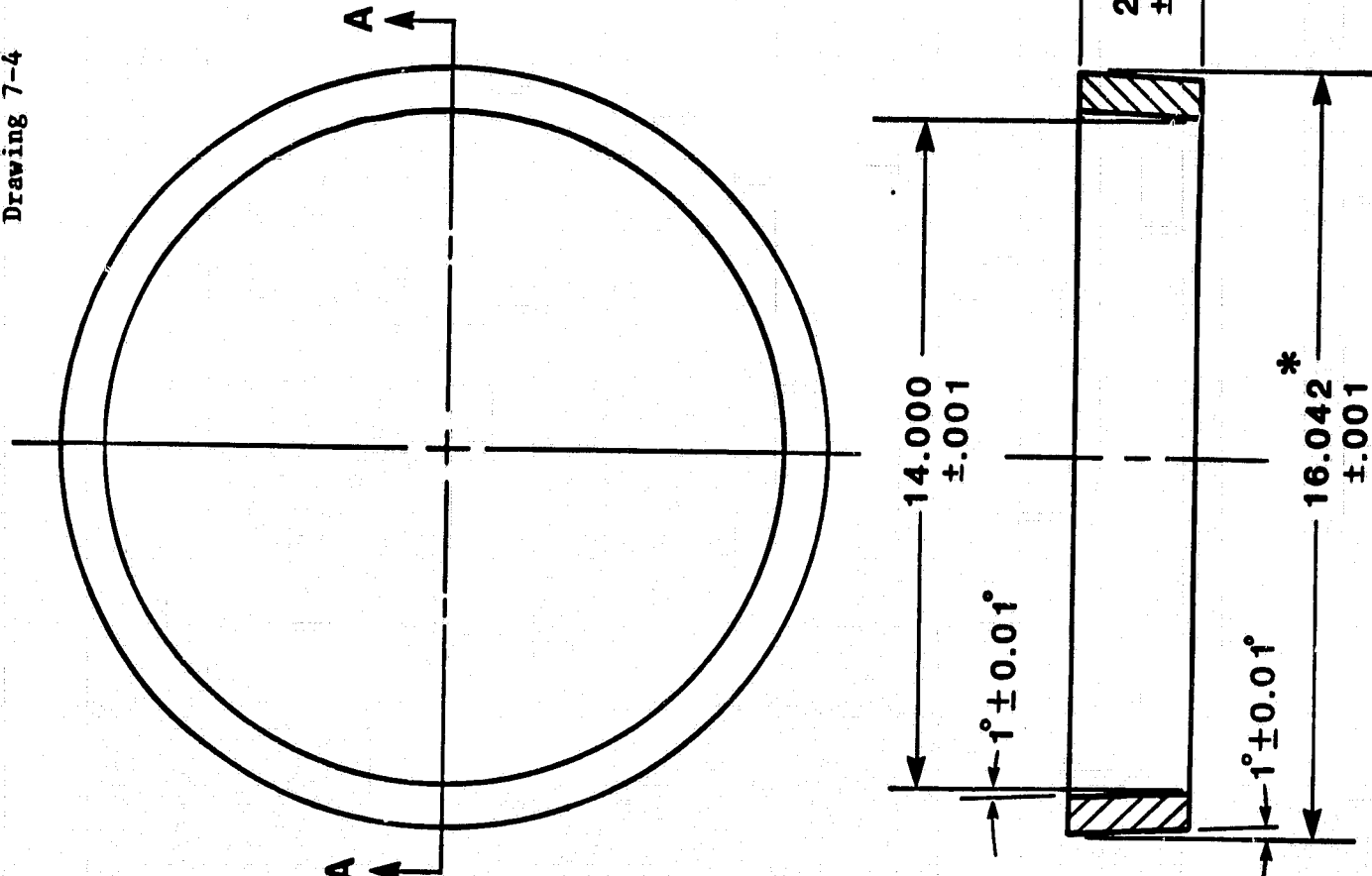
Drawing 7-4

Note: Approximate ring
weight = 7.0 lbs.

* Machine after
assembly

ORIGINAL PAGE IS
OF POOR QUALITY

Name	NASA-12
Name	Ring 4
Material	Celion 6000/Epoxy
Date	12-30-83
Scale	1:6
Tol., Unless spec.	Angles $\pm 0.1^\circ$ Dim. $\pm .001$
Designer	J A K
Graftsman	J T S



Taper angles
not to scale

Section A-A

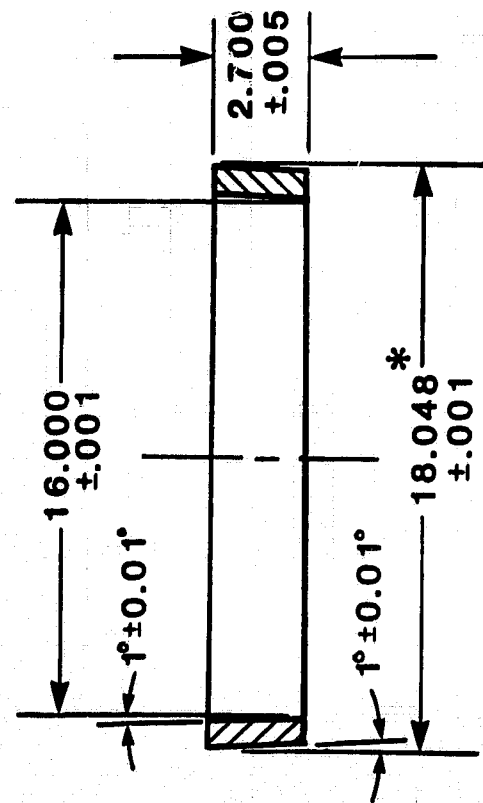
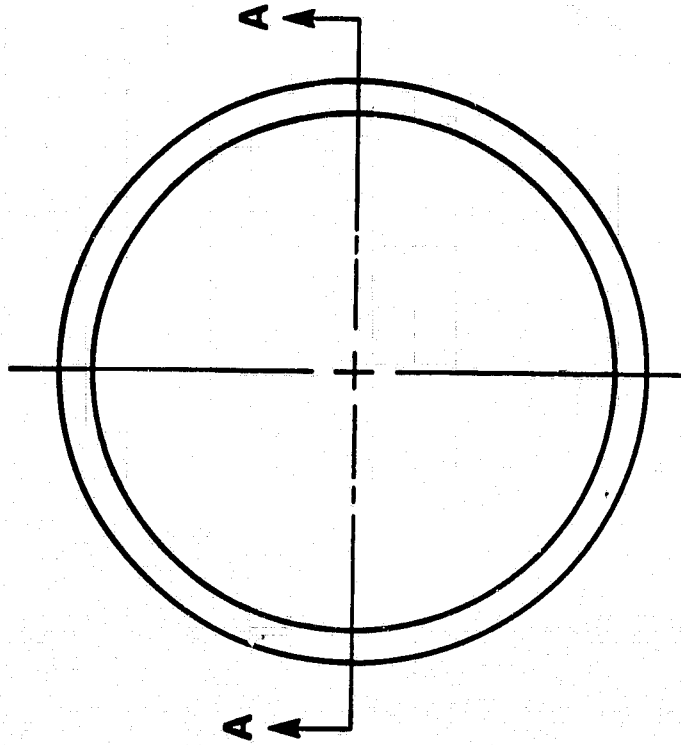
Drawing 7-5

Note: Approximate ring
weight = 7.9 lbs.

* Machine after
assembly

Name	NASA - 12
Name	Ring 5
Material	Celion 6000/Epoxy
Date	12-30-83
Scale	1:4
Tol., Unless spec.	Angles ± 0.1 Dim. $\pm .001$
Designer	J A K
Draftsman	J T S

ORIGINAL PAGE IS
OF POOR QUALITY



Section A-A

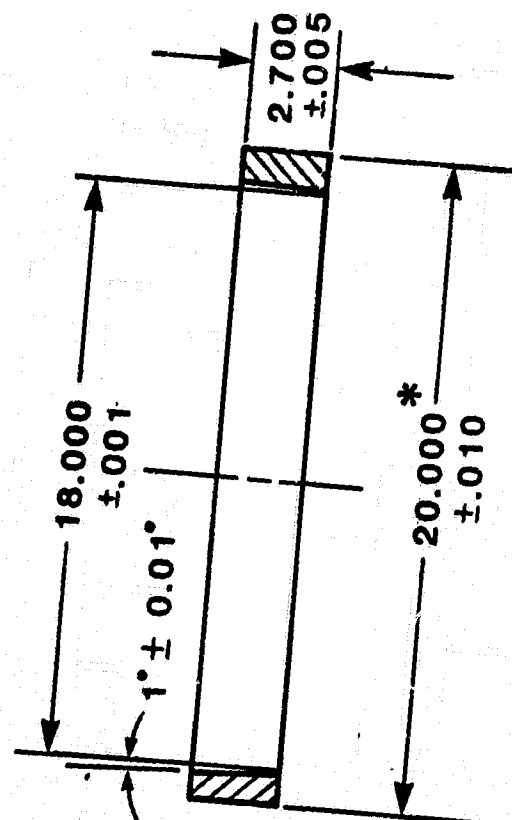
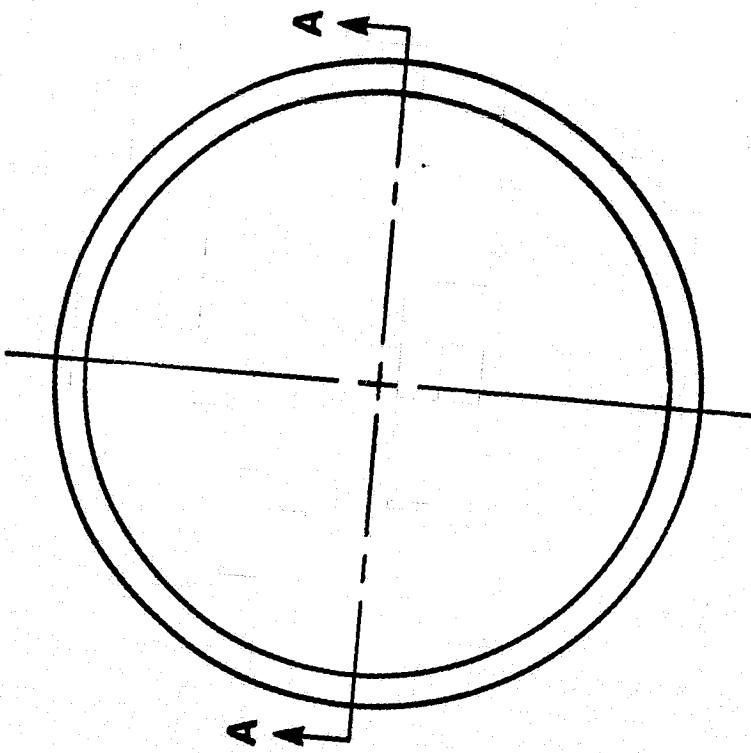
Drawing 7-6

Note: Approximate ring
weight=8.9 lbs.

* Machine after
assembly

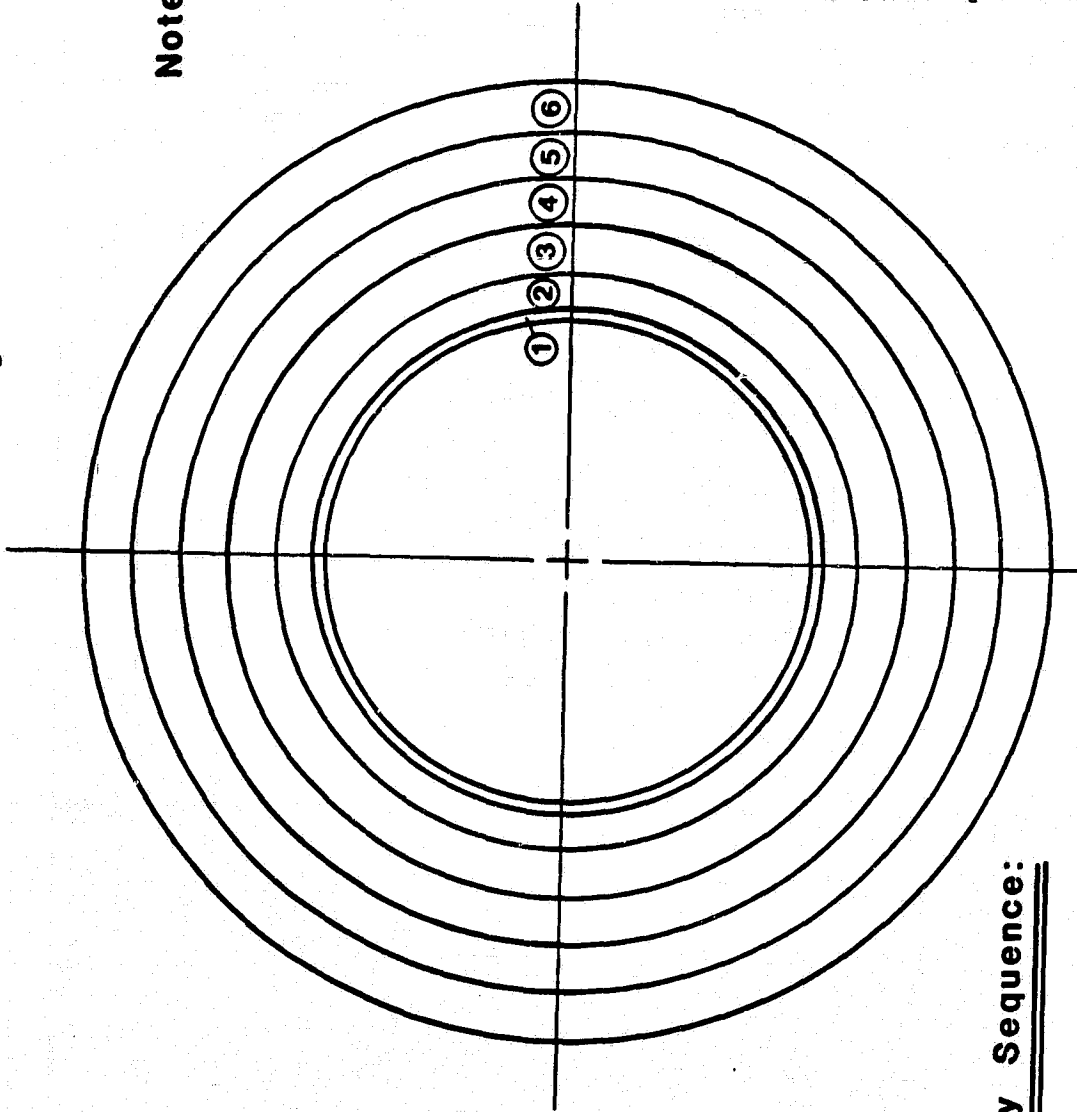
Name	NASA-12
Name	Ring 6
Material	Celion 6000/Epoxy
Date	12-30-83
Scale	1:6
Tol., Unless spec.	Angles $\pm 0.1^\circ$ Dim. $\pm .001$
Designer	J A K
Draftsman	J T S

ORIGINAL PAGE IS
OF POOR QUALITY



Taper angles
not to scale
Section A-A

- Note:**
1. Coat all interfaces with epoxy prior to assembly..
 2. Ring number in circles, \bigcirc .
 3. Machine O.D. of each ring to print spec. after assembly.



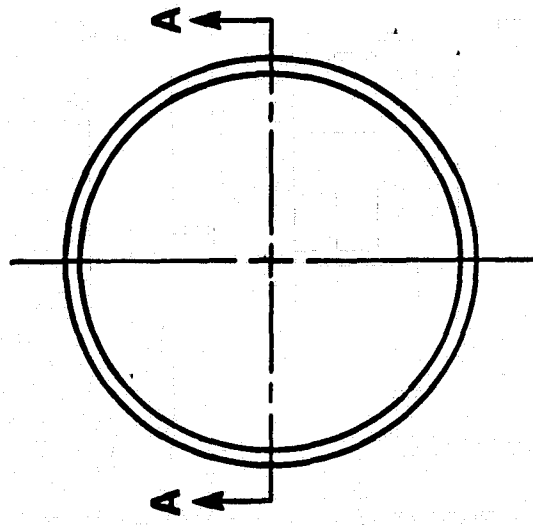
Assembly Sequence:

1. Press Ring 3 onto Ring 2. Typ. force = 44,000 lbs.
2. Press Ring 4 onto Assy. Typ. force = 59,000 lbs.
3. Press Ring 5 onto Assy. Typ. force = 67,000 lbs.
4. Press Ring 6 onto Assy. Typ. force = 73,000 lbs.
5. Bond Segmented Iron Ring 1 to Ring 2.

Name	Assembly Drwg.
Name	NASA-12
Material	
See Ring Drwg.	
Date	12-30-83
Scale	1:4
Tol., Unless spec.	Angles $\pm 0.1^\circ$, Dim. $\pm .001$
Designer	J A K
Drafterman	J T S

ORIGINAL PAGE IS
OF POOR QUALITY

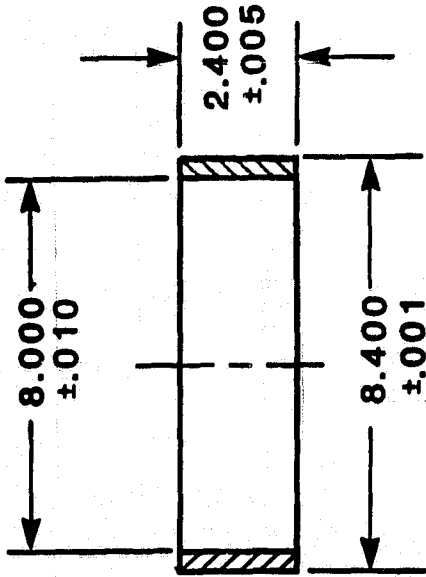
Drawing 7-1A



Note: 1. Approximate ring weight = 3.6 lbs.

2. This ring is added after all others have been assembled. Its exact design has not been determined as part of this project.

Name	NASA-20
Name	Ring 1
Material	Segmented Iron
Date	12-30-83
Scale	1:4
Tol., Unless spec.	
Angles $\pm 0.1^\circ$	Dim. $\pm .001$
Designer	J A K
Draftsman	J T S



Section A-A

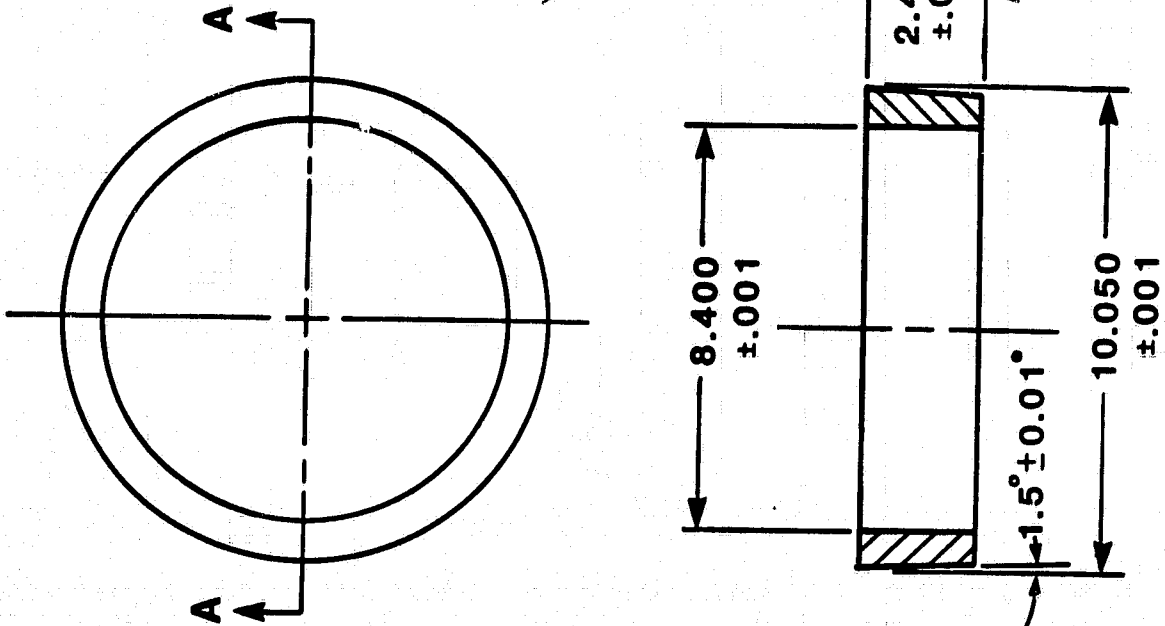
ORIGINAL PAGE IS
OF POOR QUALITY

Drawing 7-2A

Note: Approximate ring
weight = 3.1 lbs.

ORIGINAL PAGE IS
OF POOR QUALITY

Name	NASA-20
Name	Ring 2
Material	Celion 6000/Epoxy
Date	12-30-83
Scale	1:4
Tol., Unless spec.	
Angles $\pm 0.1^\circ$, Dim. $\pm .001$	
Designer	J A K
Draftsman	J T S



Taper angle
not to scale
Section A-A

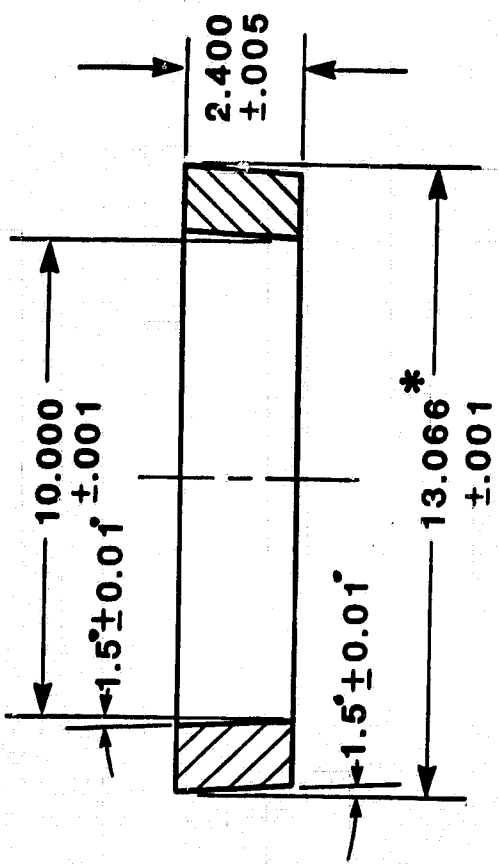
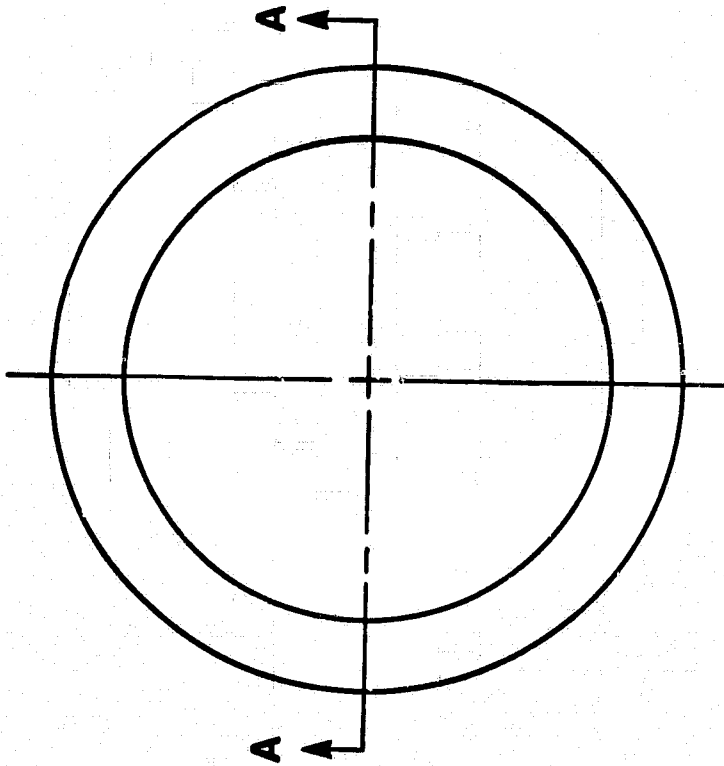
Drawing 7-3A

Note: Approximate ring weight = 7.2 lbs.

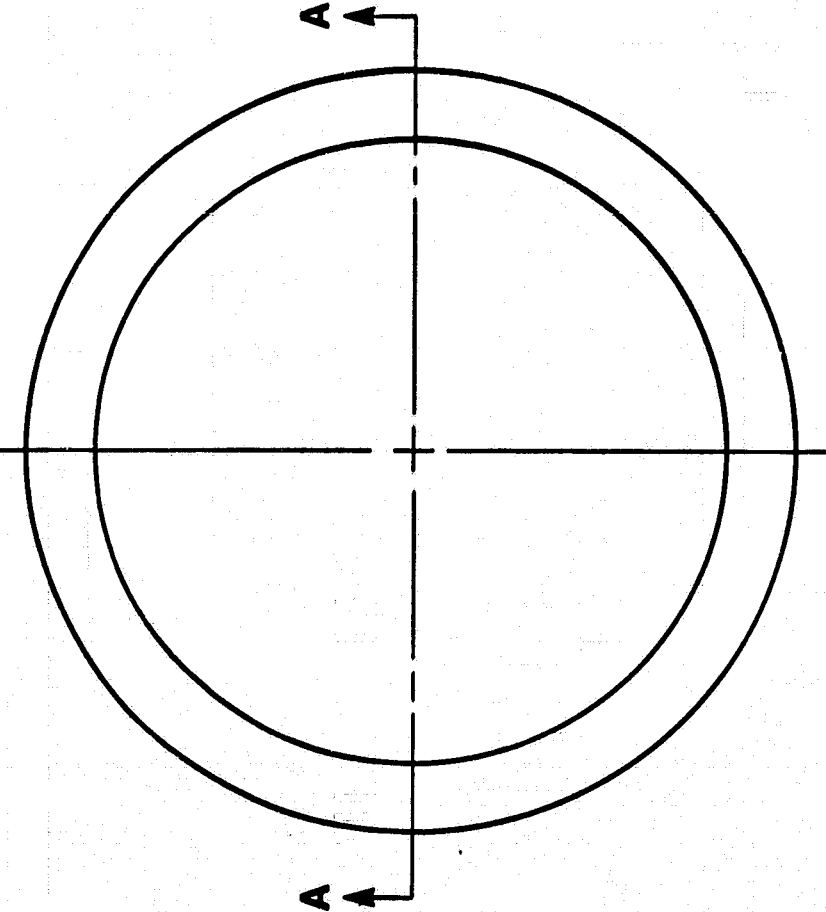
* Machine after assembly

Name	NASA-20
Name	Ring 3
Material	Cellon 6000/Epoxy
Date	12-30-83
Scale	1:4
Tol., Unless spec.	
Angle $\pm 0.1^\circ$, Dim. $\pm .001$	
Designer	J A K
Drafterman	J T S

ORIGINAL PAGE IS
OF POOR QUALITY



Drawing 7-4A

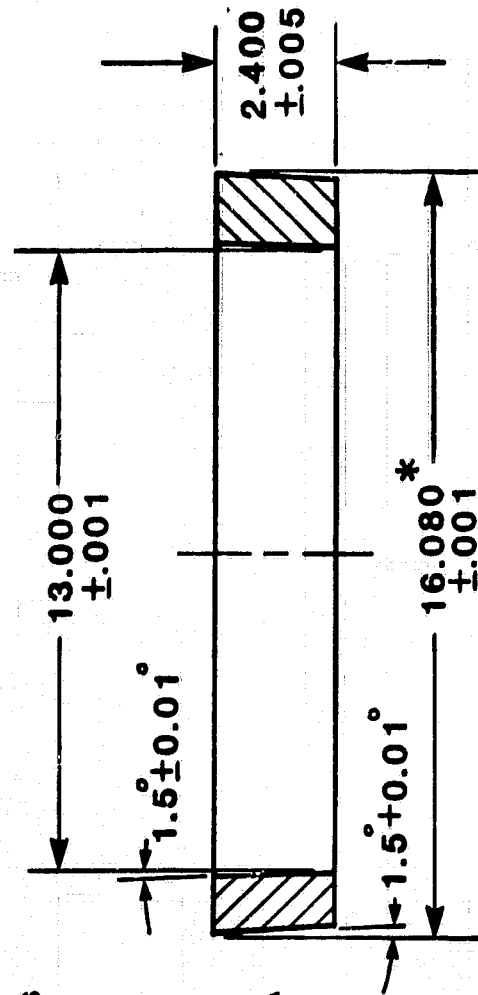


Note: Approximate ring
weight = 9.1 lbs.

* Machine after
assembly

ORIGINAL PAGE IS
OF POOR QUALITY

Name	NASA-20
Name	Ring 4
Material	Celion 6000/Epoxy
Date	12-30-83
Scale	1:4
Tol., Unless spec.	
Angles $\pm 0.1^\circ$, Dim. ± 0.01	
Designer	J A K
Draftsman	J T S



Taper angles
not to scale

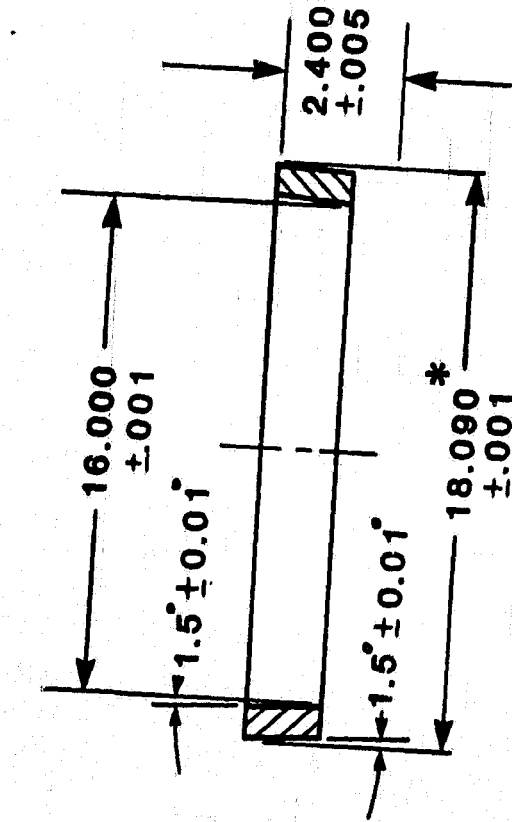
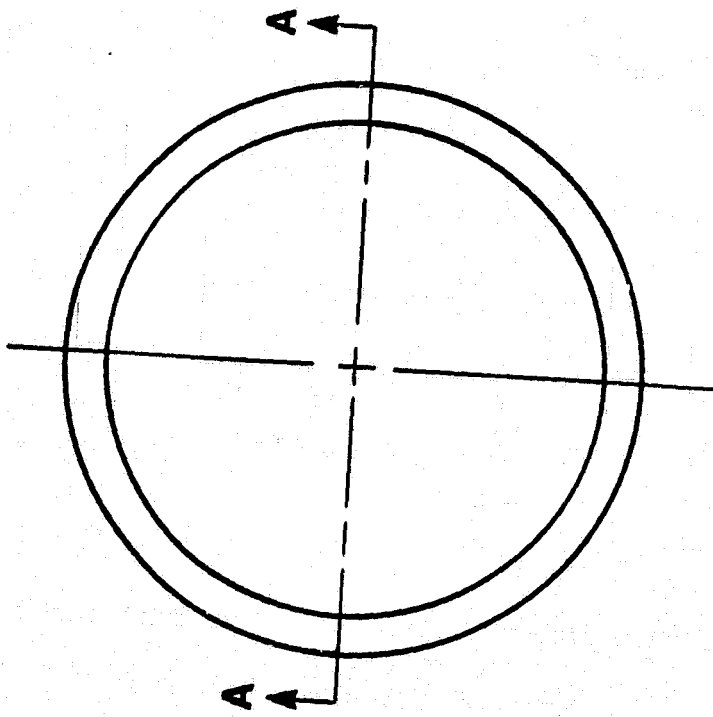
Section A-A

Note: Approximate ring weight = 7.1 lbs.

* Machine after assembly

Name	NASA-20
Name	Ring 5
Material	Celion 6000/Epoxy
Date	12-30-83
Scale	1:6
Tol., Unless spec.	Angles $\pm 0.1^\circ$; Dim. $\pm .001$
Designer	J A K
Draftsman	J T S

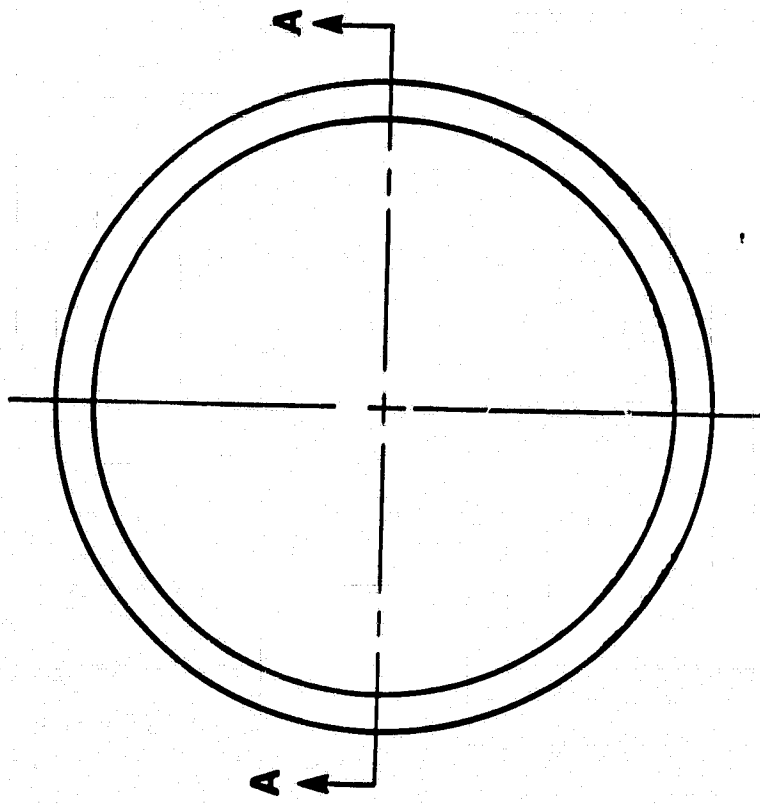
ORIGINAL PAGE IS
OF POOR QUALITY



Taper angles
not to scale

Section A-A

Drawing 7-6A

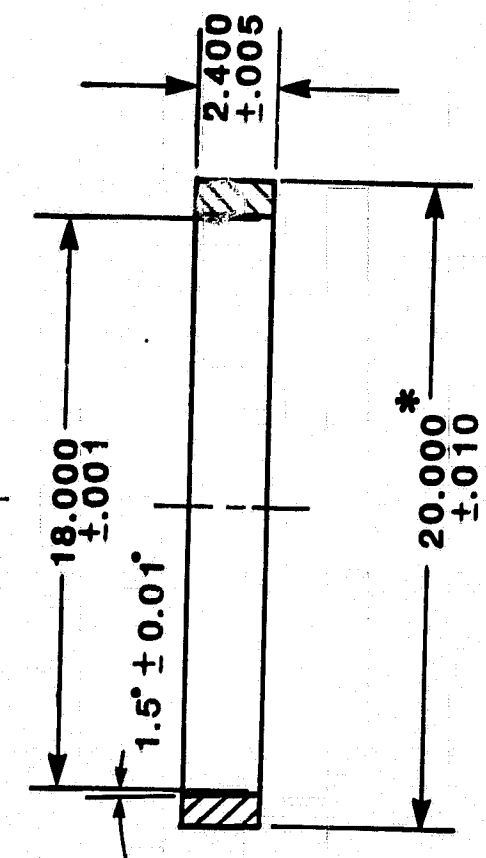


Note: Approximate ring
weight = 8.0 lbs.

* Machine after
assembly

ORIGINAL PAGE IS
OF POOR QUALITY

Name	NASA-20
Name	Ring 6
Material	Cellion 6000/Epoxy
Date	12-30-83
Scale	1:6
Tol., Unless spec.	
Angles $\pm 0.1^\circ$, Dim. $\pm .001$	
Designer	JAK
Draftsman	JTS



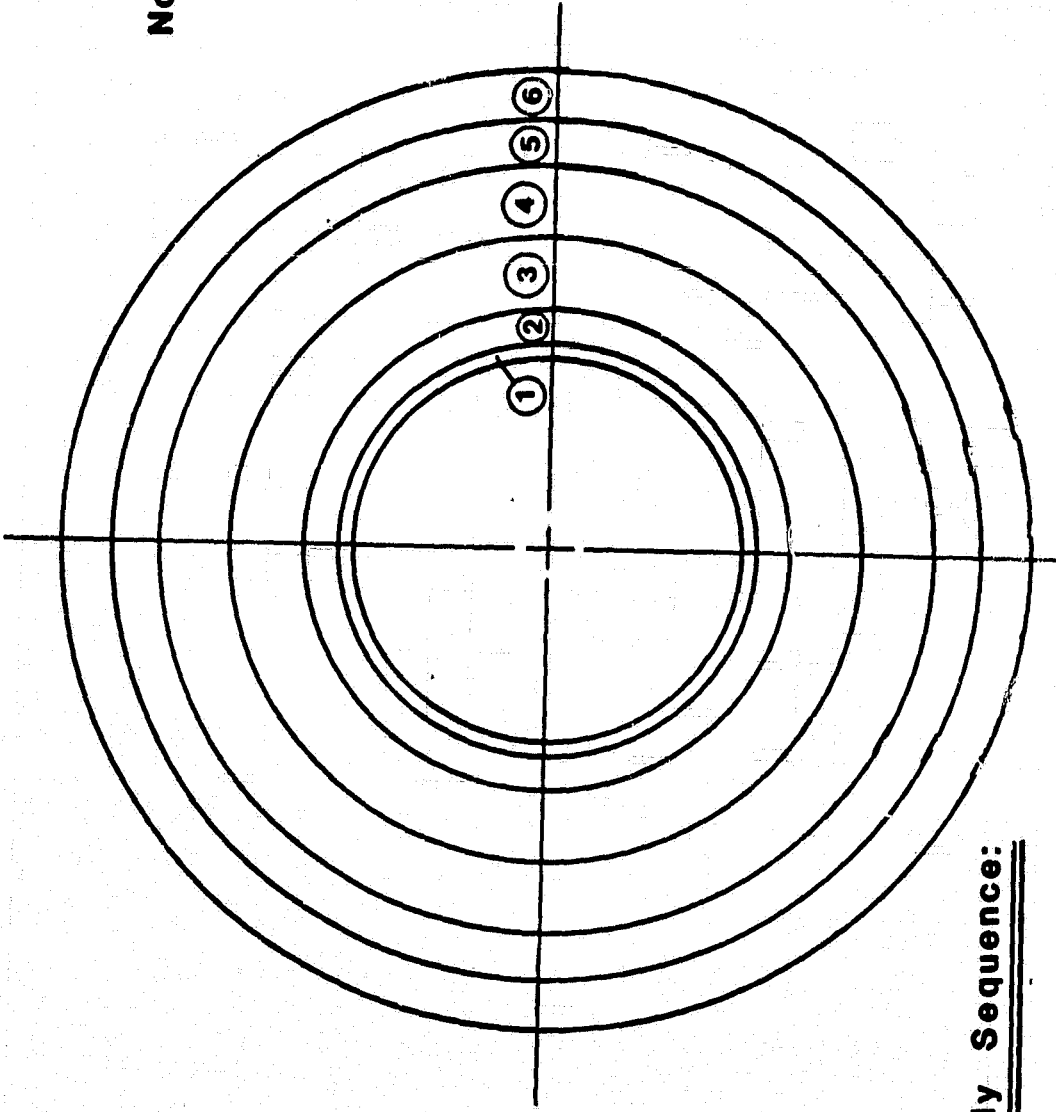
Taper angle
not to scale

Section A-A

Drawing 7-7A

Note: 1. Coat all ring interfaces with epoxy prior to assembly.

2. Ring number in circles, .
3. Machine O.D. of each ring to print spec. after assembly.



Assembly Sequence:

1. Press Ring 3 onto Ring 2. Typ. force = 82,000 lbs.
2. Press Ring 4 onto Assy. Typ. force = 125,000 lbs.
3. Press Ring 5 onto Assy. Typ. force = 117,000 lbs.
4. Press Ring 6 onto Assy. Typ. force = 123,000 lbs.
5. Bond Segmented Iron Ring 1 to Ring 2.

Name	Assembly Drwg.
Name	NASA-20
Material	
See Ring Drwg.	
Date	12-30-83
Scale	1:4
Tol., Unless spec.	
Angles $\pm 0.1^\circ$, Dim. $\pm .001$	
Designer	J A K
Draftsman	J T S

OPTIONAL PAGE E
OF POOR QUALITY